# Mechanism of Oxidation Reactions Catalyzed by Cytochrome P450 Enzymes

Bernard Meunier,*,† Samuël P. de Visser,‡ and Sason Shaik*,‡

*Laboratoire de Chimie de Coordination du CNRS, 205 route de Narbonne, 31077 Toulouse Cedex 4, France, and Department of Organic Chemistry and the Lise-Meitner-Minerva Center for Computational Quantum Chemistry, The Hebrew University of Jerusalem, Givat Ram 91904 Jerusalem, Israel*

*Received February 4, 2004*

## Contents



* To whom correspondence should be addressed. E-mail: bmeunier@lcc-toulouse.fr. E-mail: sason@yfaat.ch.huji.ac.il.
† Laboratoire de Chimie de Coordination du CNRS.
‡ The Hebrew University of Jerusalem.

## 1. Introduction

The cytochromes P450 constitute a large family of cysteinato-heme enzymes,[1−9] are present in all forms of life (plants, bacteria, and mammals), and play a key role in the oxidative transformation of endogeneous and exogeneous molecules (see refs 5 and 6 for recent reviews). The total number of members of the cytochrome P450 family is increasing rapidly (over 2000 members at the time of this writing. Updated information is available on the following web site: http://drnelson.utmem.edu/CytochromeP450.html). In all these cysteinato-heme enzymes, the prosthetic group is constituted of an iron(III) protoporphyrin-IX covalently linked to the protein by the sulfur atom of a proximal cysteine ligand (see Figure 1).

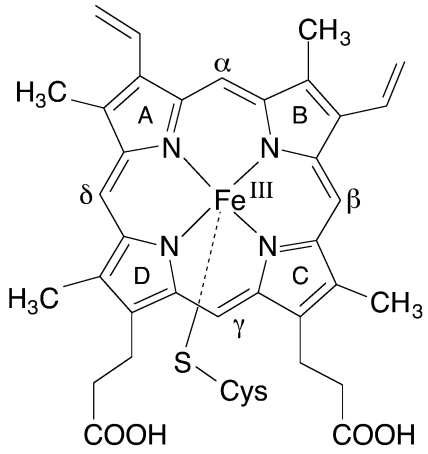


cysteinato-iron(III) protoporphyrin-IX

**Figure 1.** Prosthetic of cysteinato-heme enzymes: an iron(III) protoporphyrin-IX linked with a proximal cysteine ligand.

These enzymes are potent oxidants that are able to catalyze the hydroxylation of saturated carbon−

10.1021/cr020443g CCC: $48.50 
Published on Web 08/21/2004

Bernard Meunier was born in 1947 and educated at the Universities of Poitiers, Montpellier (with R. J. P. Corriu), and Orsay (with H. Felkin, ICSN-CNRS). After a post-doc at the University of Oxford, he joined the "Laboratoire de Chimie de Coordination du CNRS" in Toulouse in 1979. He is Director of research at the CNRS and Associate Professor at the Ecole Polytechnique at Palaiseau, near Paris. His current research interests include catalytic biomimetic oxidations, DNA cleavage, oxidation of pollutants, and the mechanism of action of drugs (antitumoral, antibiotics, and antimalarial agents). As recent awards, he received the Descartes–Huygens Prize in 2001 and the Gay Lussac–Alexander Von Humboldt Award in 2002. He is the founder of Palumed S. A., a start-up company devoted to medicinal chemistry. He is the author of 310 publications and 25 patents. He was elected a Member of the French Academy of Sciences in 1999.

Sason Shaik was born in 1948 in Iraq. The family immigrated to Israel in the Exodus of the Iraqi Jewry. He received his B.Sc. and M.Sc. in chemistry from Bar-Ilan University and his Ph.D. from the University of Washington. In 1978/9, he spent a postdoctoral year with Roald Hoffmann at Cornell University. In 1980, he started his first academic position as a Lecturer at Ben-Gurion University where he became Professor in 1988. He subsequently moved to the Hebrew University, where he is currently the director of The Lise-Meitner-Minerva Center for Computational Quantum Chemistry. Among the awards he has received are the Lise-Meitner–Alexander von Humboldt Senior Award in 1996–1999, the 2001 Israel Chemical Society Prize, and the 2001 Kolthoff Award. His research interests are in the use of quantum chemistry, and in particular of valence bond theory, to develop paradigms which can pattern data and lead to the generation and solution of new problems. He started his P450 research in 1998 and has been fascinated ever since!

Samuël de Visser was born in a village in the southwest of The Netherlands on September 17, 1968, and has been working at the Hebrew University since December 1999. He obtained an experimentally oriented Ph.D. degree in Physical Organic Mass Spectrometry from the University of Amsterdam under the supervision of Prof. Nico Nibbering (1997). He then moved to London to do postdoctoral research in Theoretical Chemistry with Prof. Mike Robb (King's College London) before moving to Israel. He won a Ramsay Memorial Fellowship (1997) and is a recipient of the Lise-Meitner-Minerva Junior Award (2003). His major research interests include the properties and reactivities of heme-type enzymes and their analogues. He recently accepted a lectureship in Biophysics from the University of Manchester Institute of Science and Technology (UMIST) in Manchester (United Kingdom).

hydrogen bonds, the epoxidation of double bonds, the oxidation of heteroatoms, dealkylation reactions, oxidations of aromatics, and so on. As the means of oxidation, the P450 uses molecular oxygen, inserts one of its oxygen atoms into a substrate (S), and reduces the second oxygen to a water molecule, utilizing two electrons that are provided by NAD(P)H via a reductase protein (eq 1). Since only one of the two oxygen atoms, initially present in $O_2$, remains in the oxidized substrate, P450s are called monooxygenases.

$$S + O_2 + 2e^- + 2H^+ \xrightarrow{\text{cytochrome P450}} SO + H_2O \quad (1)$$

Molecular oxygen, itself, is unreactive toward organic molecules at low temperatures either due to spin-forbiddenness or to high barriers.[10] Consequently, living systems mainly use enzymes that modify dioxygen to a form capable of performing the desired oxidation reaction. This modification can be achieved by metal-dependent oxygenases, like cytochromes P450 or non-heme metalloenzymes (e.g., methane monooxygenase), or by flavin-containing enzymes that do not possess a metal-based prosthetic group. Cytochrome P450 enzymes were first identified and purified nearly 40 years ago by biochemists and pharmacologists who focused on the early studies of the oxidative metabolism of drugs. This pharmacological and medicinal interest in P450 remains intense to this day, and the name cytochrome P450 can be found 2508, 2775, 2690, and 2319 times in the *Medline* database of the U.S. National Institutes of Health for the years 2000, 2001, 2002, and 2003, respectively.

The historical details of the discovery of cytochrome P450 are available in two recent review articles by Estabrook and Omura.[11,12] A few studies, conducted before the early 1960s, on the animal response to toxic molecules or pharmacologically active entities, have established that hydrophobic exogeneous molecules are modified and subsequently excreted as water-soluble forms. These two distinct steps are now described as phase I (oxidation step) and phase II

(conjugation step) (eq 2, O−X being a sulfate or a glucuronic residue).[1,13]

$$\mathrm{R{-}H} \xrightarrow{\text{cytochrome P450 (}\textit{phase I}\text{)}} \mathrm{R{-}O{-}H} \xrightarrow{\text{transferases (}\textit{phase II}\text{)}} \mathrm{R{-}O{-}X} \quad (2)$$

The main phase II drug-elimination enzymes are the aryl sulfatase, the UDP-glucuronyl transferase, and the glutathione S-transferase.

The motivation for these early studies was the necessity of establishing a paradigm of drug metabolism, a particularly important domain of molecular pharmacology. Early in 1955, Axelrod reported that the oxidative metabolism of ephedrine was mediated by the microsomal fraction (containing the endoplasmic reticulum) of a rat liver homogenate in the presence of NADPH and dioxygen.[14] In 1958, Klingenberg established that the rat liver microsomes contained an unknown carbon monoxide binding pigment.[15] Later, Omura and Sato found that the microsomal CO-binding pigment was a heme-protein having a strong absorption peak at 450 nm and therefore named this pigment as "cytochrome P450" (the strong absorption band at 450 nm corresponds to the Soret $\pi-\pi^*$ band of the PPIX−$Fe^{II}$−CO chromophore).[16] In 1963, Estabrook et al. indicated that cytochrome P450 was able to catalyze the C-21 hydroxylation of 17-hydroxyprogesterone in adrenal cortex microsomes.[17] For many years, the membrane-bound nature of these oxidative enzymes, present in the microsomal fraction of rat liver, posed difficulties for the biochemical characterization of these proteins. However, due to the combined effort of a few groups, it has become possible for the communities of biochemists, enzymologists, and pharmacologists to study the wide range of different oxidative transformations mediated by cytochrome P450 enzymes either in the liver (detoxification processes, drug metabolism, etc.) or in specific tissues or organs (biosynthetic steps that require difficult oxidative processes).

Originally found in rat liver microsomes, cytochromes P450 are, in fact, present in all eukaryotic organisms (animals, plants, and fungi) and also in some prokaryotes. The purification of these membrane-bound enzymes was facilitated by the discovery of Ichikawa and Yamano[18] in 1967 that high concentrations of glycerol were able to stabilize cytochrome P450 against detergent treatments.[18,19] Successful purifications of different cytochrome P450s were achieved in the period 1975−1980, just before the beginning of the "cloning era", initiated by the development of genetics in the early 1980s.

Cytochromes P450 have been initially classified according to the auxiliary electron-transfer proteins, which provide electrons from NADH or NADPH to the oxygenase protein (see Figure 2).[20] "Class I" refers to mammalian mitochondrial enzymes involved in steroid syntheses and to most bacterial enzymes. For this category, the electrons are transferred by an iron−sulfur protein $Fe_2S_2$.

"Class II" corresponds to mammalian enzymes located in the endoplasmic reticulum of liver cells, which are involved in drug (or any exogeneous compound) metabolism. For this second category, electrons are provided by FAD- and FMN-containing reductases (FAD serves as an electron acceptor from NADPH and the FMN moiety transfers the electrons to the oxygenase protein). All cytochromes P450 are integrated in a complex multienzymatic system, which hampers their industrial application for selective oxygenations of chemicals (sol−gel immobilization of P450 enzymes might be a way to develop their use in fine chemical syntheses).[21] In that respect, other enzymes, like hydrolytic ones, are easy to handle on the industrial scale and are now currently used in modern organic syntheses.

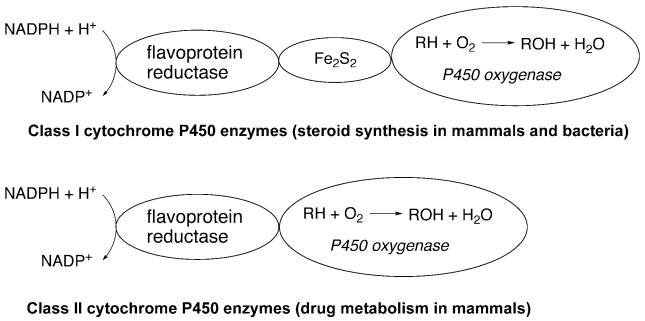


**Figure 2.** Different electron-transfer chains in class I and class II of cytochrome P450 enzymes.

## 2. Genomic Studies on Cytochromes P450

The development of genomic studies has highly facilitated the identification, the classification, and the naming of the different cytochrome P450 enzymes that have been generated by evolutional divergence from a single ancestral form.[22,23] The number of cytochrome P450 genes in the genome of a given organism ranges from 50 to 150, indicating highly diversified functions of these monooxygenases in multicellular eukaryotes.[24] The number of known individual cytochrome P450s in humans is about 57 and will not change much in the future (in comparison, the plant *Arabidopsis thaliana* has 286 cytochrome P450s). No P450 genes have been found in the genomes of several bacteria, including *Escherichia coli*; however, some prokaryotes which are using hydrocarbons (e.g., terpenes) as both carbon and energy sources contain cytochrome P450s, the classical example being *Pseudomonas putida* with its camphor-oxidizing P450 ($P450_{cam}$). Cytochrome P450 enzymes are now classified according to genetic information. The nomenclature of cytochromes P450 was originally organized according to their physiological functions and then, in the 1980s, according to serial numbers based on the degree of similarity in their amino acid sequences. For example, a cytochrome P450 able to catalyze the oxidative cleavage of the side chain of cholesterol is usually called $P450_{ssc}$ and, according to the systematic nomenclature, is now reclassified as a member of subfamily 11A of family 11 (P450 11A1 or CYP11A1) and the corresponding gene is *Cyp11A1*.[25−27] For detailed explanations of the nomenclature system adopted for cytochrome P450 enzymes, the review articles by Nelson et al. and Nebert et al. are highly recom-

mended (see also the Web site mentioned at the begining of the Introduction).[25−28]

Taken together, all P450 families make up the superfamily of cytochromes P450. The number of cytochrome P450 families is continuously growing and is now above 200. Within the same family, the sequence identity of individual P450s should be ≥59% (within a subfamily, the sequence identity should be above 70%). However, between two individual P450 enzymes, the sequence identity can be as low as 16%.

The gene analysis of the different cytochrome P450s indicates that all these metalloproteins exhibit the same so-called "P450 signature" motif of 10 amino acids, including the invariant cysteine residue that ligates the heme iron to the protein, Phe-XX-Gly-$X_b$-XX-Cys-X-Gly. The amino acid Xb is usually a basic amino acid that plays a key role in interactions with the reductase partner.[23,29] In cytochrome $P450_{cam}$, this basic amino acid is a glutamine residue (Glu-360) interacting with two cysteines: the proximal cysteine (Cys-357) of the oxygenase protein and one cysteine (Cys-39) of the ferredoxin reductase. The role of this basic amino acid has been clearly established with mutants of cytochrome $P450_{cam}$ by Morishima and co-workers.[30] Arg-112 (in $P450_{cam}$) has also an important role in the interactions between the oxygenase and the iron−sulfur protein that acts as electron transferase.[31,32]

In the future, genomic studies will provide the whole collection of P450 sequences (and consequently also the corresponding proteins) for the different living organisms. X-ray crystallography remains the main technique for structural determination of P450s. Most of the P450 proteins are still too big for routine three-dimensional (3D) structure determination by nuclear magnetic resonance (for an example of a NMR analysis of P450−substrate interaction, see ref 33). Consequently, efforts are currently being made on the comparative modeling of these metalloenzymes. With access to fast computers, the prediction of the 3D structure of P450 proteins from their amino acid sequences will become more and more accurate.[34] Computational predictions of drug interactions with P450 enzymes are also rapidly expanding and will facilitate in the future design of (i) specific P450 inhibitors or (ii) drugs with limited and/or controlled P450 metabolism.[35,36] The main human liver cytochrome P450s able to recognize and to metabolize the xenobiotics (drugs and all the other exogeneous molecules) are the following ones: CYP1A2, CYP2C9, CYP2C19, CYP2D6, and CYP3A4. Currently, these five human liver P450s contribute to the oxidative metabolism of more than 90% of the drugs in clinical use.[37] The organization of cytochrome P450 genes has been studied as well as the role of NO or RNA in the down-regulation of the expression of cytochrome P450 enzymes.[38−40]

## 3. Three-Dimensional Structures of Cytochrome P450 Enzymes

After the establishment of the first 3D structure of the bacterial cytochrome $P450_{cam}$ (=CYP101) by Poulos and co-workers in 1985, cytochrome P450 enzymes ceased being black boxes that perform oxidation.[41−44] Cytochrome $P450_{cam}$ of *P. putida* catalyzes the stereospecific hydroxylation of the exo C5−H bond of camphor (Figure 3). In turn, the microorganism uses this terpene as its only source of carbon and energy; camphor is first hydroxylated and then metabolized to isobutyrate and acetate.

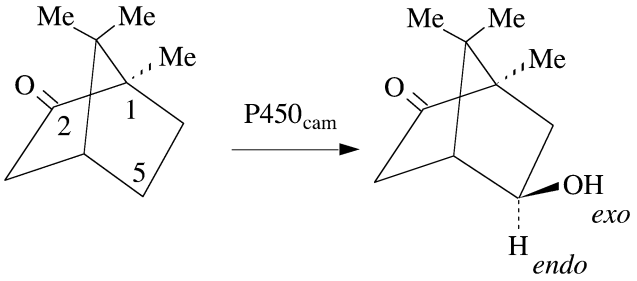


**Figure 3.** Stereospecific hydroxylation of the exo C−H bond at the C5 position of camphor by cytochrome $P450_{cam}$.

$P450_{cam}$ is a 45 000 Da polypeptide chain containing a single ferric protoporphyrin-IX and a cysteine (Cys-357) as an axial ligand (see Figure 4A for a general disposition of the different helices of the enzyme and Figure 4B for a view of the camphor substrate within the active site).

The camphor substrate is oriented within the active site of the enzyme by a combination of a hydrogen bond between the oxygen of the carbonyl group and the phenolic function of a tyrosine residue (Tyr-96) and weak hydrophobic interactions with Phe-87, Leu-244, Val-247, Thr-252, and Val-295. The entrance of the hydrophobic pocket of the active site is occupied by two phenylalanines (Phe-87 and Phe-193).

The $Fe^{III}$ state of the resting enzyme can, in principle, equilibrate between the low-spin ($S = 1/2$) and the high-spin state ($S = 5/2$). The low-spin state is favored in the absence of a substrate when the sixth position of the octahedron is occupied by a water molecule (an aqua ligand). In the presence of camphor, the axial water molecule and other water molecules are displaced from the hydrophobic pocket of the enzyme and the spin equilibrium of the iron(III) center is shifted toward the high-spin form. This modification of the coordination sphere of the metal center induces a change in the redox potential of the iron center, shifting it from −300 to −170 mV after substrate binding; such a redox shift facilitates the reduction of the pentacoordinated ferric center by the reductase.

At present, 12 other X-ray structures have been published: (i) the fatty acid hydroxylating enzyme $P450_{BM-3}$ (CYP102, molecular weight = 119 kDa) from *Bacillus megaterium* (this enzyme is the first example of a bacterial enzyme that can be classified as a class II P450),[45,46] (ii) the bacterial terpineol-hydroxylating cytochrome $P450_{terp}$ (CYP108),[47] (iii) the fungal cytochrome $P450_{eryF}$ from *Saccharopolyspora erythraea* (CYP107A1),[48−50] (iv) the fungal NO-reductase cytochrome $P450_{nor}$ from *Fusarium oxysporum* (CYP55A1),[51] (v) the acidothermophilic archaeon cytochrome CYP119 from *Sulfolobus solfataricus*,[52] (vi) the *Mycobacterium tuberculosis* cytochrome CYP51 able to demethylate 14α-sterols,[53]

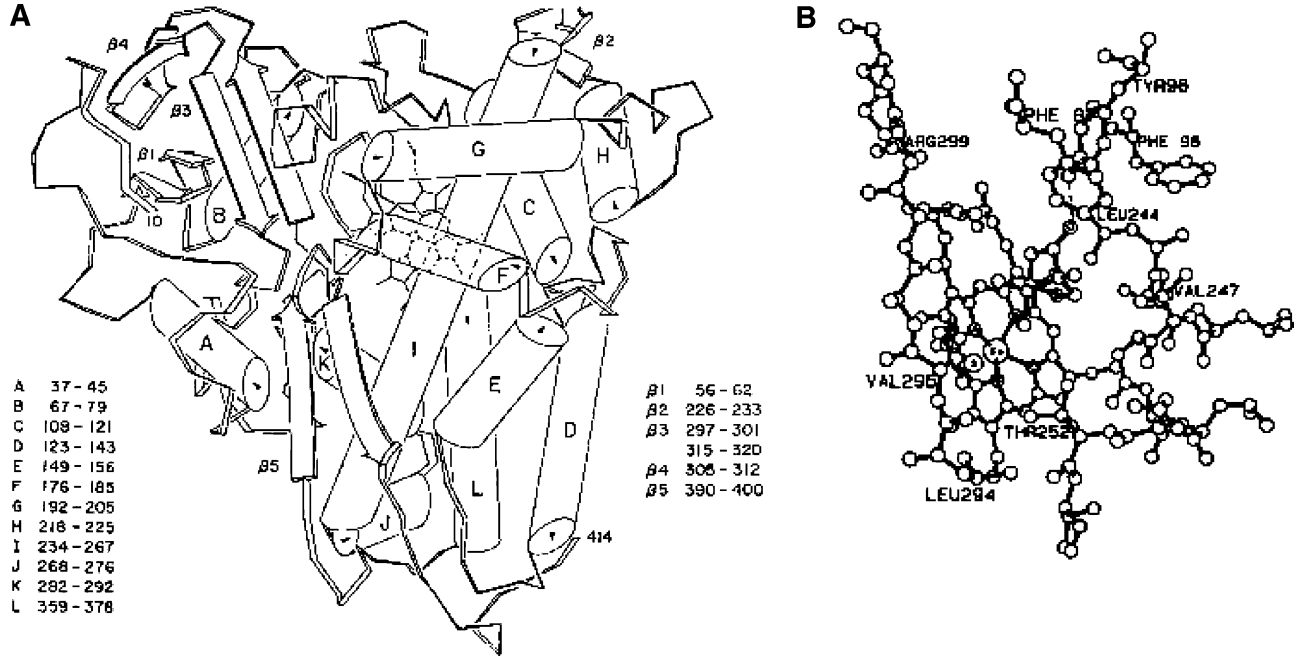


**Figure 4.** (A) General disposition of the different helices of cytochrome $P450_{cam}$ Reprinted with permission from ref 41. Copyright 1985 American Society for Biochemistry and Molecular Biology. (B) View of the camphor substrate within the active site of cytochrome $P450_{cam}$. Reprinted with permission from ref 41. Copyright 1985 American Society for Biochemistry and Molecular Biology.

**Figure 5.** Structure of the human cytochrome P450 2C9. Reprinted with permission from *Nature* (http://www.nature.com), ref 60. Copyright 2003 Nature Publishing Group.

(vii) the mammalian cytochrome CYP2C5,[54,55] (viii) the bacterial cytochrome $P450_{OxyB}$ from *Amycolatopsis orientalis* involved in vancomycin biosynthesis,[56] (ix) the macrolide-functionalizing cytochrome $CYP_{154C1}$ from the Gram-positive bacteria *Streptomyces coelicolor*,[57] (x) the fatty acid hydroxylating cytochrome $P450_{BS\beta}$ from *Bacillus subtilis*,[58] (xi) the thermostable cytochrome $CYP_{175A1}$ from *Thermus thermophilus*,[59] and (xii) also recently the mammalian cytochrome CYP2C9, one of the major human drug-metabolizing enzymes (see Figure 5 for the general structure of this P450; here the sixth coordination site of the iron is not occupied by a water molecule in the substrate-free enzyme).[60]

The X-ray structure of CYP2C9 with the anticoagulant drug *S*-warfarin indicates that the substrate is stabilized within the active site by stacking interactions between the drug phenyl group and two phenylalanine residues of the protein (Phe-476 and Phe-100).[60]

All these 3D structures of cytochrome P450 have common structural elements and an overall fold characteristic of the P450 family. The general shape of these metalloenzymes involves 12 helices and loops denoted A−L (Figure 5). The B−C and F−G helices contribute to substrate access and specificity, and the heme is located between helices I and L. In addition, a few $\beta$-sheets are present in P450 structures.

The crystal structure of the complex between the heme-containing protein and the FMN-binding domain of the reductase of bacterial cytochrome $P450_{BM-3}$ has been determined at 2.03 Å resolution by Poulos and co-workers.[61] The flavin domain is positioned at the proximal face of the heme of the oxygenase-domain, and the interface between the two proteins is strongly organized via hydrogen bonds and salts bridges. The electron-transfer "pathway" between the reductase (via a key tryptophan residue Trp-574) and the heme-domain involves a series of amino acids between two amino acid residues of the oxygenase, Pro-382 and the proximal cysteine Cys-400 of the heme. The specific flavin−protein interactions are involved in the tuning of the redox potential of the FMN entity in such a way that the flavin shuttles between the semiquinone and the fully oxidized states during the catalytic cycles of the oxygenase. The binding of the substrate to the heme-domain increases the redox potential of $Fe^{III}$−PPIX and thereby allows the electron transfer from the FMN semiquinone to the metal center (see Figure 6). The tight coupling between electron transfer and

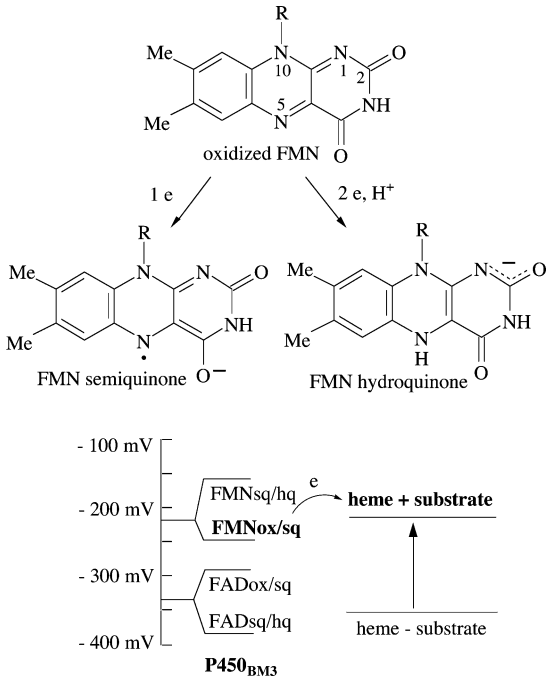


**Figure 6.** Redox potential control of the electron flow between flavin-dependent reductases in cytochrome $P450_{BM-3}$ (sq, hq, and ox stand for semiquinone, hydroquinone, and oxidized forms, respectively).

the oxygenation cycle is of great importance for a fast P450 enzyme such as $P450_{BM-3}$ since it avoids electron waste in side reactions (the turnover number of this enzyme is above 4000 catalytic cycles per min).

The availability of the 3D structures of cytochrome P450s has had a major impact on the enzymological studies of these monooxygenases. Thus, using the structural information paved the way to protein engineering by site-directed mutageneses and made it possible to carry out real molecular enzymology. In fact, this field can be called "chemical enzymology", in which all the molecular partners (enzymes, substrates, and inhibitors) can be modified according to the methods that chemists use for ordinary molecules.[62] Besides the site-directed mutagenesis studies that have been performed to understand the role of key amino acid residues in the catalytic cycle of the enzyme (see below the section devoted to the catalytic cycle of P450), many studies focused on the changes in the protein conformation with chiral inhibitors,[63] product distributions with different substrates,[64] substrate docking,[65] and the design of ruthenium-photosensitizers linked to $P450_{cam}$ substrates and able to recognize submicromolar concentrations of this particular enzyme in the presence of other heme proteins.[66] The long-chain fatty acid hydroxylase $P450_{BM-3}$ can be turned into an efficient indole-hydroxylating enzyme by a triple mutation (Phe87Val, Leu88Gln, Ala74Gly).[67]

## *4. Theoretical Methods for Studying P450 Enzymes*

One of the pioneering theoretical studies on the active species of P450 was carried out by Loew, Kert, Hjelmeland, and Kirchner,[68] using an empirical quantum mechanical (QM) method to calculate electronic structure and derive the Mössbauer parameters for the species. However, it was only after the development of density functional theory (DFT) methods that QM theory came of age and offered a tool that combines reasonable accuracy with speed. More recently, even better tools have become available when DFT calculations were combined with molecular mechanical (MM) approaches, leading to hybrid quantum mechanical/molecular mechanics (QM/MM) methods that enable study of the active species in their native protein environment. All these developments have had a considerable impact on the field and led to an ever-growing surge of theoretical activity. It was therefore deemed timely to include in this review the results and insights provided by these theoretical methods. While we mention occasionally other theoretical methods, our focus is on DFT methods,[69] of which the most successful one is the method based on the hybrid functional called B3LYP. However, there are other methods based on pure functionals, with gradient corrections, such as BP86 and so forth. The interested reader can find a concise description of the various theoretical methods in the recent monograph by Cramer.[69] The theoretical results will be embedded into the following discussion wherever theory provides an essential and complementary insight to experiment. We emphasize that the theoretical coverage is restricted here to selected P450 species and mechanisms. Fuller coverages can be found in recent reviews.[70−72]

## *5. Updated Description of the Catalytic Cycle of P450 Enzymes*

Forty-five years after the isolation and the characterization of cytochromes P450, the exact nature of the active species responsible for the oxygen insertion step is still a matter of intensive debates. After an "iron-oxenoid" period during the 1970s[2,73] came the period of the "high-valent iron-oxo" species. This last suggestion was based primarily on elegant studies using single oxygen atom donors with cytochrome P450 itself and with chemical model species made from synthetic metalloporphyrins.[74−80] More recently, the hypothesis of an electrophilic "iron(III)-hydroperoxo" appeared in the literature,[81] partially inspired by oxidations catalyzed by non-heme iron complexes and DNA sugar oxidation performed by activated iron-bleomycin within tumor cells.[82]

We shall discuss in the section below the different steps of the catalytic cycle of cytochrome P450 (mainly the case of $P450_{cam}$ which can be used as a paradigm) with particular attention to the iron oxygen-containing intermediates. Then, in the following sections, we shall review mechanistic aspects of reactions catalyzed by cytochrome P450 enzymes (hydroxylation, epoxidation, aromatic oxidation, etc.).

### 5.1. Substrate Binding and Product Release

The kinetic and thermodynamic parameters of the reversible binding of the substrate have been particularly well studied in the case of cytochrome $P450_{cam}$ by Griffin and Peterson.[83] The association of camphor is a second-order reaction with a rate

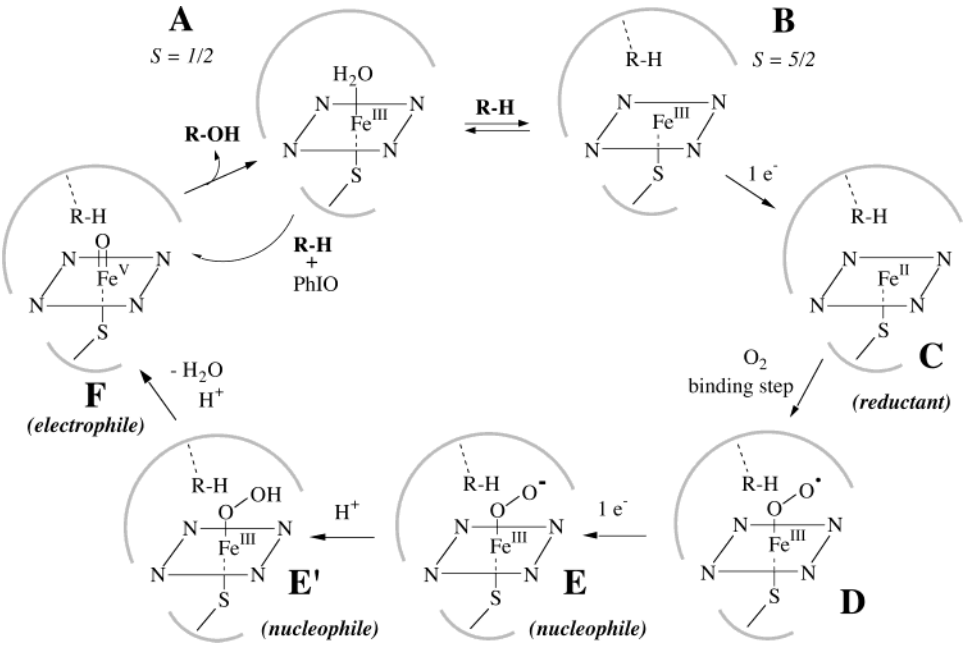


**Figure 7.** Schematic representation of the different intermediates generated during the catalytic cycle of cytochrome P450.

constant of $4.1 \times 10^6$ $M^{-1}$ $s^{-1}$, while the dissociation is a slow first-order reaction with a rate constant of 6.0 $s^{-1}$. Since the camphor binding causes release of a few water molecules from the protein pocket, this produces an entropy change ($\Delta S$) of 26 cal $mol^{-1}$ $K^{-1}$ and a free-energy change ($\Delta G$) of $-7.7$ kcal $mol^{-1}$ at 21 °C. The substrate binding is therefore an entropy-driven process.

The catalytic cycle of cytochrome $P450_{cam}$ is triggered as the camphor molecule enters into the active site and displaces the axial water molecule (**A** in Figure 7). Consequently, the displacement of the iron from the plane of the porphyrin ring increases from 0.30 Å in the resting state of the enzyme (**A**, Figure 7) to 0.44 Å in the pentacoordinated complex (**B**, Figure 7). This makes the heme a better electron sink and triggers an electron transfer from the reductase protein; this electron-transfer event then initiates the cycle. At the end of the cycle, camphor is converted to 5-exo-hydroxycamphor that forms a complex with the heme. Now Tyr-96 comes into play, which together with the product complex forms a polar environment acting as a probe for the polarity changes within the active site of the enzyme when camphor binds. Since Tyr-96 and 5-exo-hydroxycamphor favor a polar environment, this causes the reentrance of bulk water molecules into the pocket and, by displacing the 5-exo-hydroxycamphor, causes the release of the product from the enzyme.[84]

Theoretical calculations using molecular dynamics (MD) simulations lend support to the X-ray structural-based mechanistic description of substrate binding and product release. The hydration of the protein cavity was studied by Helms and Wade[85] using MD simulations of the substrate-free $P450_{cam}$. It was found that the thermodynamically most favorable water content in the pocket was six molecules; most of them occupied the site of the sixth axial ligand (distal ligand), and one was coordinated to Tyr-96. The water molecules in the pocket were spread over a larger volume than in bulk water and were therefore more mobile than bulk water molecules. MD simulations of the substrate entrance and exit channels of $P450_{cam}$, $P450_{BM-3}$, and $P450_{eryF}$ were studied by Lüdemann et al.[86] and Winn et al.[87] In all cases, the major access channels were found to coincide with the ones predicted from crystallographic data based on thermal fluctuation factors near the F/G loop and adjacent helices. All these mechanisms involve backbone motions that are specifically tailored to the physicochemical properties of the substrate. In $P450_{cam}$, the channel is typified by small backbone displacements (1.8−2.4 Å) and aromatic side chain rotations of Phe-87, Phe-193, and Tyr-29. In $P450_{BM-3}$, the positively charged Arg-47 located in the entrance of the channel makes a salt-link that guides the negatively charged substrate via its carboxylate group, while in $P450_{eryF}$ the Arg-185 residue rotates and, by making intraprotein hydrogen bonds, gates the channel opening.

## 5.2. First Reduction Step

After the substrate binding step as discussed above (**A** → **B** in Figure 7), an electron transfer from the reductase causes the reduction of the iron(III) center to the ferrous state (**C**, Figure 7). As mentioned in section 3 above, the nature and role of the different amino acids involved in this electron-transfer step have been elucidated based on the 3D structure of the "oxygenase−reductase" complex in the case of cytochrome $P450_{BM-3}$.[61] The rate constant of the first reduction step is relatively slow ($k = 35$ $s^{-1}$). The reduced form of cytochrome P450 (intermediate **C** in Figure 7) is an extremely efficient reducing agent as expected for an iron(II) porphyrin complex. For example, polyhalogenated hydrocarbons (halothane, carbon tetrachloride, etc.) produce a stable iron(II)-carbene species via a reductive dehalogenation.[73]

The sulfur−iron bond length is probably modified as the resting state, **A**, is converted to the ferrous

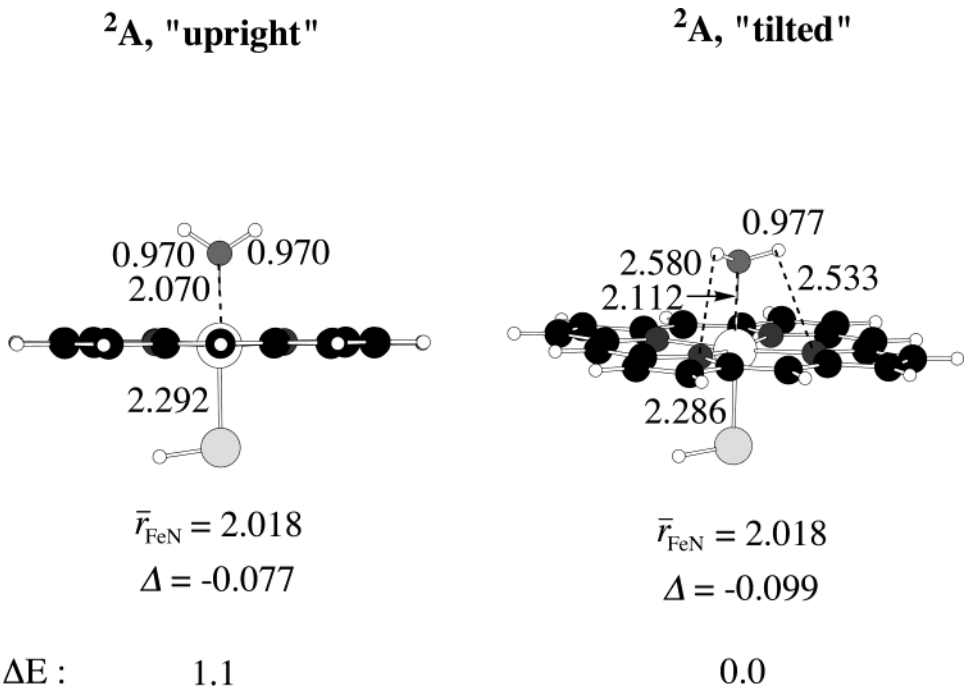


**Figure 8.** The two conformations of the resting state (**A**, see labels in Figure 7) predicted by DFT calculations for the ground doublet spin state. Bond lengths are in Å. Δ is the deviation of the iron from the porphine plane (Δ > 0 signifies that the deviation is above the plane, etc.). Δ*E* is in kcal/mol.

intermediate **C**. Thus, the sulfur−iron bond distance changes from 2.20 Å in the ferric P450$_{cam}$ (**A**, Figure 7) to 2.35−2.41 Å in the CO-adduct of intermediate **C** with the ferrous iron being only displaced by 0.02 Å from the porphyrin plane.[88] Despite the high resolution of the X-ray structure, the authors preferred to attribute this distance modification to experimental errors rather than to a possible modification of the nature of the iron−sulfur bond. The reduction of **B** leads to a negatively charged ferrous complex or to a ferrous complex with a neutral cysteine ligand (RSH, i.e., an L neutral ligand) instead of a cysteinato ligand (RS$^-$, an anionic X ligand). The protonation of the proximal cysteine would give rise to a cytochrome having a Soret band at 420 nm, excluding the hypothesis of a protonated sulfur atom, but extended Hückel calculations[89] and data on model systems[90,91] suggested that a negative charge exists on intermediate **C**. This negative charge is delocalized over the whole prosthetic group, including the sulfur atom, and probably has a key role in the heterolytic cleavage of the O−O bond of the ferric-hydroperoxo complex leading to the high-valent iron-oxo species. The cysteinato sulfur atom is hydrogen bonded to the amide proton of three amino acids in P450$_{cam}$.[88] For simplification, the negative charge is not explicitly indicated on intermediates **C**−**E′** in Figure 7, like in any other textbook on cytochrome P450, but this charge is likely to play a key role in the increase of the electron density of the iron-dioxygen intermediate. The representation of this negative charge has already been discussed (see also section 6.1).[7] The key role of the cysteinato ligand has been confirmed by site-directed mutagenesis; the Cys375His mutant of P450$_{cam}$ has a poorer substrate affinity than the wild-type cytochrome. In addition, the proximal ligand strongly facilitates the O−O bond cleavage of the iron-peroxo intermediate.[92]

The species **A**−**C** were calculated by theoretical methods. Harris and Loew[93] studied the resting state for P450 using an early phase of the QM/MM method that relied on a semiempirical QM method. They found that only with inclusion of an electrostatic field of the protein, the ground state of **A** is the low-spin doublet state, which was found to lie −1.6 kcal mol$^{-1}$ lower than the sextet high-spin state. The authors concluded that the low-spin ground state is due to the electric field of the protein and is not an intrinsic feature of the water complex. Some support for this conclusion was provided by synthesis of a model ferric water complex with a thiophenoxo ligand[94] that exhibits a ground state with a sextet spin, whereas the doublet state becomes the ground state only when water is replaced by a ligand with a stronger field such as imidazole.

This conclusion was contested by Green,[95] who calculated the resting state of cytochrome P450 using DFT and the B3LYP functional. Green's model system, which had a water-ligated iron-porphyrin and a methyl mercaptide proximal ligand, led to the conclusion that the doublet state is an intrinsic property of the resting state of P450. An early DFT study by Shaik et al.[96] used the pure functional BP86 and partial geometry optimization. The ground state was found to be a doublet state that existed in two conformations; in the "upright" conformation, the water molecule is perpendicular to the porphyrin ring, while in the "tilted" conformation the water molecule sits parallel to the ring and forms hydrogen bonds to the nitrogen atoms of the porphyrin. The water−porphyrin hydrogen bonds were found to stabilize the tilted complex by about 6.6 kcal mol$^{-1}$. The present B3LYP/LACVP(Fe),6-31G(H,C,N,O,S) calculations of Shaik and de Visser,[72] shown in Figure 8, support this conclusion but show that after geometry optimization the energy differences are small,

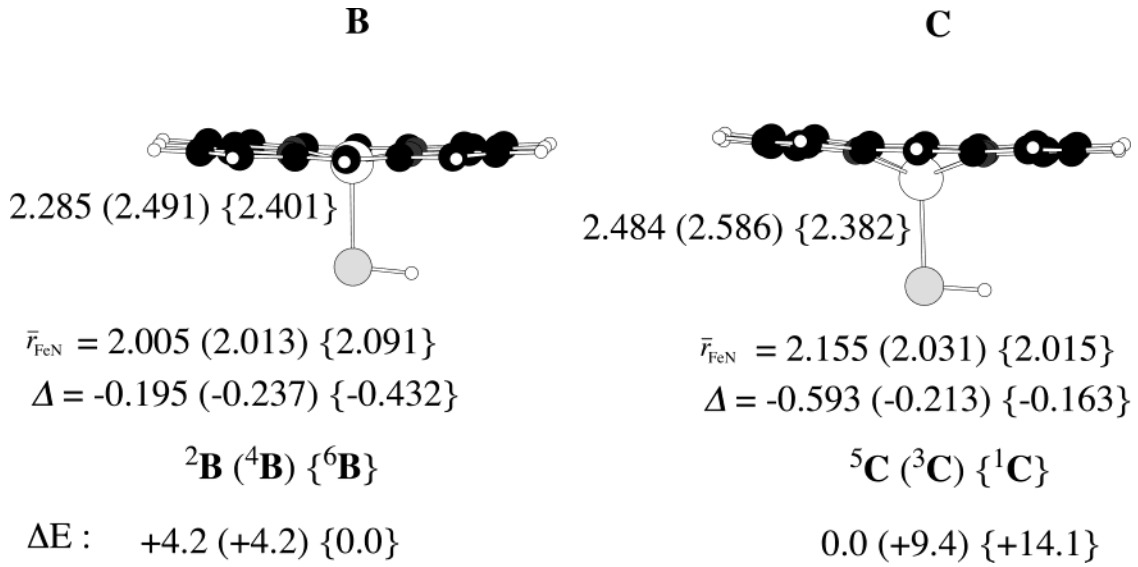


**Figure 9.** DFT geometries of the pentacoordinate Fe(III) complex (**B**) and the reduced Fe(II) complex (**C**), in their various spin states that are indicated by the superscripts. $\Delta E$ is in kcal/mol.

ca. 1.1 kcal mol$^{-1}$. Clearly, therefore, DFT calculations indicate that the resting state has an intrinsic preference for a tilted conformation, due to the propensity of the water ligand to undergo hydrogen bonding with a suitable H-bond acceptor. Within the protein pocket, this interaction can be supplied by the protein side chains that will stabilize the upright conformation, which might become the ground state or at least be in equilibrium with the tilted conformer. A QM/MM study using the BP86 functional for the QM subsystem was performed by Scherlis et al.[97] using X-ray data without geometry optimization. The studies confirm the previous DFT findings, that the doublet state is indeed the ground state. However, the study started with the upright conformer, so that the conformational question is still open. Future QM/MM calculations with full geometry optimization will be required to resolve this issue.

Shaik et al.[98] calculated the pentacoordinated ferric- and ferrous-porphyrin (**B** and **C**, Figure 7), using the B3LYP hybrid functional. Figure 9 provides optimized structures and energy separation of some of the lowest lying states. At the UB3LYP/LACV3P+* level of theory, the ground state of **B** was found to be the sextet state, whereas the quartet and doublet states were higher by 4.2 kcal mol$^{-1}$.

Reduction of $^6$**B** fills the $d_{x^2-y^2}$ orbital and generates a quintet ground state, $^5$**C** for the reduced pentacoordinated ferrous complex.[72,98] Another quintet state with a doubly filled $d_{xz}$ orbital lies only 2.1 kcal mol$^{-1}$ higher, while the triplet state lies 9.4 kcal mol$^{-1}$ higher. The singlet state lies considerably above the quintet ground state by 14.1 kcal mol$^{-1}$. Thus, basically theory converges to the experimental description of the initial species of the cycle. The next step is the binding of dioxygen to the ferrous state of this heme-enzyme.

## 5.3. Oxygen Binding Step (Formation of the Dioxygen Complex of P450 or Dioxy-P450)

Triplet dioxygen reacts with ferrous cytochrome P450$_{cam}$ with a second-order rate constant of 1.7 × 10$^6$ M$^{-1}$ s$^{-1}$ to produce a stable dioxygen adduct ($K_{aff}$ = 10$^6$ M$^{-1}$).[1] One electron from the iron(II) center and one from the triplet oxygen pair create an iron(III)−oxygen bond. This oxygen−iron complex (intermediate **D** in Figure 7) is relatively stable but can dissociate to an iron(III) and superoxide anion with a rate constant of 0.01 s$^{-1}$ at room temperature. Within the enzyme, the release of superoxide is followed by its disproportionation and generation of hydrogen peroxide, a source of harmful hydroxyl radicals. Such a step is called the "decoupling reaction" (or "uncoupling reaction") in the vocabulary of P450 enzymology.[99] The uncoupling reaction is more common in microsomal P450s than with bacterial enzymes. So, the intermediate **D** has to be regarded as an $\eta^1$-superoxide ion coordinated to an iron(III) center with an unpaired electron on the terminal oxygen atom. An O−O stretching vibration has been observed at 1141 cm$^{-1}$ in the resonance Raman spectrum of P450$_{cam}$ under catalytic conditions.[100] The Fe−O−O bending mode has been observed at 401 cm$^{-1}$ (for the Fe−O) by resonance Raman spectroscopy with an angle of approximately 125−130°.[101]

The electronic structure and the chemical properties of this dioxygen intermediate of P450 enzymes are different from the analogous stable ferrous-dioxygen states of molecular oxygen carriers such as hemoglobin and myoglobin. In these heme-dioxygen carriers, the reduced ferrous state is neutral with the proximal position being occupied by a histidine nitrogen atom, a ligand that is a poorer electron donor compared with the cysteinato ligand. In this respect, a proximal cysteine does not stabilize the Fe(II)-heme-dioxygen adduct as well as the histidine ligand does.

## 5.4. Transfer of the Second Electron to P450 (Formation of a Nucleophilic Iron-peroxo Species)

The second reduction step is the rate-determining step in many cytochrome P450s. This relatively slow step ($k$ = 17 s$^{-1}$ in cytochrome P450$_{cam}$) generates a

negatively charged iron(III)-peroxo complex (intermediate **E** in Figure 7; note that it is formally a dinegatively charged anion) which is probably quickly protonated at this stage to generate the iron(III)-hydroperoxo complex **E′**. The intermediate **E** with a red-shifted band at 350−450 nm and a split Soret band has been observed by UV−visible spectroscopy in a Asp251Asn $P450_{cam}$ mutant (the aspartic residue at 251 being replaced by an asparagine).[102,103] The aspartic residue plays a key role in the kinetics of the proton transfer to this intermediate **E**. In that mutant Asp251Asn, the rate-determining step is not the reduction step, but the proton transfer that generates an Fe−OOH entity (complex **E′** in Figure 7). The turnover rate for camphor hydroxylation of this mutant is 1−2 orders of magnitude slower than for native $P450_{cam}$.[103]

This unprotonated iron(III)-peroxo complex **E** is obviously an excellent candidate to explain some particular P450-catalyzed reactions that involve a nucleophilic oxidant intermediate. This is the case with both the oxidative decarbonylation of aldehydes and the final step of the aromatization of the cycle A of androstenedione in the biosynthesis of estrone (see section 7.8). The intermediate **E** is certainly a stronger nucleophile than **E′**, the corresponding protonated form $Fe^{III}$−OOH. However, both entities can be involved in these nucleophilic oxidations depending on the relative rates of the nucleophilic addition of the nonprotonated iron-peroxo to an electrophilic center of the substrate present in the active site and that of the protonation of intermediate **E**. If the proton transfer is faster than the nucleophilic attack, then P450−$Fe^{III}$−OOH is the only intermediate responsible for the nucleophilic oxidations observed with some particular substrates.

Theoretical calculations of **D** and **E** provide further support for the experimental characterization of these species. The first DFT calculations on **D** and **E** were reported by Harris and Loew[104] and Harris et al.,[105] using the BPW91 and BLYP pure density functionals; the two functionals gave virtually the same results, which are in good agreement with experimental data. The most stable form of ferrous dioxygen (**D**) is an end-on complex in accord with the experimental predictions, while the symmetrically bridged isomer was found to be much higher in energy, by ca. 28 kcal $mol^{-1}$. Reduction of **D** to **E** resulted in elongation of the Fe−O and Fe−S bonds, while leaving the O−O bond length intact, albeit the O−O bond order decreased from 1.20 to 0.87.[104] In agreement with its silent electron spin resonance (ESR) behavior, **D** was found to have a singlet ground state, with the triplet state only 1.1 kcal $mol^{-1}$ higher. By comparison, **E** was reported to have a doublet ground state with spin densities distributed over both oxygen atoms, in agreement with ESR data. Electronic spectra of both the ferrous and ferric dioxygen species, calculated with the semiempirical INDO/S/CI method,[105] exhibit, in agreement with experiment, a split Soret band. The corresponding Mössbauer parameters of **D** and **E** were calculated too, and those for **D** show a good fit to experimental data.

Figure 10 compares the structures of $^1$**D** and $^2$**E** (superscripts indicate the spin state) as derived by Shaik et al.,[72] using the B3LYP functional, vis-à-vis the BPW91 results of Harris et al.[105] in parentheses. The structures show a general fit, with the exception of $^1$**D** that appears more open in B3LYP compared with BPW91. Transformation of the DFT orbitals for $^1$**D** revealed that its electronic structure is the open-shell singlet $\delta^2 d_{xz}^2 \pi^*_{yz}{}^1 \pi^*_{OO}{}^1$ configuration. The $\pi^*_{yz}$ orbital has a strong mixing with the corresponding $\pi$ and $\pi^*$ orbitals of the dioxygen moiety, and as such, an appropriate description of $^1$**D** is a resonating mixture of the ferrous and ferric forms, $Fe^{II}O_2$ and $Fe^{III}O_2^-$. This conjugation requires that the dioxygen moiety, in the $Fe^{II}O_2$ form, will be in its singlet state, so that the empty $\pi^*$(O−O) orbital can mix with the doubly occupied $d_{yz}$ (Fe) orbital; as such there is a very low lying triplet state, $^3$**D**, only 1.1 kcal $mol^{-1}$ higher than $^1$**D**.

An orbital analysis reveals that the odd electron in $^2$**E** populates predominantly the $\pi^*$(O−O)-type orbital of the dioxygen ligand, as found by Harris et al.[105] In reasonable agreement with Harris and Loew,[104] the reduction $^1$**D** → $^2$**E** was found by Shaik and de Visser[72] to be endothermic, by 46.5 kcal $mol^{-1}$. However, in the presence of a medium modeled by a dielectric constant of $\epsilon = 5.7$,[72] the reduction energy becomes exothermic by 48.1 kcal $mol^{-1}$.

The effect of the protein environment on $^1$**D** and/or $^2$**E** was studied initially by molecular dynamics simulations of $P450_{cam}$ and $P450_{eryF}$, using MM/MD calculations.[106,107] The study showed that the ferrous dioxygen species is stabilized by a hydrogen bond from Thr-252.[106] In the case of the species $^2$**E** of $P450_{eryF}$, Harris and Loew[107] found that the distal oxygen of $^2$**E** is linked through a hydrogen-bonding network involving neighboring amino acids, such as Ala-241 and Ser-246, and several water molecules. This stable hydrogen-bonding network was implicated as the root of the double protonation that eventually converts **E** to the active species **F** (Figure 7).

## 5.5. First Protonation Step (Generation of a Nucleophilic Iron(III)-hydroperoxo Species)

Threonine-252 in $P450_{cam}$ plays a key role in the protonation of the iron-peroxo intermediate **E** (see Figure 11). The protonation of the terminal oxygen atom of intermediate **E** is not going to change the oxidation state of the iron center which is already III.

The first protonation produces a P450−$Fe^{III}$−OOH intermediate which can behave as a nucleophile (see above for the discussion on the reduced nucleophilicity of this protonated form compared to the corresponding nonprotonated species, intermediate **E** in Figure 7). The close interaction of Thr-252 with Asp-251 allows two fast proton transfers from protonated forms of Lys-178 and Arg-186. When Thr-252 is replaced in $P450_{cam}$ by an alanine, the mutant enzyme produces hydrogen peroxide and water molecules in large excess compared to the expected camphor hydroxylation (the so-called uncoupling reactions).[108,109]

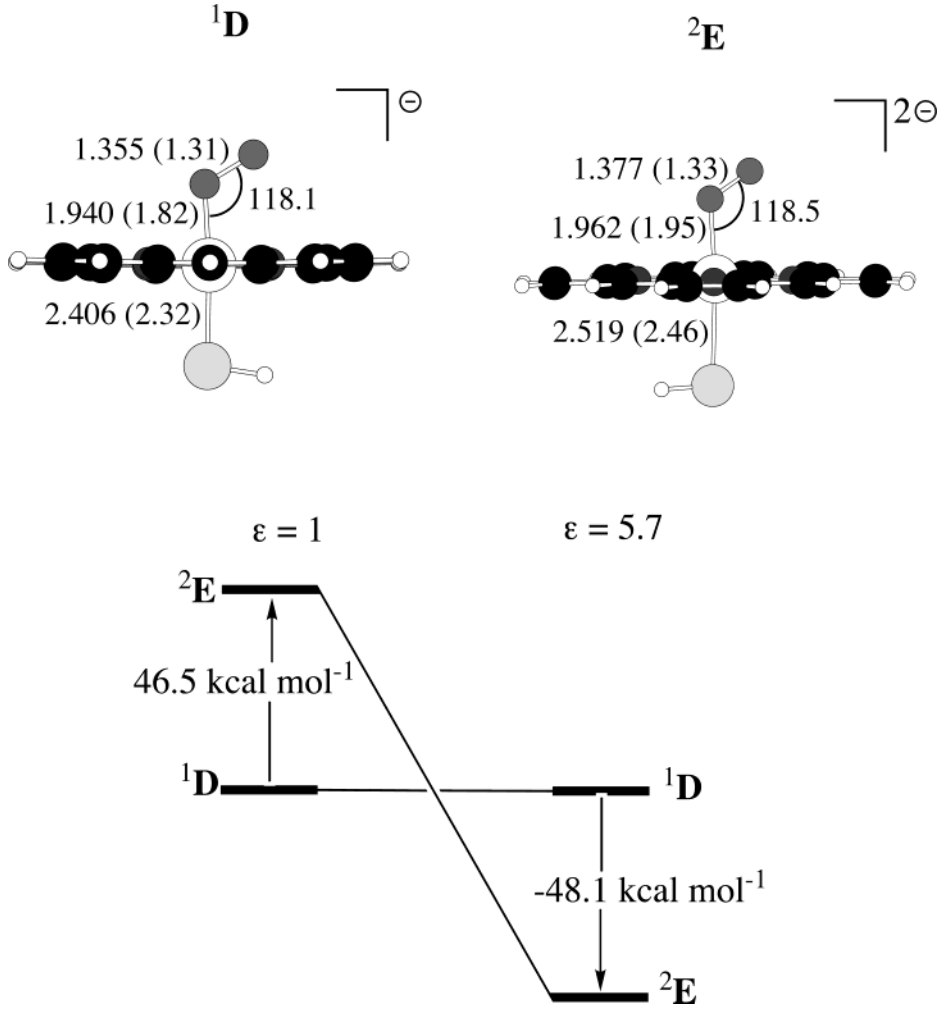


**Figure 10.** DFT geometries of the singlet-state $Fe^{II}-O_2$ complex ($^1$**D**) and its reduced form ($^2$**E**). In parentheses are the BPW91 values obtained in ref 104. Out of parentheses are the B3LYP values from ref 98. The energy digram underneath the drawings shows the effect of a dielectric constant on the B3LYP reduction energy $^1\mathbf{D} \rightarrow {}^2\mathbf{E}$.

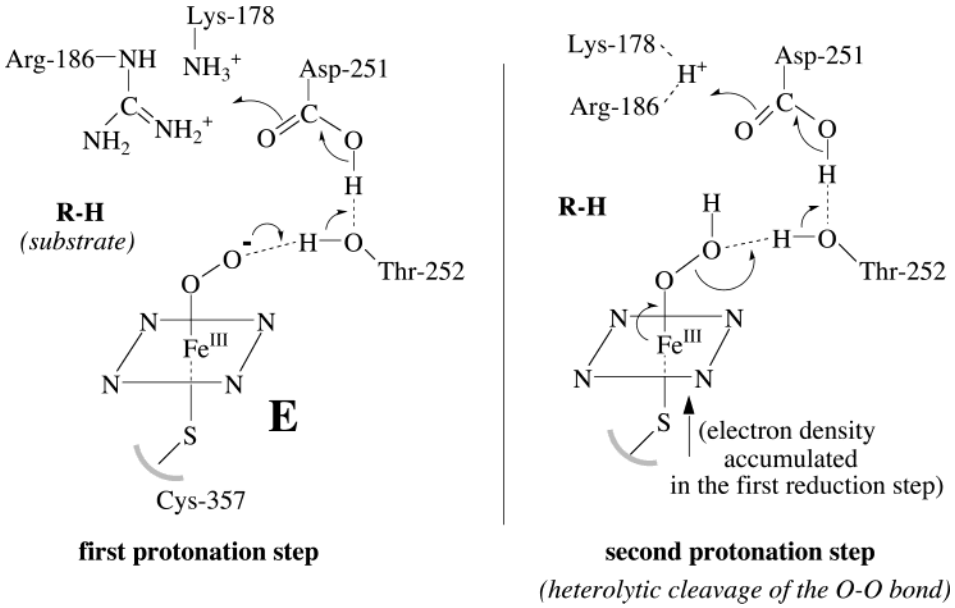


**Figure 11.** Essential role of Thr-252 and Asp-251 residues in the proton delivery to the iron−dioxygen intermediate during the catalytic cycle of cytochrome $P450_{cam}$. Reprinted with permission from ref 7. Copyright 2000 Springer-Verlag Heidelberg.

The essential role of the Asp-251 in the proton transfer to the $Fe^{III}-O-O^-$ intermediate **E** has been studied in cytochrome $P450_{cam}$ using site-directed mutagenesis, crystallography, and kinetic solvent isotope effects.[59] The turnover rates of the Asp251Asn mutant in various proton−deuterium mixtures have

been determined. The kinetic solvent isotope effect is larger, with a value of 10, compared to 1.8 for the wild-type enzyme. The hydrogen-bond network created with the aspartic residue is broken in the mutant, and the dioxygen adduct is more open to bulk water molecules.

This threonine residue is highly conserved among cytochrome P450s (see the similar role of Thr-268 in cytochrome $P450_{BM-3}$).[110] In this latter case, it should be mentioned that a Thr-268-Ala mutant still has a low oxygenase activity (this is not the case for $P450_{cam}$).

As shall be seen in sections 6 and 7, the same $Fe^{III}$—OOH intermediate **E′**, mainly considered as a strong nucleophile, has been proposed by Newcomb, Coon, and some other colleagues as being an electrophilic intermediate in olefin epoxidations mediated by cytochrome P450.[111,112]

## 5.6. Second Protonation Step (Generation of an Electrophilic Iron-oxo Species)

As in the case of the first protonation step, the second proton which is necessary to produce an iron(V)-oxo species (intermediate **F** in Figure 7) and a water molecule after protonation of the terminal oxygen atom of the $Fe^{III}$—OOH entity **E′** is also provided by Thr-252 and involves the contribution of Asp-251, Lys-178, and Arg-186. This protonation is probably assisted by the negative charge accumulated on the proximal cysteine in the first reduction step (see section 5.2), which is one of the driving forces of the heterolytic cleavage of the O—O bond leading to the electrophilic high-valent Fe(V)-oxo species **F**.[92] Since the protonation steps are faster than the second reduction step in wild-type P450s, no lifetimes can be determined for the $Fe^{III}$—OOH and Fe(V)═O species; both are very short-lived entities. The hydroxylation product is observed very quickly after the injection of the second electron.[113] This is the reason the exact nature of the hydroxylating species in cytochrome P450 is still a matter of debate. The very elegant work on $P450_{cam}$ crystals by Schlichting et al.[114] has provided in a single study the 3D structures of different intermediates of the catalytic cycle of this cytochrome P450, including possibly the high-valent iron-oxo species having an iron—oxygen distance of 1.65 Å (Figure 12).

However, this latter structure has been questioned since kinetic data are suggesting that the iron-oxo will not be able to accumulate before the oxygen transfer step.[113] This argument may not be entirely applicable to this particular protein, which crystallizes in a monoclinic space group with two protein molecules within the asymmetric unit that are connected to each other via a potassium ion. Such strong interactions between the two proteins produce a real constraint for the camphor itself, which was kept away from the ideal position required for an oxygen transfer step. This may explain why the high-valent iron-oxo could have accumulated in this particular type of P450 crystals.[115]

It has been possible to generate reactive iron—oxygen species with cytochrome P450 enzymes by using peroxides or single oxygen atom donors, supporting that the reactive species **F** is, in fact, a high-valent iron with only one oxygen atom linked to it.[74] This so-called "peroxide shunt" opened successfully the modeling of cytochromes P450 with single oxygen atoms donors such as PhIO, NaOCl, $KHSO_5$, $H_2O_2$, and so forth.[74−80]

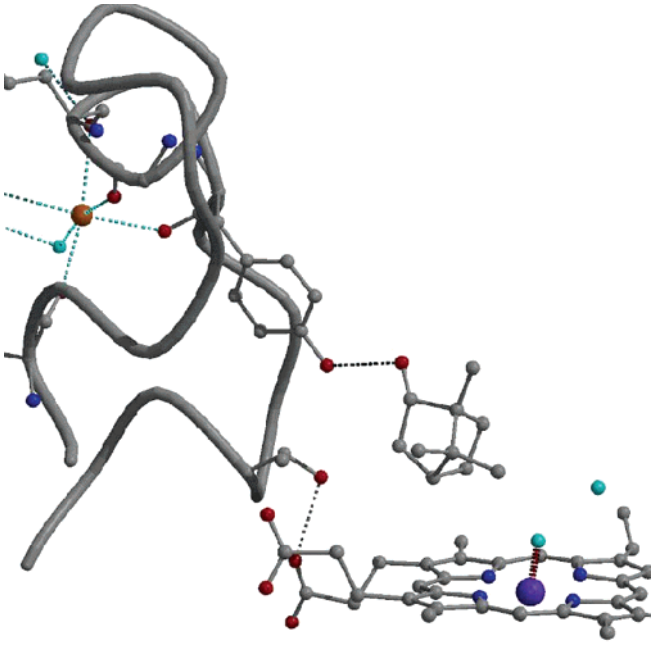

**Figure 12.** X-ray structure of the high-valent iron-oxo species in cytochrome P450. This structure has been kindly provided by Dr. Ilme Schlichting (see ref 114).

Theory has also addressed the ferric hydroperoxo species **E′**, called sometimes compound 0 (Cpd 0), and its protonation to yield **F**. DFT calculations, in Figure 13, show that ferric peroxide, Cpd 0, is a fairly strong base with a high proton affinity.[98,104,116] In both studies, **E′** was found to be the stable isomer by ca. 18.4[104] (23.3[116]) kcal $mol^{-1}$, relative to the isomer with a proton on the proximal oxygen, and to possess a doublet ground state, labeled $^2\Pi_{yz}$ ($Fe^{III}$),[116] a symbol that denotes its singly occupied $\pi^*_{yz}$ orbital. An interesting feature of the ferric peroxide is the internal hydrogen bond between the hydroxo proton and the nitrogen of the porphyrin ring.[116] Application of a weakly polar environment simulated by a dielectric constant of $\epsilon = 5.7$ further shortened the Fe—S bond and the OH---N hydrogen bond.[116] Whether this hydrogen bond will or will not survive in the protein pocket is an interesting question that will await QM/MM calculations.

As mentioned already, the protonation mechanism is thought to occur from a hydronium ion sequestered in $P450_{cam}$ by Asp-251 and Thr-252.[103] A recent DFT study of Kamachi and Yoshizawa[117] used a model similar to the one proposed by Vidakovic et al.,[103] with two water molecules sequestered between the carboxylate end, $CO_2^-$, of Asp-251 and the hydroxyl side chain of Thr-252, as shown in Figure 14. The protonation starts with a proton transfer from Thr-252 to the distal oxygen of Cpd 0, followed by the departure of a water molecule that is trapped through hydrogen bonding to the Thr-252 anion and the array of the two waters that are linked by hydrogen

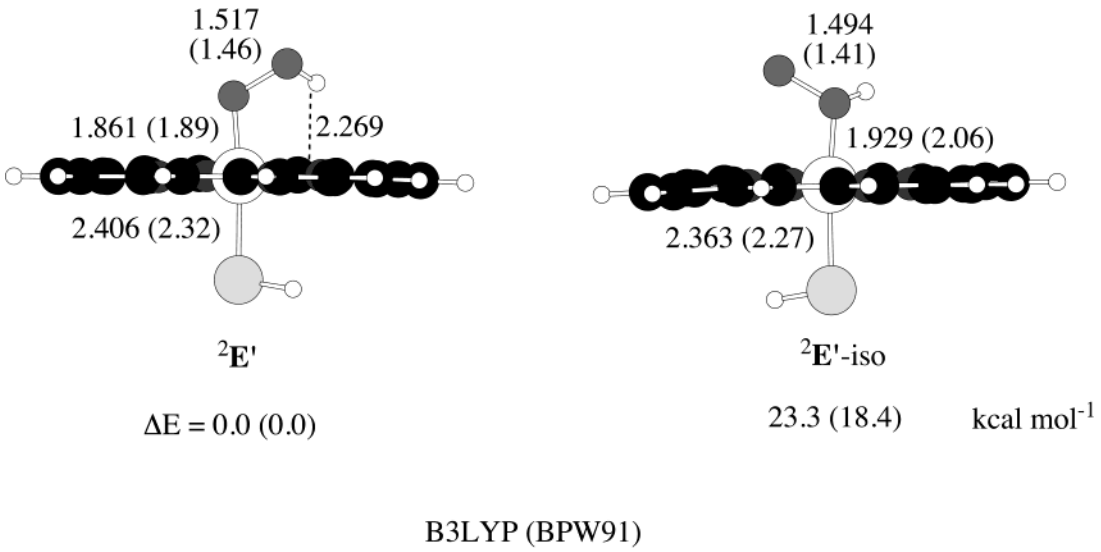


**Figure 13.** DFT geometries of the $Fe^{III}$−OOH intermediate, $^2$**E′**, and its isomer, $^2$**E′**-iso. Values in parentheses are BPW91 values from ref 104; out of parentheses are B3LYP values from ref 116.

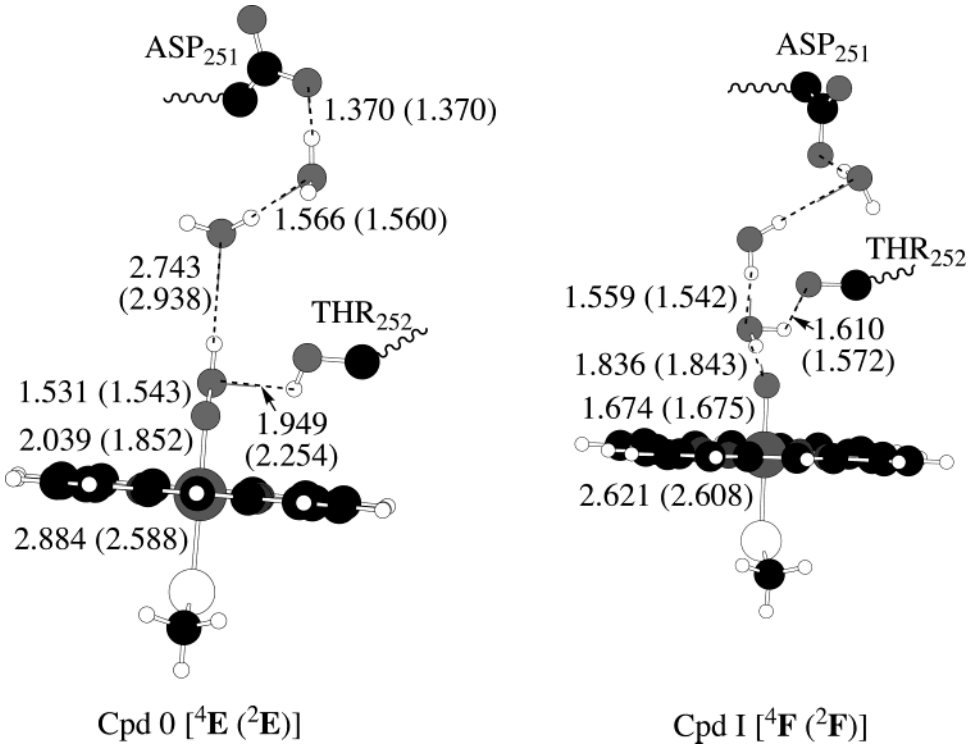


**Figure 14.** DFT geometries and mechanisms for the protonation mechanisms **D** → **E** → **F**, adapted from ref 117.

bonding to the Asp-251 anion. This mechanism predicts that the protonation of Cpd 0 and formation of **F** is exothermic by 13.1 and 5.5 kcal $mol^{-1}$ for the quartet and doublet states, respectively. The entire protonation process from $^{2,4}$**E** to $^{2,4}$**F** by this Asp-251−Thr-252 machinery was calculated to be exothermic by 74.6 kcal $mol^{-1}$ for the doublet state and 55.6 kcal $mol^{-1}$ for the quartet state.[117] However, the barrier was not calculated for this process. Alternatively, the protonation mechanism may be nascent from a hydrogen-bonding array of water molecules similar to the one discussed by Gualar et al.[118] and Harris[119] for the conversion of **D** to **E**. This protonation mechanism is significantly gentler and less exothermic. Taken together, the two mechanisms suggest strongly that there should exist a variety of alternative protonation mechanisms that eventually lead to species **F**.

In principle, protonation of Cpd 0 can occur on either the proximal or the distal oxygen of the complex. Distal protonation results in the splitting of a water molecule and generation of Cpd I (**F**, see below for a comment on this manner of naming **F**). Alternatively, proximal protonation gives a hydrogen peroxide complex. The latter complex is able to release $H_2O_2$ and return to the resting state by coordination to a water molecule, thereby leading to decoupling. Energetically, the formation of the hydrogen peroxide complex from Cpd 0 is only 6 kcal $mol^{-1}$ less exothermic than that of **F** from Cpd 0,[104] such that the decoupling reaction is a serious competitor with the productive process that leads to **F**.

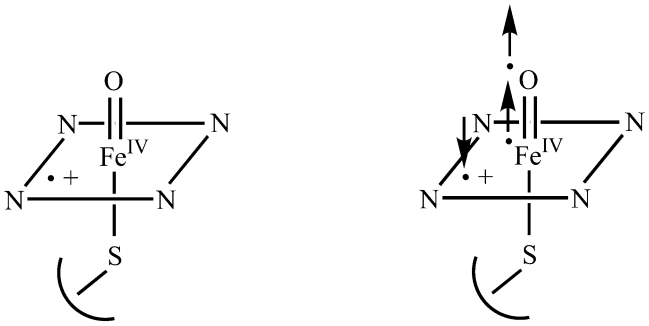

**F iron(IV)-oxo porphyrin-radical cation**

**Figure 15.** Two cartoons representing different electronic aspects of the iron(V)-oxo species, **F**. On the left, the doubly bonded FeO moiety represents the fact that like in $O_2$, here too the bond order is 2. However, like in $O_2$, here too the FeO moiety has two triplet coupled electrons. This is represented on the right, where we added the spins of the unpaired electrons in the FeO and porphyrin moieties. The effective oxidation state of V is the combination of Fe(IV) and $Por^{\bullet+}$.

Not much is yet known about this competition. Clearly, a future theoretical study is required to explore alternative protonation pathways that can reveal the intricate behavior of the wild-type and mutant enzymes.

## 5.7. Properties of the Iron-oxo Species

In this second protonation step, the formal oxidation state of the iron center increases from III to V with the formation of the iron-oxo species **F** (Figure 15).

As reasoned by Shaik et al.,[120] using bonding principles, the Fe═O moiety of this species is a triplet state, much like the ground state of the dioxygen molecule. In addition, there is an odd electron, formally on the porphyrin, making the macrocycle a radical-cation species. The three electrons are, in turn, coupled into two closely lying spin states: one is a ferromagnetic state with all three electrons having the same spin, and one an antiferromagnetic one, where the spin of the electron in the porphyrin is opposite to the spins on the Fe═O moiety; the latter is the ground state and is shown in the drawing in Figure 15. Such Fe(IV)-oxo radical-cation species have been fully characterized in heme-peroxidases: these entities are the so-called compound I (see refs 121 and 122 for reviews on peroxidases). Initially, the name compound I was only used for peroxidases, but recently several authors have been using it for naming the high-valent iron species of P450 enzymes.

Within this review article, the active species of P450 resulting from the heterolytic cleavage of the O−O bond of $Fe^{III}$−OOH by protonation will be named compound I (Cpd I) or iron(V)-oxo, this latter description being useful for electron counting and for emphasizing that this active species corresponds to a two-electron oxidation with respect to the resting state Fe(III) of the enzyme. This will become clearer in the theoretical description of Cpd I. An iron(III)-oxene has been used as another possible resonance

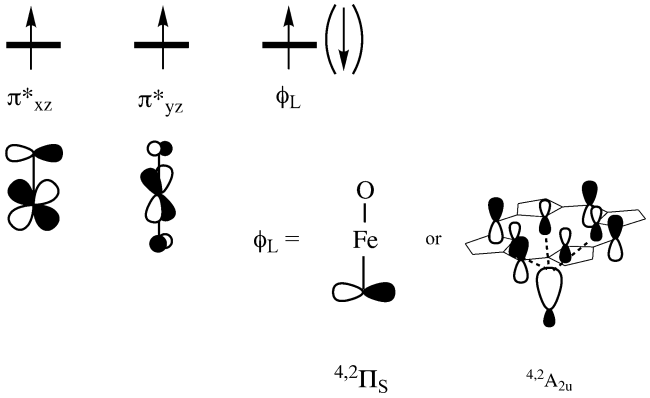

**Figure 16.** The three unpaired electrons of the iron-oxo species occupy $\pi^*$ orbitals and a ligand orbital, $\phi_L$. Some calculations suggest that $\phi_L$ is virtually a pure sulfur orbital; others lead to a porphyrin $a_{2u}$−sulfur combination orbital. QM/MM calculations (ref 132) show that the latter is the correct state.

form for the representation of the active electrophilic species of P450 (with this representation, the two electrons of the oxo ligand are back on the iron, thus corresponding formally to the coordination of an atomic oxygen to an iron(III) center). However, such electronic structure has not been observed when oxidizing iron(III) porphyrins with oxygen atom donors. In all cases, the oxidation state of the iron center is at least IV as determined by magnetic data on isolated complexes; see refs 74 and 78−80. Consequently, there is no longer a reason to use the name "iron-oxene" that has been utilized in 1960−1975 to describe the reaction iron−oxygen species of P450 enzymes.

Detailed theoretical calculations support the above picture of Cpd I as a species having three unpaired electrons coupled to two closely lying spin states. Initial DFT studies of Cpd I were done for the bare molecule, that is, in vacuum or gas phase conditions, and showed sensitivity to the thiolate used to model the cysteinate ligand, as well as to the functional used to calculate the species. Nevertheless, all the calculations agreed that the species is a triradicaloid with three singly occupied orbitals. Two of these are the $\pi^*_{xz}$ and $\pi^*_{yz}$ orbitals, depicted below in Figure 16, which appear in all calculations including the CASSCF study of the reduced Cpd I (so-called Cpd II).[123] However, the various studies differ significantly in the description of the third orbital, depending on the manner in which the study models the thiolate proximal ligand.[8,70−72,104,124−129] The studies, especially those using mercaptide[128,129] or cysteinate anion devoid of its internal hydrogen bonding,[129] predicted that the third singly occupied orbital is the $p_\pi$ lone pair orbital on sulfur leading to a $^{4,2}\Pi_S$ ($\pi^*_{xz}{}^1$ $\pi^*_{yz}{}^1$ $\pi_S{}^1$) state (Figure 16) with spin density almost exclusively on the sulfur while the porphyrin is closed shell. Other studies[125,126] that used $HS^-$ or cysteinate with its internal hydrogen-bonding interactions found that the third singly occupied orbital is $a_{2u}$ strongly mixed with the sulfur $\sigma$-hybrid (see Figure 16); this occupancy leads to $^{4,2}A_{2u}$ states, with spin density distributed over the porphyrin and sulfur. It was found[125,130] that with $HS^-$ or cysteinate as ligands, the $^{4,2}\Pi_S$ electronic states are more than 5 kcal $mol^{-1}$

higher in energy than the $^{4,2}A_{2u}$ state, whereas with mercaptide all the four states were condensed to within 1 kcal mol$^{-1}$. This difference is not only academic. Had Cpd I been a $^2\Pi_S$ ground state, it would have been red, as the Cpd II species with closed shell porphyrin, while if the ground state had been $^{4,2}A_{2u}$ type, the compound would have been green.

These considerations and other findings prompted a DFT study of the effect of the NH---S hydrogen bonding and the protein electric field on the nature of Cpd I, using simple modeling of these effects.[126,131] Inclusion of these effects showed that the ground state of Cpd I for P450 is $^{4,2}A_{2u}$, where the third electron resides in an orbital which is a combination of porphyrin $a_{2u}$ and the $\sigma$-hybrid of the sulfur, as depicted in Figure 15. Recent QM(DFT)/MM calculations of Cpd I of $P450_{cam}$[132] retrieved the important NH---S hydrogen bonds, donated to the sulfur by Leu-358, Gly-359, and Gln-360, and assigned Cpd I in a definitive manner as the doublet $^2A_{2u}$ state with a very closely lying $^4A_{2u}$ state; the same QM/MM description was found irrespective of whether the proximal ligand was $HS^-$, $CH_3S^-$, or a more extensive chunk of the cysteine loop. Thus, in accord with experimental results on the analogous Cpd I species of the enzyme chloroperoxidase,[133] Cpd I of $P450_{cam}$ is a doublet state and it corresponds to the "green species". Having this definitive theoretical assignment, we can return to deal with the question of the best cartoon that describes the species and with the oxidation state of the iron in it, as depicted above in Figure 15. The FeO moiety of the species has the same bonding as the $O_2$ molecule (one filled $\sigma$-FeO orbital, two filled $\pi$-FeO orbitals, and two singly occupied $\pi^*$-FeO orbitals), and as such the FeO bond order is two. For this reason, we used in Figure 15 the doubly bonded cartoon, Fe═O, that signifies this bond order. In addition, since the two $\pi^*$ electrons maintain a triplet couple, we added in Figure 15 the arrows for two triplet electrons on the FeO moiety. With this electronic structure, Fe has formally four electrons (two in a $\delta$ orbital, the pure $d_{x^2-y^2}$, and two in the $\pi^*$-FeO orbitals that are considered as the $d_{xz}$ and $d_{yz}$ iron orbitals) and is hence Fe(IV). The third unpaired electron of Cpd I is largely on the porphyrin moiety, which appears therefore as radical-cationic species $Por^{\bullet+}$. Thus, Cpd I contains two oxidation equivalents higher than the resting state and can be described either as $Por^{\bullet+}Fe(IV)$-oxo or simply as iron-(V)-oxo.

In the next section, we summarize the role of chemical model molecules used to understand the nature of reactive species generated during the catalytic cycles of these monooxygenases.

## *6. Role of Chemical Models of Cytochromes P450 Used To Understand the Nature of the Reactive Species Generated during the Catalytic Cycle of These Monooxygenases*

For three decades, synthetic metalloporphyrin complexes have been made and used as models of the iron(III)-peroxo and the iron(V)-oxo species, which are generated during the catalytic cycle of cytochrome P450.

### 6.1. Reactivity of Iron(III)-peroxo Porphyrin Complexes

The nucleophilicity of iron(III)-peroxo porphyrin complexes has been demonstrated by Valentine and co-workers,[134−137] using electron-deficient olefins (unsaturated ketones or quinones). The peroxo complex $[Fe^{III}(TMP)O_2]^-$ reacts quickly with menadione (2-methyl-1,4-naphthoquinone) to produce the corresponding 2,3-epoxide, whereas no reaction was observed with cyclohexene.[134] In contrast, such an electron-rich cis olefin is easily epoxidized by single oxygen atom donors (iodosylbenzene, hypochlorite, monopersulfate) using metalloporphyrin catalysts.[74−80]

Replacement of the electron-donating porphyrin ligand by an electron-withdrawing porphyrin containing perfluorophenyl substituents at the meso positions caused a reduction of the nucleophilicity of the corresponding iron-peroxo. But the presence of an axial ligand can restore its reactivity by opening the side-on peroxo to a more reactive end-on structure.[135] The peroxo complex $[Fe^{III}(TMP)O_2]^-$ is also able to mimic the deformylation step of aromatase.[137]

What are the necessary modifications that are required to enable the iron-peroxo porphyrin complex to epoxidize electron-rich olefins? To remove electron density from the iron-peroxo, highly electron-deficient porphyrin ligands[138,139] should be used and, if possible, the proximal ligand should be made electron-withdrawing. These properties are precisely the opposite of the electronic properties possessed by the prosthetic group of cytochrome P450: the natural protoporphyrin-IX is a very good electron reservoir, and the proximal cysteinate ligand is a good electron donor as well. *Both factors work against an electrophilic behavior of iron-peroxo intermediates in cytochrome P450s; instead they would argue for a nucleophilic iron-peroxo intermediate.*

Non-heme metal-peroxo complexes that are able to react with electron-rich olefins (di- or trisubstituted aliphatic olefins) have electron-withdrawing ligands in their coordination sphere. In the case of iron polypyridine complexes, many oxygenation reactions that have been originally claimed as being due to an iron-peroxo reactive intermediate are now reconsidered as being due to high-valent iron-oxo species (using oxygen-labeled studies).[140,141]

### 6.2. Characterization and Reactivity of High-Valent Metal-oxo Porphyrin Complexes

The first high-valent iron-oxo porphyrin complex has been isolated by Groves et al. by oxidation at low temperature of Fe(TMP)Cl with *meta*-chloroperbenzoic acid.[142] The resulting "green" compound is an iron(IV)-oxo complex with a radical-cation on the porphyrin ring resembling compound I of heme-peroxidases (see refs 74, 75, and 80 for review articles on the preparation and characterization of high-valent iron-oxo porphyrin complexes). Many other compound I models have been obtained with various substituted metalloporphyrins. However, in all these

model systems, the exchange between the spin $S = 1$ of the oxo-ferryl group with the spin $S' = 1/2$ of the porphyrin radical-cation was found to be ferromagnetic in contrast to the weak ferromagnetic or antiferromagnetic coupling usually observed with Cpd I derivatives.[143,144]

Up to now, a genuine iron(V)-oxo porphyrin complex has not been identified. This might be related to the fact that most of the pentacoordinated high-valent iron-oxo complexes isolated up to now have no proximal anionic ligand as in cytochrome P450 or a neutral one as in horseradish peroxidase which has a proximal histidine. The P450 models with a proximal sulfur-containing ligand appear to be more reactive than the corresponding models without this cysteine analogue. They might be the only suitable P450 models which in the future should allow the isolation of a true perferryl complex.[145,146] Oxygen-containing proximal ligands reduce the oxygenase activity of synthetic metalloporphyrins compared to the corresponding complexes with nitrogen-containing axial ligands.[147]

Synthetic manganese porphyrins have also been extensively used as P450 models, and both Mn(IV)-oxo and Mn(V)-oxo porphyrin complexes have been characterized recently (see ref 148 for an early attempt). A (Por)Mn(IV)═O complex has been characterized by X-ray absorption spectroscopy.[149] The Mn−O bond distance is 1.69 Å, and the complex has an $S = 3/2$ spin state corresponding to a high-spin $d^3$ configuration.

More recently, it has been possible to characterize by stopped-flow spectrophotometry a manganese(V)-oxo porphyrin complex generated with hypochlorite or monopersulfate.[150] This (TMPyP)(X)Mn(V) ═O exhibits a Soret band at 443 nm between that of (TMPyP)Mn(IV) ═O (428 nm) and Mn(III)(TMPyP) (462 nm). The half-lifetime of this Mn(V)-oxo is 25 ms at room temperature at pH 7.4. When the methyl groups of the pyridinium substituents of the porphyrin are in ortho positions instead of para, then the manganese(V)-oxo porphyrin complex has a longer lifetime (a few minutes) so that the acquisition of a diamagnetic proton NMR spectrum is possible.[151] This fact supports a low-spin $d^2$ electronic structure for the ground state of this manganese(V)-oxo complex. As proposed recently based on DFT calculations,[152,153] in addition to the singlet Mn(V)═O state, one should consider also higher spin states with Mn(IV)═O coupled to a porphyrin radical-cation situation. The state ordering depends on the porphyrin substituents and the proximal ligand.

## 6.3. Oxo–Hydroxo Tautomerism with Water-Soluble Metalloporphyrins

When not characterized by structural studies, high-valent metal-oxo porphyrin complexes can be studied via product analyses and labeling experiments. Such O-labeling experiments related to the oxygenation reactions mediated by these high-valent metal-oxo complexes will be reviewed in the present section. Most of the studies on P450 models have been performed with hydrophobic metalloporphyrins and an organic oxidant (PhIO) or water-soluble oxidants

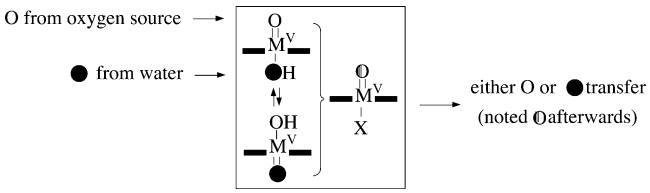


**Figure 17.** The oxo−hydroxo tautomerism mediates that the oxygen incorporated into the oxidation product consists of 50% from the primary oxidant and 50% from water. X = hydroxo ligand. Reprinted with permission from ref 7. Copyright 2000 Springer-Verlag Heidelberg.

(NaOCl, $KHSO_5$, $H_2O_2$, etc.).[74,75,79] With these catalysts operating in organic solvents, the oxygen atom incorporated during the oxygenation reaction (hydroxylation or epoxidation) originates from the oxidant.[74,154,155] But when these metalloporphyrin-catalyzed oxygenations are performed in aqueous solvents, such metal-oxo species are able to transfer an oxygen atom coming either from the oxygen source or from bulk water.[156−161] Because the intermolecular exchange of metal-oxo with bulk water is slow, an intramolecular exchange of labeled oxygen atoms via the so-called *oxo−hydroxo tautomerism* has been proposed.[78,156,159] This mechanism involves a rapid shift of two electrons and one proton from a hydroxo ligand (electron-rich ligand formed by deprotonation of an aqua ligand) to the trans oxo species (electron-poor ligand) leading to the transformation of the hydroxo ligand into an electrophilic oxo entity on the opposite side of the initial oxo (see Figure 17 for a representation of this tautomeric equilibrium).

The rate of this equilibrium depends on the experimental conditions (pH, temperature, composition of the medium, nature of the axial ligands, etc.). Based on the observed label distribution in oxidation products modulated by this oxo−hydroxo tautomerism, it is possible to unambiguously distinguish between oxygenation reactions occurring (i) via an O-transfer from a high-valent metal-oxo complex or (ii) via an autoxidation mechanism in metalloporphyrin-catalyzed oxygenations carried out in the presence of $H_2{}^{18}O$ (see ref 157 for a review on this controversial debate). The main consequence of the oxo−hydroxo tautomerism is the incorporation within the substrate of an oxygen atom coming from either the oxidant or from bulk water, respectively in the ratio 1:1 (Figure 17). Other recent reports support the concept of oxo−hydroxo tautomerism, not only with metalloporphyrins[150,158−164] but also with non-heme oxygenation catalysts.[140]

An example of oxo−hydroxo tautomerism has also been identified in the oxidation of deoxyribose C−H bonds of DNA by Mn(TMPyP)/$KHSO_5$.[165] Hydroxylation at carbon-1′ of deoxyribose gives 5-methylene-2-furanone (5-MF) in several steps, as final sugar residue. In the presence of labeled $H_2{}^{18}O$, 50% of oxygen incorporated in 5-MF comes from the primary oxidant ($^{16}O$ from $KHSO_5$) and 50% from the solvent ($^{18}O$ from $H_2{}^{18}O$), supporting a metal-oxo-mediated DNA cleavage with an oxo−hydroxo tautomerism to explain the $^{18}O$-incorporation in the oxidation product of DNA sugar.

The oxo−hydroxo tautomerism emphasizes in fact the role of the axial ligand trans to a high-valent

metal-oxo porphyrin species. This in turn suggests that the proximal cysteinato ligand in cytochrome P450 enzymes plays a key role as an electron shuttle during the oxidation of the iron center.[78] This electron-releasing property of the thiolate ligand has gained theoretical support from recent DFT calculations.[98]

The current mechanistic proposals for the different reactions catalyzed by cytochromes P450 will be discussed in the following sections.

## 7. Mechanistic Proposals for Different Reactions Catalyzed by Cytochromes P450

The mechanistic proposals that will be presented below reflect the views of molecular chemists on cytochrome P450 enzymes, and they are not a simple compilation of literature data. The key role of cytochrome P450 enzymes in drug metabolism will not be discussed extensively in the present review (see refs 1−9 for books or reviews concerning that field), but a selection of P450-catalyzed reactions will be presented in detail in order to achieve a "molecular view" of the mechanisms of the catalytic cycles of these unique monooxygenases that are able to perform such different reactions (oxygenations, dealkylations, aromatic oxidations, dehalogenations, etc.), essential for the development of life.

### 7.1. Hydroxylation of an $sp^3$ C–H Bond (Hydroxylase Activity of P450 Enzymes)

The insertion of an oxygen atom within the C−H of a saturated carbon atom is one of the most difficult reactions to achieve with a catalyst at room temperature. This is all the more difficult when the oxidant is molecular oxygen since customarily hydrogen peroxide or water is generated as a waste byproduct.

Two main mechanisms have been proposed and discussed depending on the nature of the substrate and on the enzyme itself: a cage-controlled radical mechanism (the "oxygen rebound" mechanism, see ref 74) or a concerted mechanism without formation of a radical intermediate based on the use of ultrafast "radical clocks" (see refs 112, 166, and 167 for reports on this aspect). Both possible reaction pathways are depicted in Figure 18. A third mechanism, called two-state reactivity (TSR)[130] was suggested by theory and will be discussed later.

Hydroxylation reactions catalyzed by P450s are not always stereospecific. The loss of stereochemistry has been shown with a tetradeuterated norbornane derivative and with many other substrates; the same type of stereochemical scrambling was observed when a synthetic Cpd I was used, thus showing that the iron-oxo species is the source of this loss of stereochemistry.[1,168] The partial loss of stereochemistry is easily explained by the oxygen rebound mechanism, if one assumes that the rate of the formation of the carbon−oxygen bond is very close to the rate of skeletal rearrangement (e.g., inversion) of the intermediate radical generated after abstraction of a H-atom by the high-valent iron-oxo species (see Figure 19).

The abstraction of a hydrogen atom by the active species of P450 is consistent with the high intrinsic

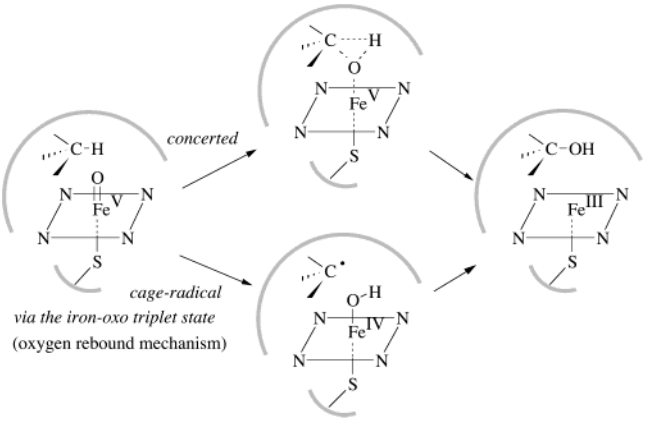


**Figure 18.** Two possible reaction pathways in hydroxylation reactions catalyzed by P450 enzymes: a concerted mechanism and a cage controlled radical pathway (the oxygen rebound mechanism). Reprinted with permission from ref 7. Copyright 2000 Springer-Verlag Heidelberg.

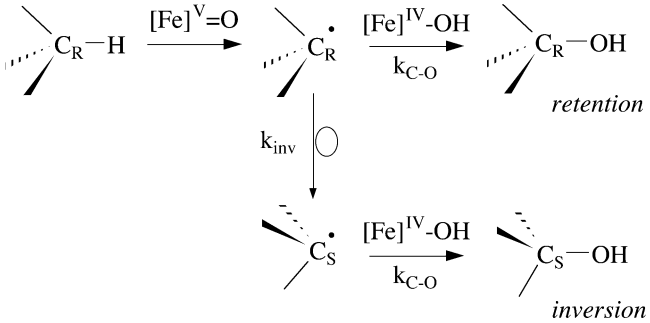


**Figure 19.** A mechanism for the possible loss of stereochemical configuration during hydroxylation reactions involving an oxygen rebound mechanism. Reprinted with permission from ref 7. Copyright 2000 Springer-Verlag Heidelberg.

isotope effects observed in hydroxylation reactions catalyzed by these heme-monooxygenases.[1,169,170] The $k_H/k_D$ values range from 5 to 12, depending on the substrates and the isoform of P450. In addition, the value of the intrinsic isotope effect for the hydroxylation process could be masked by the other enzymatic steps, reversible substrate binding, product release, and so forth. In fact, the kinetic isotope effect (KIE) values determined with P450 and *t*-BuO$^\bullet$ (a pure H-atom abstractor) in a series of different substrates are very similar, suggesting that both reagents have a H-atom transfer step in common.[170] However, if relative rates of product formation are masked by other steps in the enzymatic cycle, then linear free-energy relationship data obtained in intermolecular isotope effect studies must be interpreted with caution to avoid an overinterpretation of the nature of the oxygenating species in cytochromes P450. Clearly, to avoid the masking of relative rates in KIE studies, intramolecular KIE evaluations should be preferred and masking is significantly reduced when the used substrates contain hydrogen and deuterium bonded to the same carbon atom.[171] The kinetic isotope effect on the product distribution has been recently used to tentatively demonstrate that two different electrophilic oxidants (an electrophilic iron-hydroperoxo, **E′**, and an iron-oxo, **F**) are involved in P450-catalyzed hydroxylations (Figure 20).[172] However, even significant

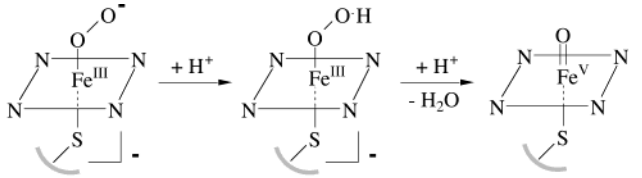


**Figure 20.** Formal descriptions of iron(III)-peroxo, iron(III)-hydroperoxo, and iron(V)-oxo species with indication of the negative charges. The roles "electrophile" or "nucleophile" are assigned according to the charge type. Reprinted with permission from ref 7. Copyright 2000 Springer-Verlag Heidelberg.

differences in product isotope effect data can be differently interpreted as shown by a recent theoretical treatment.[173]

At the outset, it is important to emphasize that the involvement of species other than Cpd I has to be considered very carefully, in view of the fact that *all the preceding species carry negative charge, which makes them good nucleophiles and good bases but not electrophiles* (see Figure 20). Discussions concerning published schemes with confusing charge distribution on oxygenating P450 intermediates have already been mentioned in the literature.[7] The iron(III)-peroxo species **E**, in Figure 20, has two negative charges and is probably the "supernucleophile" in P450 catalytic cycles (see above for the mechanism of aldehyde deformylation). When the first proton is added to the terminal oxygen atom of the peroxo species, the so-obtained iron(III)-hydroperoxo species **E′** has still one negative charge (see Figure 20). The second proton delivery by the threonine to the hydroperoxo ligand gives two neutral molecules, the iron(V)-oxo **F** and a water molecule. The nature and the reactivity of iron-peroxo species are certainly highly modulated by the nature of the coordination sphere of the iron (for a study concerning the behavior of non-heme iron-peroxo complexes, see the recent work of Que et al.).[174]

Kinetic data on the hydroxylation reaction catalyzed by P450s have been obtained by using several different radical clocks, of *trans*-1-alkyl-2-arylcyclopropane, to probe the rate of the oxygen atom transfer step in the rebound mechanism (Figure 19).[112] Formation of a radical with these probes would lead to opening of the cyclopropane ring and the formation of both unrearranged and rearranged alcohol products. Newcomb et al. observed that the amount of rearranged product depended on the substrate, such that for the poorer electron donor, that is, for *p*-$CF_3C_6H_4$ as the aryl group, one observes significant rearrangement, while when the alkyl group is *iso*-propyl the amount of rearrangement is virtually nil.[112] Using the percentage of rearrangement for the various probes, Newcomb et al. derived lifetimes as short as 70−100 fs. One might argue that inside the protein pocket the rate of radical rearrangement is slowed, and therefore these lifetimes are underestimated. This however requires proof, since several quite bulky substrates were found to tumble freely, or virtually so, within the pocket.[175,176]

Theoretical arguments[120] and DFT calculations, carried out on a variety of substrates,[70−72,130,173] have offered a reasonable rationale for these controversial findings of the ultrashort radical lifetimes. B3LYP calculations were used to model the mechanism of methane hydroxylation,[130,177−179] allylic hydroxylation of propene,[180] and recently also of *trans*-1-methyl-2-phenylcyclopropane,[173] which is one of Newcomb's probes. In all these cases, the lowest energy mechanism was found to involve a hydrogen abstraction like TS ($TS_{abs}$), as shown schematically in Figure 21. However, the calculations reveal that the mechanism involves two reaction profiles, one high-spin (HS) and the other low-spin (LS), which result from the two virtually degenerate ground states of Cpd I. The reaction pathway has three phases: (i) a C−H abstraction phase that leads to an alkyl radical coordinated to the iron-hydroxo complex by a weak OH---C hydrogen bond, labeled as $^{4,2}C_I$; (ii) an alkyl (or OH) rotation phase whereby the alkyl group achieves a favorable orientation for rebound; and (iii) a rebound phase that leads to C−O bond making and the ferric−alcohol complexes, $^{4,2}P$. The two profiles remain close in energy throughout the first two phases and then bifurcate. Whereas the HS state exhibits a significant barrier and a genuine TS for rebound, in the LS state, once the right orientation of the alkyl group is achieved, the LS rebound proceeds in a virtually barrier-free fashion to the alcohol. As such, alkane hydroxylation proceeds by TSR,[70−72,120] in which the HS mechanism is truly stepwise with a finite lifetime for the radical intermediate, whereas the LS mechanism is effectively concerted with an ultrashort lifetime for the radical intermediate. Subsequent studies of ethane and camphor hydroxylation by the Yoshizawa group[117,181−183] arrived at basically the same conclusion, that the mechanism is typified by TSR. The differences between the results of Shaik et al.[130,173,177−180] and Yoshizawa et al.[117,181−183] were rationalized recently[71,72] and shown to arise owing to technical problems and the choice of the mercaptide ligand,[117,181−183] which is a powerful electron donor and is too far from the representation of cysteine in the protein environment. The most recent study of camphor hydroxylation, which was done at a higher quality,[117] converged to the picture reported by Shaik et al.[130,173,177−180] and shows a stepwise HS process with a barrier of more than 3 kcal/mol for C−O bond formation by rebound of the camphoryl radical vis-à-vis an effectively concerted LS process for which this barrier is 0.7 kcal $mol^{-1}$ and is the rotational barrier for reaching the rebound position.

By referring to Figure 21, it is possible to rationalize the clock data of Newcomb in a simple manner. The apparent lifetimes are based on the assumption that there is a single state that leads to the reaction, such that the radical lifetime can be quantitated from the rate constant of free radical rearrangement and the ratio of rearranged to unrearranged alcohol product. However, in TSR, the rearranged (**R**) product is formed only/mainly on the HS surface, while the unrearranged (**U**) product is formed mainly on

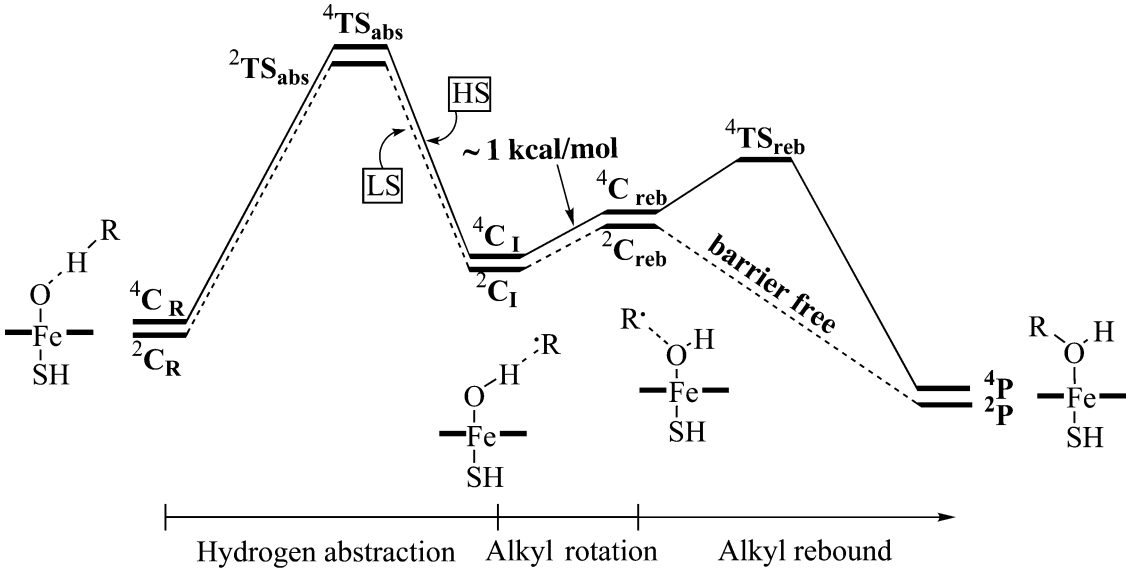


**Figure 21.** The DFT-based TSR mechanism of alkane hydroxylation (ref 131); HS corresponds to the quartet spin state, and LS to the doublet spin state. Adapted from ref 71 with permission of Wiley-VCH.

the LS surface. Therefore, the ratio of rearranged to unrearranged alcohol is associated with the relative yields of the HS vis-à-vis the LS reactions and not with the radical lifetime as such.[70,71,130,179] A simple TSR scheme leads to the following expression for the ratio of the real to the apparent lifetimes (eq 3):

$$\tau_{real}(\mathrm{TSR})/\tau_{app} = \{[\mathbf{U/R}](1 + F_{HS/LS})\}/\{[\mathbf{U/R}] - F_{HS/LS}\} > 1 \qquad F_{HS/LS} = [\mathbf{LS/HS}] \quad (3)$$

where the quantity $F_{HS/LS}$ is the relative yield of the LS to HS reactions. It is clear that the real lifetime of the radicals on the HS surface is longer than the apparent lifetime in proportion to the value of $F_{HS/LS}$, the LS vis-à-vis HS yield. Since in the calculations the LS bond activation barrier is lower than the corresponding HS barrier, $F_{HS/LS}$ is larger than unity; in the case of allylic hydroxylation[180] it reaches even values of the order of 10 when the effect of the protein electric field and hydrogen bonding are taken into account. As such, the apparent radical lifetimes will be unrealistically short compared with the real lifetimes. Furthermore, analysis of the rebound process itself[70,71,131,179] shows that the quantity [**U/R**] should increase significantly as the alkane and its derived radical become better electron donors. Therefore, in such a series the [**U/R**] quantity gradually increases, such that some critical donor-ability of the radical is reached when the HS rebound barrier altogether vanishes, the [**U/R**] quantity converges to infinity, and the apparent lifetime becomes strictly meaningless. This trend fits perfectly the series of probe substrates (*trans*-1-alkyl-2-phenylcyclopropane) used by Newcomb et al.[112] where the amount of rearranged product, which is significant for alkyl = methyl, becomes virtually zero for alkyl = *iso*-propyl.

Using another probe substrate, *trans*,*trans*-2-methoxy-3-phenyl-methylcyclopropane, Newcomb et al.[112,184] found two minor products that were obtained besides the unrearranged alcohol: a benzylic alcohol resulting from the homolytic cleavage of the C1−C3 bond (expected rearranged product with a radical clock) and an aldehyde presumably resulting from a cation generated on the methyl group attached at C1 via the protonated alcohol produced after O-insertion within the substrate (see Figure 22). To explain this latter product, the authors[112,184] invoked the $Fe^{III}$−OOH species as a "second oxidant that generates the cationic intermediate by the direct insertion of $HO^+$ into the C−H bond".

Figures 22 and 23 delineate an alternative hypothesis[185−188] for the origins of the cation, the precursor of the observed aldehyde product. Upon hydrogen abstraction, the high-valent iron-oxo is converted to an iron(IV)-hydroxo intermediate (the same oxidation level as compound II in a peroxidase). The electron affinity of this species is quite high,[71,98] and therefore the iron(IV)-hydroxo complex might abstract one electron from easily oxidizable radicals, before the rebound step of the hydroxylation reaction (see Figure 23). The resulting species will most likely be an intimate ion-pair in which the carbocation is coordinated to the iron(III)-hydroxo anion. Such ion-pairs are supported by theory[71] (see later also the discussion of benzene hydroxylation). Within the protein environment, some of these ion-pairs may dissociate to produce diffusive cations.

This step is reminiscent of the intramolecular electron transfer that was observed by Meunier et al.[185−187] during the alkylation of heme by antimalarial artemisinin derivatives. In that case, the electron transfer took place between a radical on one Cα pyrrolic position of the protoporphyrin-IX and the central iron(III) (the radical and the metal center being separated by two bonds). In a P450 hydroxylation, the C-centered radical of the substrate can be generated at a similar distance from the iron(IV), a stronger oxidant than iron(III). To our knowledge, no study has been considered to identify the origin of the oxygen atom in products derived from the rearrangement of the intermediate cation: it could be the $Fe^{III}$−OH itself or a water molecule (O-labeling studies will provide an answer).

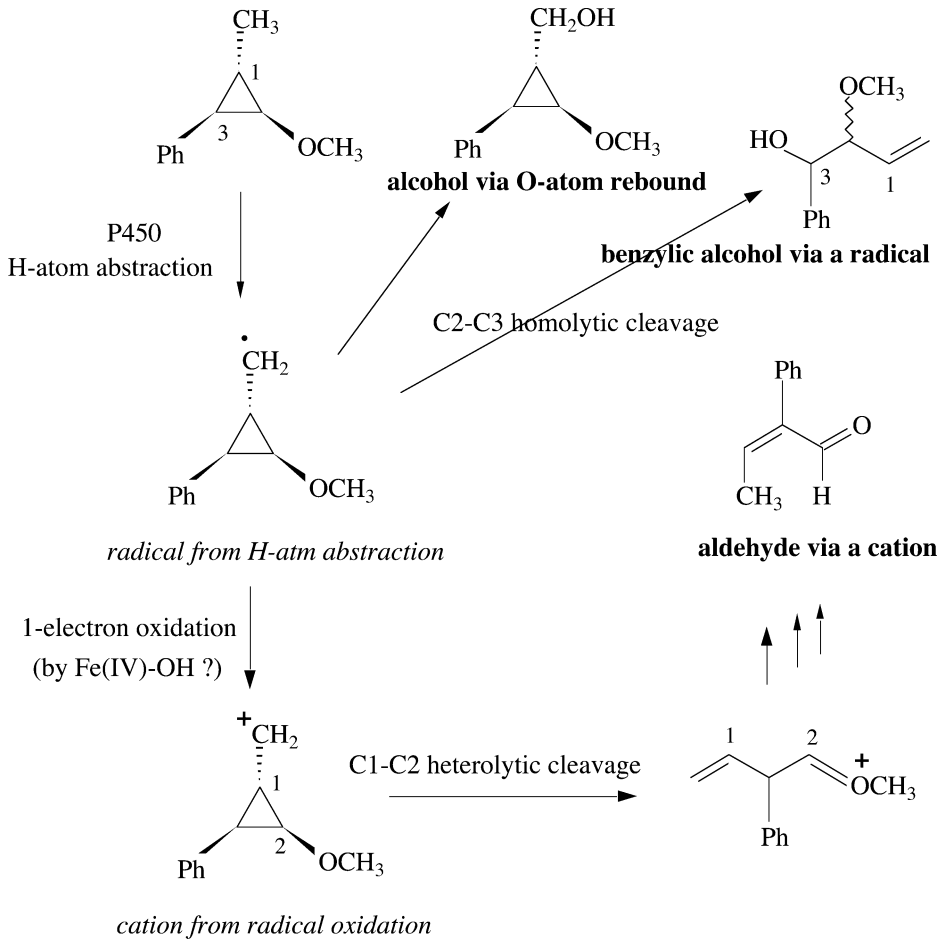


**Figure 22.** Products obtained in the oxidation of *trans,trans*-2-methoxy-3-phenyl-methylcyclopropane by cytochrome P450.

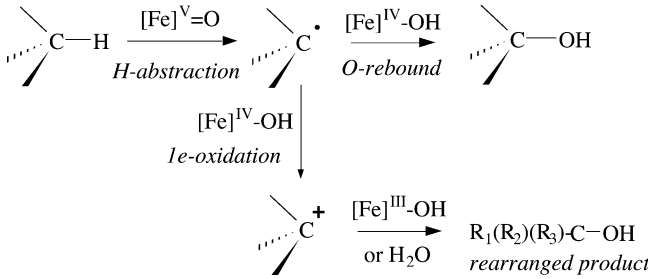


**Figure 23.** Formation of cation-derived oxidation products via the one-electron oxidation of the intermediate radical resulting from the H-atom abstraction by the high-valent iron-oxo species.

Recently, the oxidation of the radical clock norcarane has been revisited by two independent groups, Groves−Ortiz de Montellano on one hand and Newcomb−Coon−Hollenberg−Lippard on the other hand, with different cytochrome P450s and one methane monooxygenase (see Figure 24).[188,189]

With the two bacterial P450s ($P450_{cam}$ and $P450_{BM-3}$), the rat CYP2B1 and the human CYP2E1, the apparent lifetimes of the 2-norcaranyl radical generated by H-atom abstraction were 52, 44, 16, and 35 ps, respectively, supporting an oxygen rebound mechanism (product distributions obtained with $P450_{cam}$ are indicated in Figure 24).[188] With four rabbit enzymes, CYP2B4, CYPΔ2B4, CYPΔ2E1, and CYPΔ2E1-Thr303Ala, and two sMMO enzymes from *Methylcoccus capsulatus* (Bath) or from *Methylosinus trichosporium* (OB3b), Newcomb et al. found in all different cases similar distribution products with the ratio of 4-cyclohepten-1-ol (arising from a cation intermediate) ranging from 0.1 to 0.6% for the four P450s and being 2.6 and 1.2% for *Mc. capsulatus* and *Ms. trichosporium*, respectively. The ratio of the radical rearranged products was found to range from 0.4 to 3.3% within the different six enzymes. However, for some reason, the case of norcarane was considered by Newcomb et al. as being a particular case and they proposed that the observed radical pathway should not be generalized to other P450 enzymes or other non-heme monooxygenases.[189] Once again, if we consider that the cationic rearranged product is a byproduct produced by the one-electron oxidation of the initial radical by an $Fe^{IV}$−OH generated by H-atom abstraction from the substrate, then there is no need to invoke a second oxidant that effects an $OH^+$ insertion into the C−H bond of the substrate. Furthermore, since the $Fe^{IV}$−OH moiety of MMO is a better electron acceptor than the same moiety in P450, the former enzyme (MMO) is expected to give less radical rearrangment products and more cations.[71] The slight increase of both radical and cation rearranged products, which was observed with the threonine mutant CYPΔ2E1-T303A, may simply reflect a delicate balance of the competing processes that generate and consume the original radical. Thus, the absence of the threonine reduces the rate of formation of the iron-oxo species and thereby affects the rate of radical production. It may similarly affect

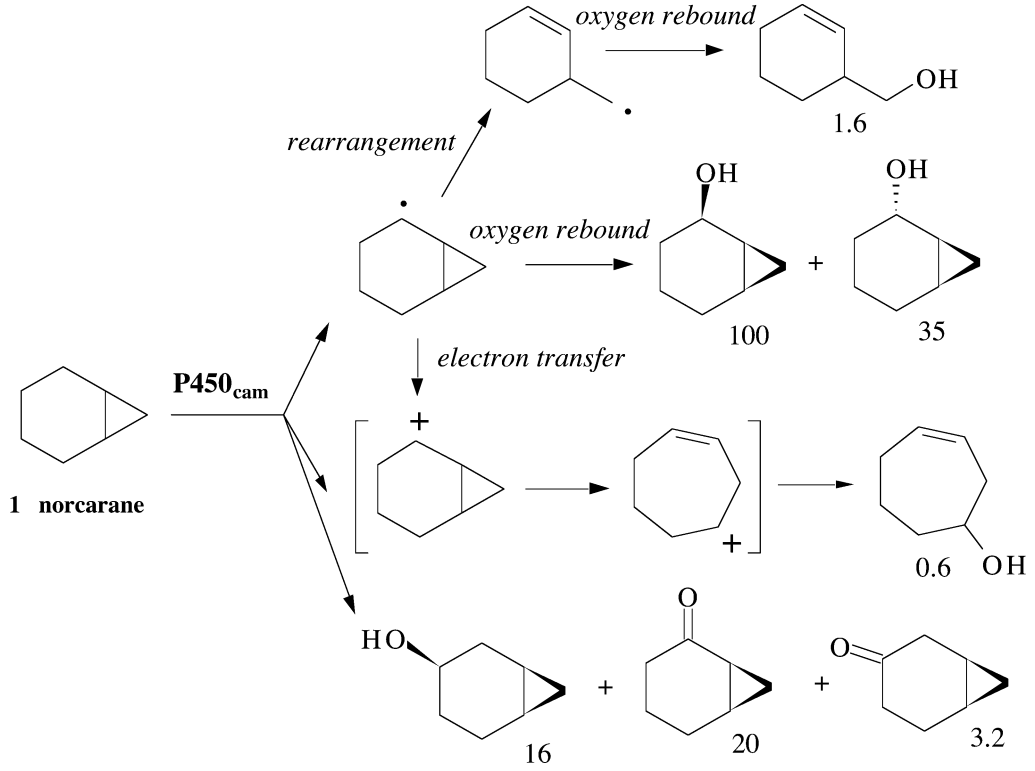


**Figure 24.** Rearrangement pathways and product distribution resulting from formation of a radical or a cation intermediate upon oxidation of norcarane **1** by cytochrome $P450_{cam}$. Adapted from ref 188.

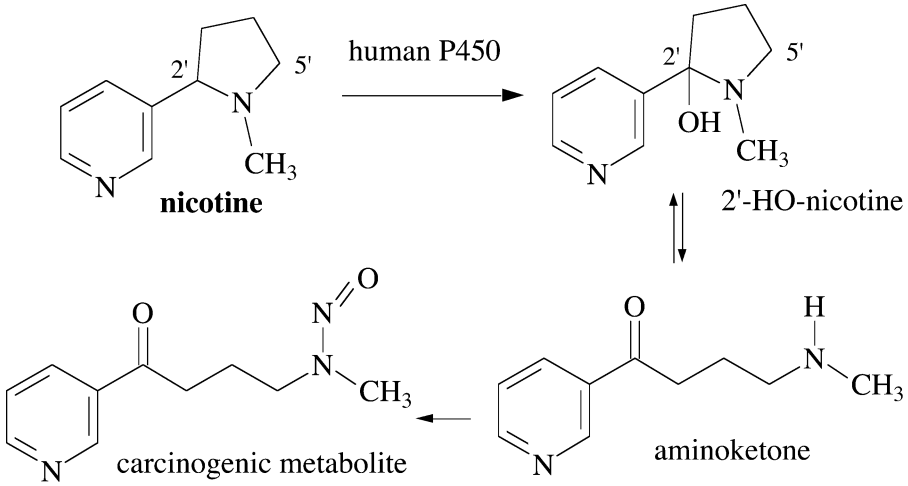


**Figure 25.** Formation of a carcinogenic metabolite by human P450-mediated 2′-hydroxylation of nicotine.

also the rates for the C−O bond formation and the generation of cation by electron transfer. Finally, it should be mentioned that most of the mechanistic conclusions, regarding these reports on the oxidation of norcarane, are dependent on the measurements (and the accuracy of these measurements) of low levels of diagnostic products.

To end this section on the hydroxylation mechanisms, we add two interesting reactions. Thus, the transformation of ethanol to acetic acid by a recombinant human cytochrome P450 is the result of two consecutive hydroxylation reactions: the first one leads to acetaldehyde, and the second one converts the intermediate aldehyde to the acid without dissociation of acetaldehyde from the active site of the enzyme.[190] A recent study on the metabolism of nicotine with the human cytochrome $P450_{2A6}$ and liver microsomes has provided a new metabolic pathway (a 2′-hydroxylation besides the known 5′-hydroxylation) leading to a potent lung carcinogenic precursor (Figure 25).[191]

The hydroxylation at 2′ directly generates an aminoketone, by opening of the oxidized pyrrolidine ring, which can be nitrosylated to produce the tobacco-specific lung carcinogen 4-(methylnitrosoamino)-1-(3-pyridyl)-1-butanone.

## 7.2. Epoxidation of Olefins

Olefins are easily epoxidized by cytochrome P450 enzymes and usually occur with retention of stereochemistry in the *cis*-olefin, strongly suggesting a concerted mechanism.[1] However, the P450-catalyzed epoxidations of some olefins produce side products

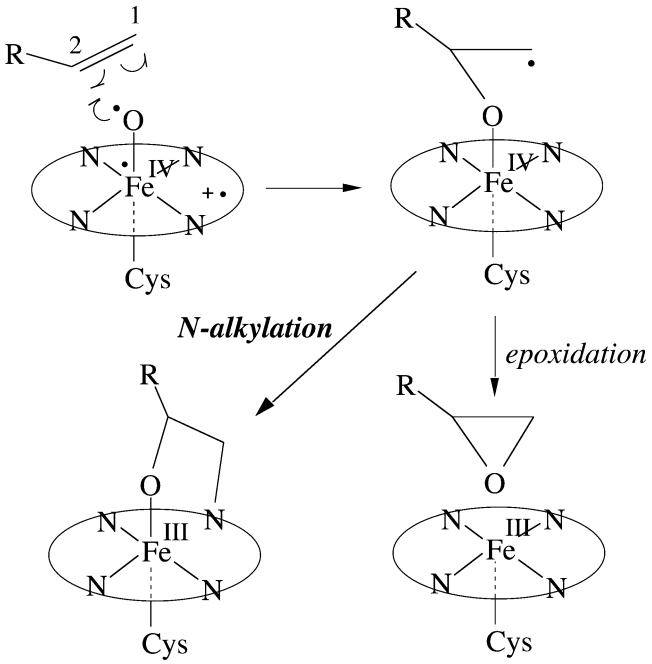


**Figure 26.** A mechanism for porphyrin *N*-alkylation during the epooxidation of terminal olefins.

besides the corresponding epoxides, indicating that the oxidation of olefins is not always a fully concerted process. This is the case of terminal olefins that produce the inhibition of cytochrome P450 by formation of an irreversible porphyrin *N*-alkylation product (the "green pigment" of rat liver is intoxicated with high levels of terminal olefins). The new carbon−nitrogen bond is formed with the terminal carbon atom $C_1$ of the olefin, and the internal one $C_2$ is bearing an oxygen atom derived from molecular oxygen.[192] The proposed mechanism is depicted in Figure 26. Here, to show more clearly the electro reorganization, we described the iron-oxo species by focusing only on the two triplet coupled electrons of the FeO moiety.

Since Cpd I has a triplet FeO moiety, with one electron each on Fe and O, the radical character of the oxyl entity initiates the formation of an intermediate with a radical on $C_2$ of the terminal olefin. The so-formed intermediate will subsequently undergo competition between $C_1-O$ bond formation (to yield an epoxide) and $C_1-N$ bond formation with one of the nitrogen atoms of the porphyrin ring (the corresponding Fe−N bond being broken at the same time by homolysis). Then the *N*-adduct complex can be easy demetalated leading to an *N*-alkylporphyrin with an alcohol function at $C_2$.

The trichloroacetaldehyde formation, observed along with the epoxide formation, in P450 oxidations of trichloroethylene[6,193] can be explained by the formation of an intermediate cation produced by the one-electron oxidation of the C-radical generated by a nonconcerted addition of Fe(IV)-oxyl onto the less-substituted carbon atom (Figure 27). Again, this intermediate formation of a cation involves an intramolecular one-electron transfer between a C-radical and an Fe(IV) ion separated by only three bonds.

Recently, Vaz and Coon proposed the role of the ferric hydroperoxide as a second oxidant in olefin epoxidations catalyzed by the Thr303Ala mutant of cytochrome $P450_{2E1}$ where the proton-delivery threonine has been replaced by an alanine residue (in such mutant, the protons come directly from bulk water and not via a cascade involving a threonine and an aspartate residue).[81] This mutant enhanced the epoxidation of three different olefins (styrene, cyclohexene, and *trans*-2-butene) along with a decreased allylic oxidation of cyclohexene and *trans*-2-butene.

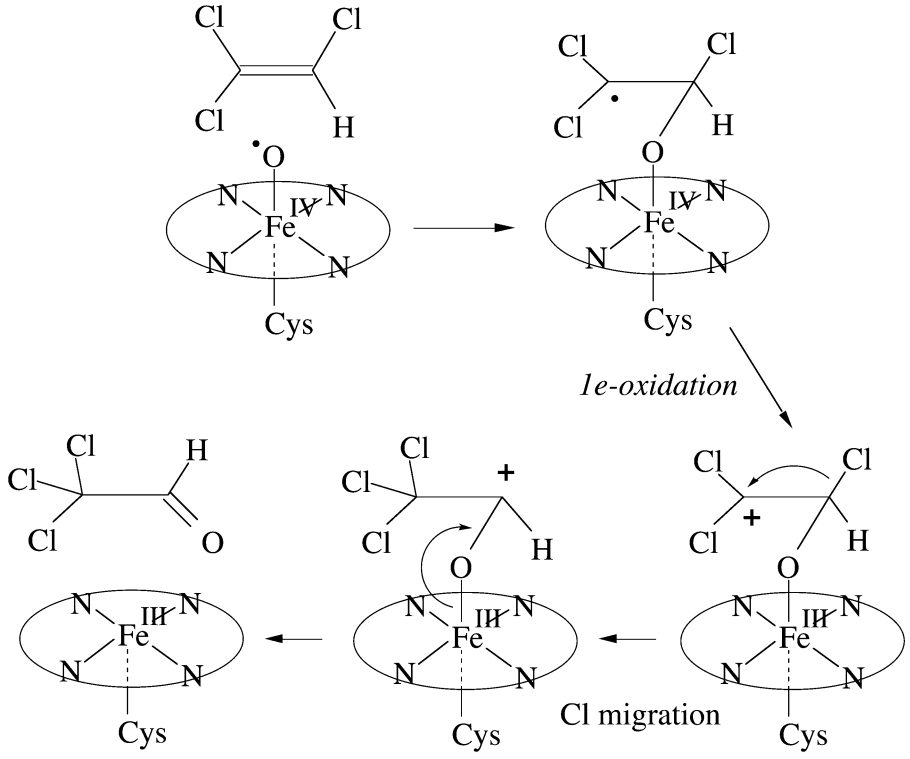


**Figure 27.** Formation of an aldehyde in the oxidation of trichloroethylene by cytochrome P450.

Dawson and Sligar have also reported that the Thr252Ala mutant of cytochrome $P450_{cam}$, a mutant unable to hydroxylate camphor, was able to epoxidize 5,6-dihydrocamphor and 5-methylenylcamphor at a rate which was 15−20% of the rate of the wild-type enzyme with the same olefins.[194]

These data have been interpreted as evidence of the electrophilic properties of the $Fe^{III}-OOH^-$ intermediate. However, many chemists have difficulties in accepting that a hydroperoxide species is able to behave both as a nucleophile in aldehyde deformylation and as an electrophile in epoxidation. Such electrophilic behavior is observed for organic peracids which are able to perform epoxidation of Baeyer−Villiger reactions.[195] However, peracids are certainly highly electrophilic species, while $Fe^{III}-OOH^-$ is not. In fact, the observed differences in product formation between the wild and mutant enzymes might be attributed to an enhanced proton delivery by bulk water as observed in the Asp-251 mutant of $P450_{cam}$ (see ref 103) and also by a modified shape of the mutant active site that will facilitate the approach of the olefin with respect to the iron-oxo species. Polarity and hydrogen-bonding effects on the C=C/C−H oxidation ratio by Cpd I have been demonstrated by recent DFT studies[180] and may well add to these trends, without a need to invoke participation of $Fe^{III}-OOH$.

Theory lends support to the idea that the $Fe^{III}-OOH$ species **E′** is an extremely sluggish epoxidizing agent compared with Cpd I. Thus, by contrast to the very large barriers for ethene epoxidation by $Fe^{III-}OOH$,[116,196] the barriers for ethene and propene epoxidation by Cpd I are very small, <14 kcal/mol.[180,197] However, theory shows also that epoxidation by Cpd I is nonsynchronous and is a two-state reaction,[180,197] much like the C−H hydroxylation mechanism. By reference to Figure 26, the initial C=C bond activation produces the carbon radical intermediate complex, $Fe^{IV}O-CRHCH_2^{\bullet}$, in two spin states, doublet and quartet.[180,197] The doublet-state complex collapses to the ferric epoxide complex without a barrier, while the quartet-state complex has a small but finite barrier for ring closure. This quartet-state intermediate will have a sufficient lifetime to lose some stereochemistry, since its ring closure barrier is of the order of the C−C rotational barrier. Theory[180,197] further shows that there exists another quartet-state intermediate; this is the $(Por^{\bullet+})Fe^{III}O-CRHCH_2^{\bullet}$ radical complex that has a significant barrier for ring closure (∼7−10 kcal/mol) and hence a long lifetime. It is this last quartet-state species that is responsible for the porphyrin alkylation products[198] as well as for the aldehyde side product; the latter is produced by conversion of $(Por^{\bullet+})Fe^{III}O-CRHCH_2^{\bullet}$ to the corresponding quartet-state cation, $PorFe^{III}O-CRHCH_2^{+}$.[199] Despite this conclusive picture that accounts for most of the facts based on two states of Cpd I, theory still has an important role, to probe the feasibility of either a proton-assisted epoxidation by $Fe^{III}-OOH$ or by its protonated form, by the ferric hydrogen peroxide complex.

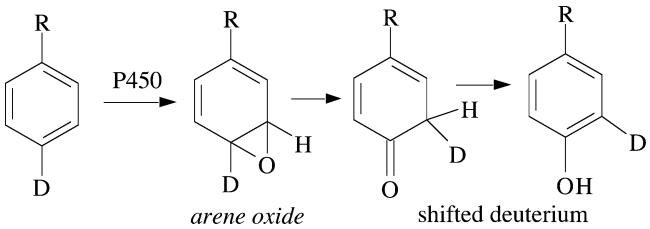


**Figure 28.** The NIH shift via an arene oxide in benzene oxidation catalyzed by cytochrome P450.

## 7.3. Aromatic Oxidation

Benzene is one of the most stable molecules toward oxidation. The homolytic cleavage of a benzene C−H bond is not easy, the bond dissociation energy being 111 kcal/mol, which is well above the values for aliphatic alkanes (90−101 kcal/mol) and even methane (105 kcal/mol).[200] In addition, benzene has a very high redox potential, making the formation of a radical-cation difficult by a one-electron oxidation process (recall, benzene and toluene are not oxidized by peroxidases). Consequently, the P450-mediated oxidation of benzene to phenol cannot result from a H-atom abstraction, like in aliphatic hydroxylation reactions, or from an initial one-electron oxidation (this latter mode of action has been evidenced though in the P450 oxidation of polymethoxylated benzene derivatives).[201]

The first mechanistic proposal of benzene hydroxylation was made by Jerina and co-workers at the National Institutes of Health (NIH) in 1969. As shown in Figure 28, the mechanism involves initial formation of an arene oxide that subsequently rearranges to a phenol derivative via the so-called "NIH" shift that leads to retention of the original H(D) of the activated C−H(D) bond.[202] The breakdown of the arene oxide via a cation has been generally accepted to explain the migration of the deuterium atom to the adjacent position and hence its eventual retention in the product.

Small isotope effects have been observed in the oxidation of different deuterated chlorobenzenes (ranging from 0.95 to 1.27), suggesting again that these aromatic oxidations are not due to a H-atom abstraction.[203] This NIH shift has been considered as the signature of an arene oxide intermediate, but an alternative mechanism involving the nonconcerted addition of an iron(IV)-oxyl species to the aromatic ring is also consistent with such migration of the label (Figure 29).[5,204] The cationic intermediate may be generated either independently or via an electron transfer from the radical intermediate shown in Figure 29. Such a cation at the meso position will induce the deuterium shift without formation of an arene oxide. The same mechanism has also been proposed by Trager et al. for the retention of deuterium observed in the P450-mediated hydroxylation of deuterated warfarin derivatives (warfarin is a widely used anticoagulant drug).[205]

Theory supports a mechanism similar to that in Figure 29, where the phenol and ketone products are formed independently of the arene-oxide.[206,207] Two different DFT studies of arene hydroxylation have been published recently, by de Visser and Shaik[206]

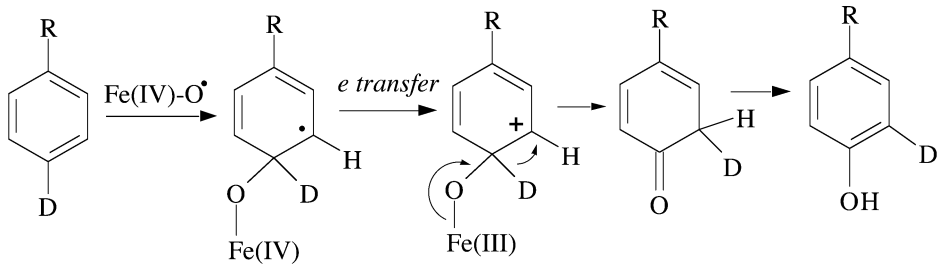


**Figure 29.** An alternative mechanism that accounts for the NIH shift without arene oxide formation.

and by Harvey et al.[207] Both studies show that the bond activation proceeds via a doublet-state mechanism. Two different mechanisms emerged from the calculations, based on spin density and charge density criteria;[206] one mechanism results in a radical $\sigma$-complex[206] (as in Figure 29), and the other in the corresponding cationic $\sigma$-complex (as in Figure 29).[206,207] Although theory does not rule out that the cation complex is generated from the radical complex via an internal electron transfer, as in Figure 29, the calculations[206] show that the radical and cationic intermediates are generated by their own independent pathways. The electrophilic path, leading to the cationic complex, is lower in energy and is further preferred over the radical mechanism by polarity and the NH---S hydrogen-bonding effect.[206] Thus, both DFT calculations predict that the major pathway for arene hydroxylation will be the electrophilic pathway.[206,207]

The so-formed intermediates subsequently bifurcate either to the ferric benzene-oxide complex by ring closure or to phenol and ketone by proton migration.[206,207] According to the study by de Visser and Shaik,[206] the ketone and phenol are formed via initial proton transfer from the ipso carbon of the benzene moiety to one of the nitrogens of the porphyrin, and the latter intermediate reshuttles the proton either to the oxo group to give phenol or to the ortho carbon to give the ketone. This process has extremely small barriers (<1 kcal/mol).[206] The study of Harvey et al.[207] implied, though did not state specifically, that the ketone and phenol were formed only by direct proton migration from the cationic intermediate. In correspondence, Harvey made it clear that they also identified the proton-shuttle mechanisms and found their barriers to be smaller than those for the direct rearrangements. Be that as it may, theory suggests that there is an enzymatic pathway that leads to all the products of arene hydroxylation. The oxidative metabolism of polyaromatics has been extensively studied due to its direct correlation with the formation of epoxide-diol derivatives that are the origin of DNA-alkylating species. The mechanism of formation of the oxidation products is similar to that described in Figure 29, whereas a recent report suggests that 3- or 6-fluorobenzo[*a*]pyrene is metabolized by P450 enzymes via an initial electron transfer generating a radical-cation on the polyaromatic substrate that collapses onto the iron-oxo, compound II, of the P450, the latter surprisingly acting as a nucleophile able to displace the fluorine atom.[208] In our opinion, there is no reason to consider that the iron(IV)-oxo of a cytochrome P450 is a nucleophile. The elimination of fluoride in the oxidative metabolism of 3-fluorobenzo[*a*]pyrene might be due to the nucleophilic attack of a water molecule on the radical-cation at the C3 position. While this mechanistic proposal has still to be checked with labeling experiments, it has already been observed in the demethoxylation reaction of a polyaromatic substrate catalyzed by a peroxidase.[209]

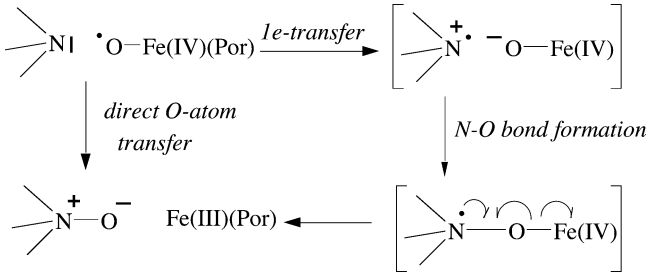


**Figure 30.** Formation of *N*-oxides by cytochrome P450 enzymes.

All the experiments on the oxidative biotransformation of aromatics are of real importance for understanding the potential risk of aromatic metabolites generated by the different monooxygenases involved in detoxification processes (or drug metabolism). However, the results of these studies, including animal studies, should be handled with care to avoid extrapolations to human risk without direct considerations of the capacity of the human biotransformation processes. For example, the oxidation of 1,2-dichlorobenzene by P450 generates reactive hepatotoxic epoxides which are poorly eliminated in rat by a nonenzymatic GSH addition, whereas the elimination of these electrophilic metabolites in human is more efficiently performed by a glutathione-*S*-transferase.[210] *Consequently, as clearly mentioned by the authors of this work, the "human risk after exposure to 1,2-dichlorobenzene will be overestimated when risk assessment is solely based on toxicity studies conducted in rat".*

## 7.4. Heteroatom Oxidations (Nitrogen and Sulfur)

Cytochrome P450s are able to add an oxygen atom to nitrogen, sulfur, phosphorus, and iodine atoms, generating the corresponding oxides.[1,211,212] These oxygen-transfer reactions can be considered as being due to the electrophilic compound I ($Por^{\bullet+}Fe^{IV}O$) species with two events of one-electron transfer, as suggested by the lack of a Hammett relationship.[213,214] Figure 30 suggests a mechanistic alternative that bypasses the unreasonable heteroatom dication.

The abstraction of one electron by the iron(IV)-oxyl species will generate a radical-cation of the nitrogen

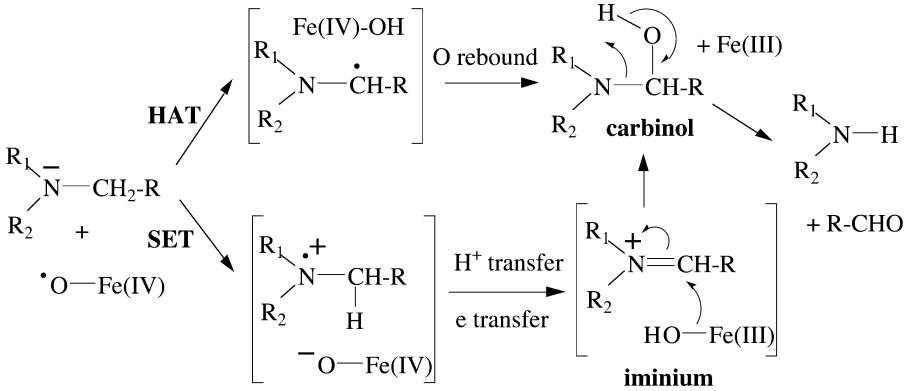


**Figure 31.** The two possible mechanisms in *N*-dealkylation of tertiary amines catalyzed by cytochrome P450 enzymes: H-atom abstraction (HAT) versus single electron transfer (SET).

facing a negatively charged oxygen atom linked to Fe(IV); a concomitant homolysis of the iron−oxygen bond with the coupling of the unpaired electron of the nitrogen with one electron of the O−Fe bond produces the *N*-oxide derivative. Alternatively, the process may involve a concerted oxygen transfer from the high-valent metal-oxo species to the heteroatom. The oxidative metabolism of amine derivatives is not limited to the oxidation of the nitrogen atom. *N*-Dealkylations are also observed, and the mechanism of these reactions can be related to heteroatom oxidation or hydroxylation depending on the structure of the substrates and the nature of cytochrome P450s involved.

Cytochrome P450 enzymes catalyze the oxidation of thiols to the corresponding sulfenic and sulfonic derivatives and the oxidation of sulfides to sulfoxides; some of these *S*-oxidations are generating electrophilic species able to alkylate P450 proteins.[211,215] The oxygen atom of the sulfoxides originates from molecular oxygen,[216] and the stereoselectivity of the sulfoxidation of one particular substrate by liver cytochromes P450 is different from that observed with liver flavin-containing monooxygenases.[217] As for hydroxylation reactions, the possible role of an iron(III)-hydroperoxo as the active species in sulfoxidations catalyzed by cytochrome P450 has also been investigated.[218] A recent theoretical study[219] shows that in the case of sulfoxidation, the iron(III)-hydroperoxo is again a sluggish oxidant, and the process involves an oxygen abstraction from compound I.

## 7.5. *N*- and *O*-Dealkylation Reactions

Two mechanisms have been observed in *N*-dealkylation reactions: (i) a formal hydroxylation of a C−H bond on the carbon adjacent to the heteroatom (HAT, H-atom transfer) and (ii) a one-electron oxidation of the heteroatom itself (SET, single-electron transfer) (Figure 31).

Both mechanisms have been debated by many different authors, and recent review articles are providing a rather exhaustive survey of these oxidative dealkylation reactions.[1,5,6] The following presentation is restricted to the recent developments on the mechanism of *N*- and *O*-dealkylation reactions.

The HAT mechanism is supported by the identification of carbinolamines in the *N*-dealkylation of particular substrates and by the fact that their oxygen atom originates from molecular oxygen ($^{18}$O-labeling experiments).[220] On the other hand, relatively low kinetic isotope effects have been observed in *N*-dealkylations (values ranging from 2.4 to 4.1)[221,222] compared to aliphatic hydroxylations or *O*-dealkylations.[223] Consequently the SET mechanism is supported by many authors.[5] Nevertheless, this is not conclusive since small isotope effects may result from highly asymmetric transition states for HAT.[221] A recent work by Hanzlik and co-workers with *N*-cyclopropyl-*N*-methylaniline indicates that the cyclopropyl ring is opened only when this substrate is oxidized by horseradish (SET mechanism) but not in oxidation mediated by phenobarbital-induced rat liver microsomes (HAT mechanism).[224] A comparison between the oxidation of *N*-cyclopropyl-*N*-alkyl-*p*-chloroanilines by rat liver microsomal P450 and $[Fe(III)(Phen)_3]^{3+}$, a one-electron oxidant, favored the HAT mechanism.[225] However, the SET mechanism, as depicted in Figure 31, might also involve the formation of a carbinolamine resulting from the nucleophilic addition of the hydroxo ligand of an $Fe^{III}$−OH onto the iminium intermediate within the active site of the enzyme (this latter proposal would account for all experimental evidence published by different authors favoring the SET mechanism). Preliminary DFT calculations indicate that a hydrogen atom transfer mechanism is at work, between trimethylamine and a model compound I species of P450.[226] Thus, these proposals require more work, and in our opinion, there should not be a clear-cut either−or on the mechanism of the oxidative dealkylation of amines. Both mechanisms might be possible, and small changes in the chemical and electronic structures of substrates and/or differences in the nature of P450 enzymes might be able to produce a shift between the two mechanisms, hydroxylation versus electron abstraction. In both cases, a carbinolamine might be a common intermediate.

*O*-Dealkylation reactions are definitively considered as resulting from a C−H bond hydroxylation on the carbon atom adjacent to the ether oxygen atom.[5,6,227] In *O*-dealkylation reactions of methyl ethers, the methyl group departs as formaldehyde, whereas horseradish peroxidase oxidizes methyl ether functions by an electron-transfer mechanism and the methoxy group is, in fact, released as methanol.[209]

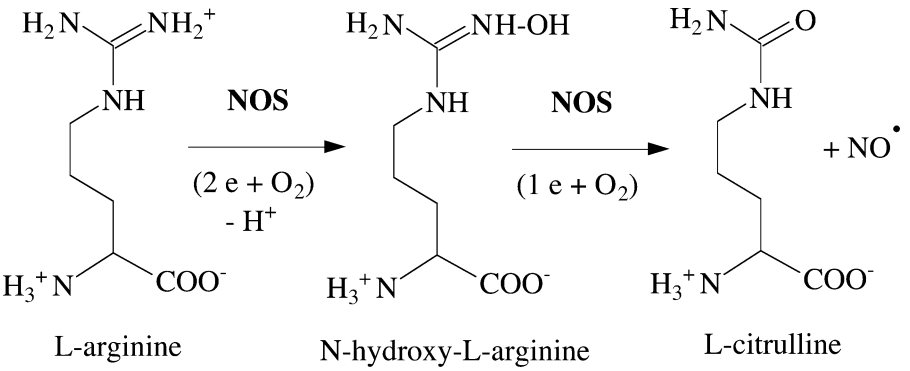


**Figure 32.** The oxidation sequence of L-arginine to L-citrulline and nitric oxide by NO-synthase.

At the end of this section on P450-catalyzed dealkylation reactions, we will only briefly touch on the oxidation of L-arginine by nitric oxide synthases (NO-synthase or NOS) since these heme-monooxygenases are able to generate NO, an important signaling molecule, which is involved in many different physiological functions and in some pathologies. Abundant studies on this class of P450 enzymes have created a new rather independent research field within less than a decade.[228−231] Three isoforms of NOSs have been isolated from various mammalian cells: neuronal NOS, inducible NOS, and endothelial NOS, and several of these proteins have been crystallized.[232−236]

Electrons are funneled from NADPH via FAD and FMN to the heme located at the N-terminal side of the protein. The heme-flavin domain interactions are regulated by calmodulin. NO-synthases catalyze the following two steps to produce NO from L-arginine: (i) a first quite specific hydroxylation of a N−H bond of the guanidinum group (except homo-L-arginine, other guanidinium-containing molecules are not oxidized by NOS) leading to $N^{\omega}$-hydroxy-L-arginine (this step consumes two electrons and a dioxygen molecule) and then (ii) a second step producing NO and L-citrulline (the step consumes only one electron and one dioxygen) (Figure 32).

This second step is less specific than the first one, and many different *N*-hydroxyguanidines are able to produce NO when oxidized by NOS.[237,238] Two structures of nNOS with different *N*-hydroxyguanidine derivatives suggest how the ferric-superoxo intermediate could participate in the final liberation of NO from the oxidized hydroxyguanidine.[239] This study demonstrates the key role of the glutamic-592 residue in orientating the *N*-hydroxyguanidine derivative within the active site. The study further indicates that the N−OH group is facing the carbonyl group of a tryptophan (Trp-587) and pointing away from the heme residue. Therefore, the attack of the $Fe^{III}$−OO species on the hydroxyguanidine appears complicated. Poulos and co-workers[239,240] have suggested a mechanism, which is depicted in Figure 33 in a simplified version.

The key step is the formation of a C−O bond between the terminal oxygen atom of the ferric-superoxo species (being formed after the dioxygen addition onto the intermediate resulting from the one-electron reduction of the resting ferric state of the enzyme) and the central carbon atom of the guanidine. Then the heterolytic cleavage of the

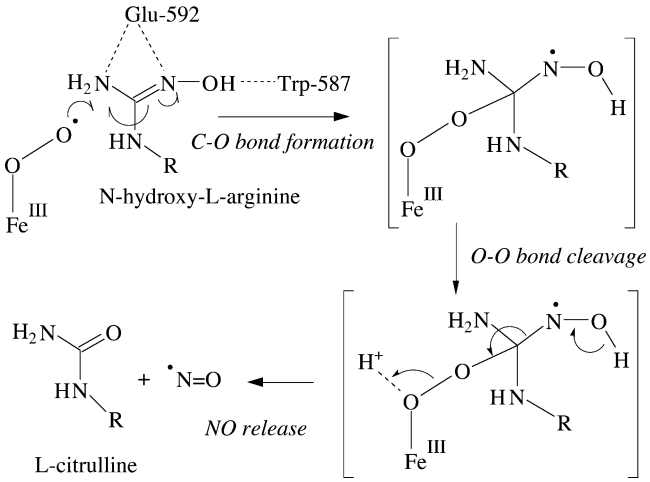


**Figure 33.** A proposed mechanism for the addition of the ferric(III)-superoxo species of NOS onto the *N*-hydroxyarginine to generate nitric oxide and L-citrulline.

intermediate peroxide bond triggers the cleavage of the C−N bond of the radical hydroxylamine, generating nitric oxide and L-citrulline (for other alternatives, the reader may consult a recent review: Groves, J. T.; Wang, C. C. Y. *Curr. Opin. Chem. Biol.* **2000**, *4*, 687).

## 7.6. Aldehyde Oxidations

Aldehydes are usually oxidized to carboxylic acids by cytochrome P450s via the hydroxylation of the aldehydic C−H bond, but a second reaction pathway has been identified with some substrates. For example, cyclohexene is formed during the oxidation of cyclohexanecarboxaldehyde catalyzed by $P450_{2B4}$, a liver P450 induced by phenobarbital (Figure 34).[241,242] This reaction was not observed when iodosylbenzene was used as single oxygen atom source, indicating clearly that the high-valent iron-oxo intermediate was not involved in this reaction. The initial nucleophilic attack of the iron-peroxo entity on the carbonyl function is probably followed by a concerted reaction involving a six-electron process as in a Grob fragmentation (see Figure 34). The carbon atom of the aldehyde function is eliminated as formic acid.

The same oxidative deformylation has been observed with other aldehydes including citronellal.[243] With some aldehydes, the deformylation reaction causes inactivation of cytochrome P450 via the formation of a heme-adduct at the $\gamma$-position located

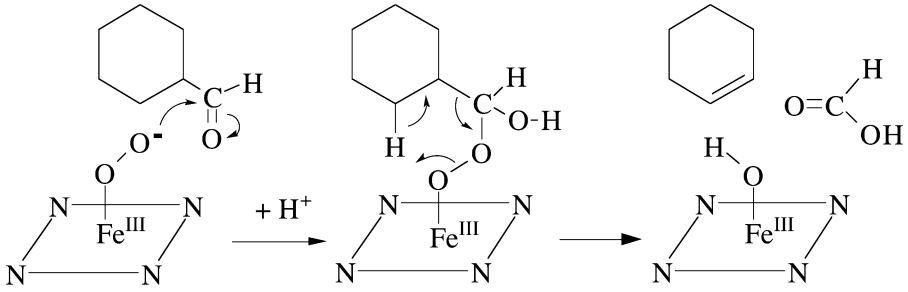

**Figure 34.** Oxidative decarbonylation of cyclohexanecarboxaldehyde to cyclohexene and formic acid catalyzed by cytochrome P450. Reprinted with permission from ref 7. Copyright 2000 Springer-Verlag Heidelberg.

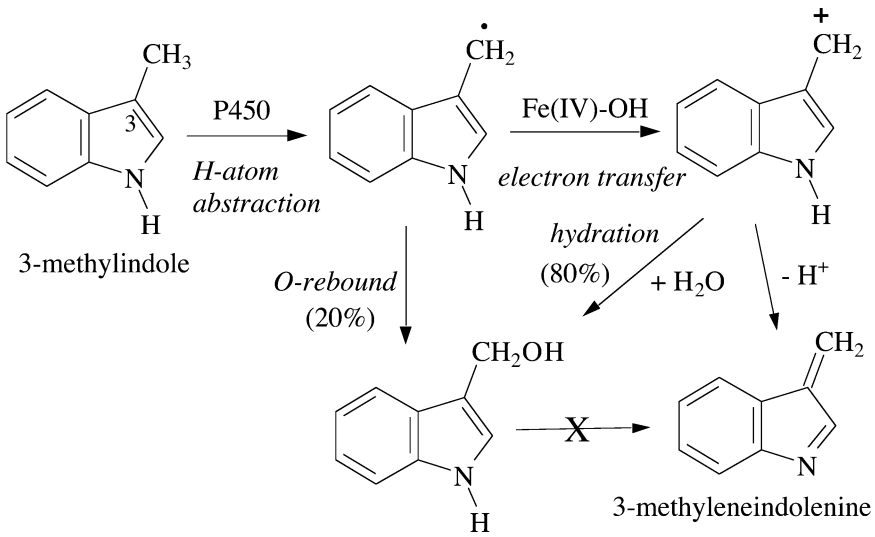

**Figure 35.** Dehydrogenation of 3-methylindole to 3-methyleneindolenine by cytochrome P450.

between the two propionic substituents. The structure of the $\gamma$-meso adduct generated during the oxidation of 3-phenylpropionaldehyde has been established by mass spectrometry and 2D-NMR data (the oxidation has been performed with cytochrome $P450_{2B4}$ in the presence of hydrogen peroxide).[244] The organic radical is generated by the homolytic cleavage of the intermediate peroxy-hemiacetal generated by the nucleophilic attack of $Fe^{III}$—OOH on the carbonyl group of the aldehyde.[245]

## 7.7. Dehydrogenation Reactions

P450 enzymes can also catalyze the dehydrogenation of some organic molecules instead of carrying out the oxygenation of the substrate. In this manner, P450 converts all the dioxygen into water and generates an olefin, thus exhibiting a mixed function as an oxidase−dehydrogenase enzyme. In particular, valproic acid is converted not only to 3- and 4-hydroxyvalproic acid but also to 2-*n*-propyl-2-*E*-pentenoic acid.[246] A KIE study indicates that the product-determining step of the dehydrogenation is the H-atom abstraction at C4 and not at C5, suggesting that the radical at C4 can be oxidized by Fe(IV)-oxo to generate a cation at C4 that can eliminate a proton from the methyl group to produce the terminal olefin.[246]

The formation of the pulmonary toxic 3-methyleneindolenine by the P450-mediated oxidation of 3-methylindole is an additional example of the formation of a double bond after an initial H-atom abstraction.[247] An intramolecular KIE of 5.5 supports the H-atom abstraction on the methyl group as being the rate-determining step (Figure 35).

Labeling studies with $^{18}O$-water indicate that only 20% of the indole-3-carbinol is produced via an oxygen rebound mechanism, 80% being obtained by hydration of 3-methyleneindolenine, a strong electrophile that is usually detoxified by glutathione.

More and more frequently, detailed studies on drug metabolism revealed the formation of dehydrogenation derivatives in parallel to classical reaction pathways. Dehydrogenation products have been found in the oxidative metabolism by human P450s of ezlopitant (a novel nonpeptide antagonist of the substance P receptor)[248] and capsaicin (a common dietary constituent and a popular homeopathic treatment for chronic pain).[249]

## 7.8. Aromatase Activity and Related Reactions

Among the different cytochrome P450 enzymes, aromatase has a special place for two reasons: (i) this enzyme is specific for the conversion of androgens to estrogens (the aromatase is the product of a single gene),[250] and (ii) this cytochrome is able to catalyze three successive oxidative transformations of the same substrate molecule before releasing the product of the reaction outside the enzyme pocket (many other P450 enzymes are also able to perform this multicycle activity, but the mechanism of aromatase has been particularly well-studied and the third step is now one of the classical examples of the role of a

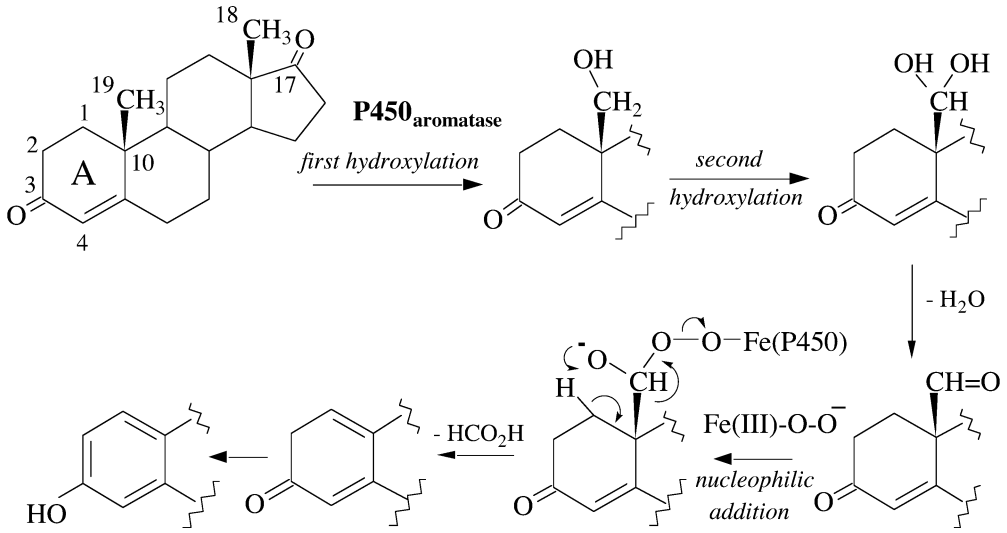


**Figure 36.** A mechanism of the aromatization of the A-ring of androst-4-ene-3,17-dione to estrone catalyzed by human placental aromatase.

nucleophilic iron-peroxo species in a P450 catalytic cycle).[1,5,6,136]

The aromatization reaction of the A-ring of androst-4-ene-3,17-dione to estrone is catalyzed by human placental aromatase.[251−254] This reaction involves three consecutive oxidative steps: two hydroxylations at the 19-methyl group and a final oxidative decarbonylation of the intermediate 19-aldehyde. All three reactions are stereospecific. The first hydroxylation at the 19-methyl group occurs with retention of configuration of the methyl group, and the second removes the 19-pro-*R* hydrogen atom yielding a *gem*-diol that produces the 19-aldehyde derivative (Figure 36).

The final step is the nucleophilic attack of the iron-peroxo intermediate $Fe^{III}-OO^-$ (or its protonated form) generated during the third catalytic cycle. This decarbonylation reaction involves the stereospecific removal of the 1$\beta$ and the 2$\beta$ hydrogens to produce the phenolic A-ring of estrone while the 19-methyl group is eliminated as formic acid. As already mentioned in section 6.1, synthetic peroxo-metalloporphyrins are able to catalyze this decarbonylation step.[134,135] The same mechanism with a nucleophilic addition of the Fe(III)-peroxo species onto a carbonyl function is also involved in the final step of the formation of 17$\alpha$-hydroxyandrogen (androst-5-ene-3$\beta$,17$\alpha$-diol) from pregnenolone, the cleavage of the C−C step generating an acetic acid molecule.[255]

Another interesting example of an unusual reactivity of a $PPIX-Fe^{III}-OOH$ intermediate is related to the oxidation of heme to biliverdin by heme oxygenase which is commonly ascribed to an electrophilic behavior of the iron(III)-peroxo species.[256,257] Heme oxygenase is a unique enzyme able to remove the excess of free heme by oxidation of the $\alpha$-meso position of heme which is the prosthetic group and the substrate of the enzyme. The formation of $\alpha$-*meso*-hydroheme might also be explained by the homolytic cleavage of the O−O bond of the $Fe^{III}-OOH$ intermediate, the generated hydroxyl radical being trapped by the $\alpha$-meso position. Then the resulting porphyrin radical can be oxidized by the Fe(IV)-oxo leading to the final product (such mechanism is reminiscent of that of the meso-alkylation of PPIX by artemisinin already mentioned).[186] Recent DFT calculations[258] support an O−O bond homolysis mechanism in the heme oxygenase and demonstrate that the hydroxyl radical $HO^{\bullet}$ is trapped by the heme macrocycle, hence leading to regioselective attack on the meso carbon of the porphyrin.

## 7.9. Inhibition of Cytochrome P450 Enzymes

Inhibitors of cytochrome P450 enzymes can be classified in three categories: (i) reversible inhibitors, that is, molecules with high affinity for the active site of the enzymes, but without formation of covalent bonds with the prosthetic group or with the apoprotein; (ii) quasi-irreversible inhibitors, that is, molecules containing a heteroatom (for example, a nitrogen atom of an aromatic heterocycle) and able to bind to the prosthetic group via a covalent iron−heteroatom bond (the stability of the inhibitor−P450 adduct is related to the strength of the iron−heteroatom bond which is usually also dependent on the oxidation state of the metal center); and (iii) irreversible inhibitors (suicide inhibitors) which are covalently linked to the protein itself after being activated during one of the different steps of the catalytic cycle of the enzyme. The present section is focused only on some recent mechanistic aspects of P450 inhibition by drugs or drug candidates (for a general and exhaustive review on P450 inhibitors, see ref 215).

The understanding of P450 inhibition at the molecular level is of particular importance in drug development and drug therapy, since the pharmacological activity of a drug can be highly modulated by its metabolism by native or drug-induced P450 enzymes. The overproduction of a toxic metabolite from a drug by a P450 induced via the uptake of a second drug can be at the origin of alarming toxicological situations during multidrug therapies, in particular with drugs having a narrow therapeutic window. Fortunately, this is not the case when both drugs have low affinities for the enzyme; then no

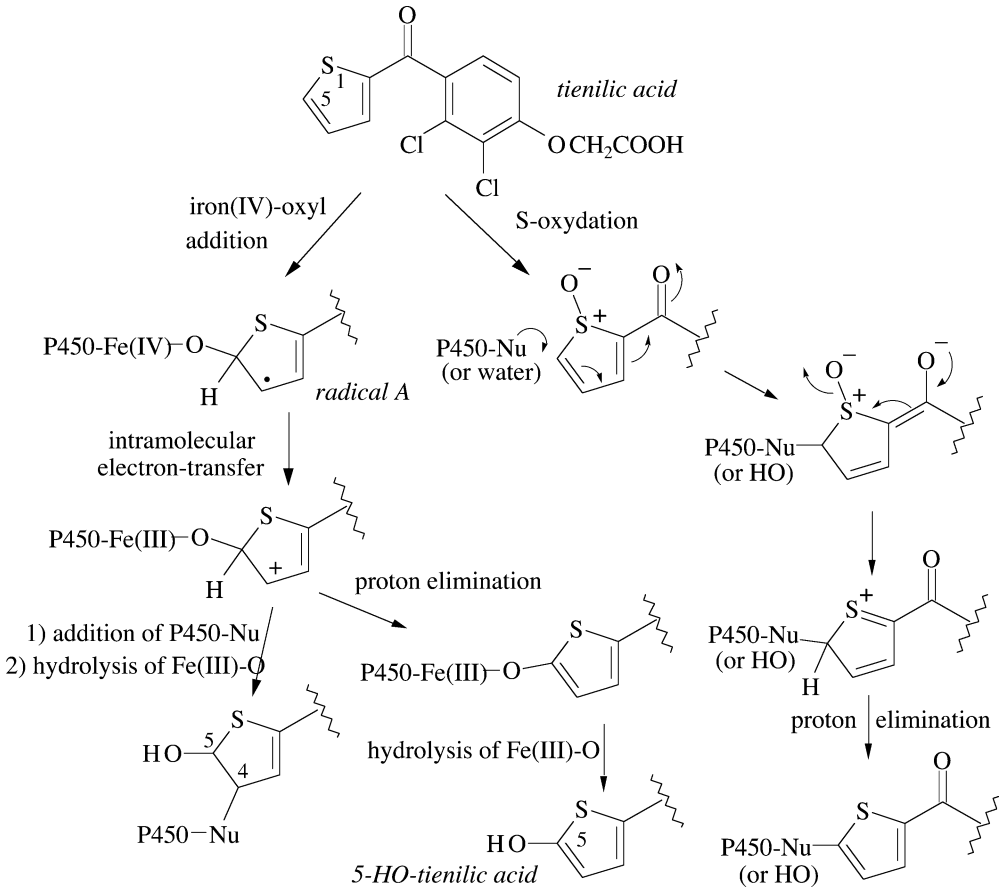


**Figure 37.** Inhibition of cytochrome P450 during the oxidative metabolization of tienilic acid, a diuretic drug.

interaction is observed at the low level of drug normally seen in vivo. Similarly, the overexpression of a particular P450 enzyme can lead to the fast elimination of a drug, which thereby limits its pharmacological activity. A significant drug−drug interaction occurs when two or more drugs compete for the same P450 enzyme and when the metabolic pathway is a major elimination pathway. Among the recent examples of drug−drug interactions, one should take note of the inhibition of human liver microsomal oxidation of nicotine by menthol, a classical flavoring ingredient of cigarettes.[259] These ADME-toxicology factors correspond to 70% of the failures observed in preclinical and clinical development of drugs (ADME: absorption−distribution−metabolism−excretion) and have recently favored the growth of more efficient in silico based models of metabolism and biodistribution.[260]

Around 70% of human liver P450 is represented by CYP1A2, 2A6, 2B6, 2C, 2D6, 2E1, and 3A enzymes (the subfamilies CYP3A and CYP2C are the most abundant ones).[261] Despite a sequence similarity as high as 80%, substrate specificity can be very high. This is the case for CYP2C9, which is responsible for the metabolization of diclofenac or tienilic acid, and for CYP2C8 which is involved in the oxidation of retinoic acid or benzo[*a*]pyrene.[262] Tienilic acid is a diuretic drug acting as a specific inhibitor of human cytochrome P450 2C9 after being oxidized by the same isozyme.[263,264] The high-performance liquid chromatography/electrospray ionization mass spectrometry data indicate that CYP2C9 can be alkylated one or two times by the electrophilic metabolite of tienilic acid. Two different oxidation routes have been proposed for product formation (5-hydroxytienilic acid) and the irreversible cytochrome P450 inactivation: (i) an addition of the iron(IV)-oxyl species to the C4−C5 bond (left side of Figure 37) or sulfoxidation of the thiophene (right side). An intermediate epoxide can be generated from the transient radical A via the homolytic cleavage of the iron(IV)−oxygen bond.

This figure is a personal (by one of us, B.M.) interpretation of the data reported by Trager et al.,[264] but these mechanistic proposals are fully compatible with the reported experimental data. In addition, the intramolecular electron transfer proposed after the addition of the iron-oxyl entity will predict the addition of a nucleophilic amino acid residue of CYP2C9 at carbon C4 (the nucleophilic addition being favored at C5 in the *S*-oxide route).

CYP3A4 is major cytochrome P450 isoform present in human liver and is responsible for the oxidative metabolism of over 60% of clinically relevant drugs (acetaminophen, cyclosporin, lovastatin, erythromycin, lidocaine, etc.). A study of the inhibition of this particular P450 by a potential HIV protease inhibitor (L-754,394, see Figure 38) indicates that a reactive furanopyridine epoxide intermediate is responsible for the covalent binding of the drug to the protein, probably via the nucleophilic addition of Glu-307.[265]

This later hypothesis is compatible with a computer-generated structure of CYP3A4 containing the drug candidate.

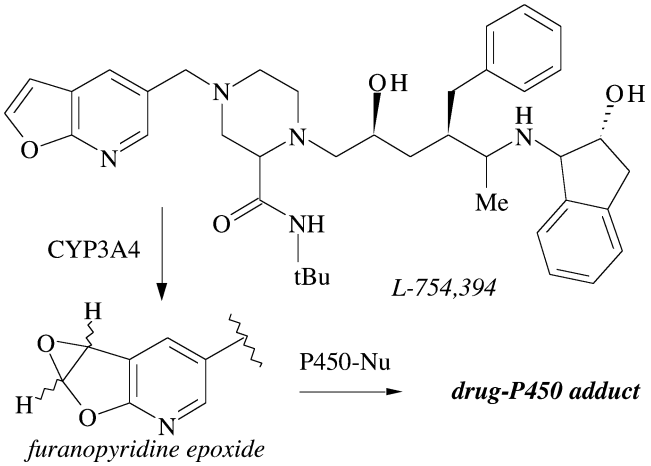


**Figure 38.** Inhibition of cytochrome P450 by L-754,394, a HIV protease inhibitor.

Clopidogrel (SR25990C, Plavix) is a potent anti-aggregant drug able to prevent thrombotic problems (myocardial infarction and stroke).[266] The specific pharmacological target of this drug is the ADP-induced platelet activation process, and the activity of clopidogrel is dependent on its biotransformation to an active metabolite by cytochrome P450 to generate the drug-target adduct. The same active species, a thiol-containing intermediate (see Figure 39), is able to inhibit $CYP_{2C9}$ and $CYP_{1A2}$ via the formation of a disulfide bridge with a cysteine residue of the enzyme.[267]

The improved understanding of the mechanisms of P450-catalyzed reactions accumulated over the past decade is now generating the expected benefit to all the studies concerning the inhibition of cytochromes P450 by drugs and the delicate problem of drug−drug interactions mediated by cytochromes P450.

## 8. Example of a P450-Mediated Oxidation without Strong Mechanistic Proposal (Orphan Mechanism!)

The biosynthesis of pregnenolone involves the degradation of the side chain of cholesterol by a specific mitochondrial cytochrome $P450_{scc}$. The C20−C22 bond of cholesterol is cleaved via three consecutive oxidation steps.[252,268] The first two steps, that is, the 22(*R*)- and 20(*S*)-hydroxylations, are easy to understand, but the mechanism of the C−C bond cleavage of the intermediate glycol (third step) is obscure and is still a matter of debate with many different speculative hypotheses.[269] Despite recent efforts on the mechanism of C−C bond cleavage in tertiary alcohol oxidations with biomimetic catalytic systems,[270,271] the cleavage of a C−C bond of a diol by a cytochrome P450 is still a black box. We propose two different hypotheses (see Figure 40) concerning the mechanism of the C−C bond cleavage of the diol: (i) a concerted reaction within a seven-membered ring transition state (Figure 40A) or (ii) the formation of an intermediate iron-peroxide that will be the driving force for the heterolytic cleavage of the C−C bond (Figure 40B).

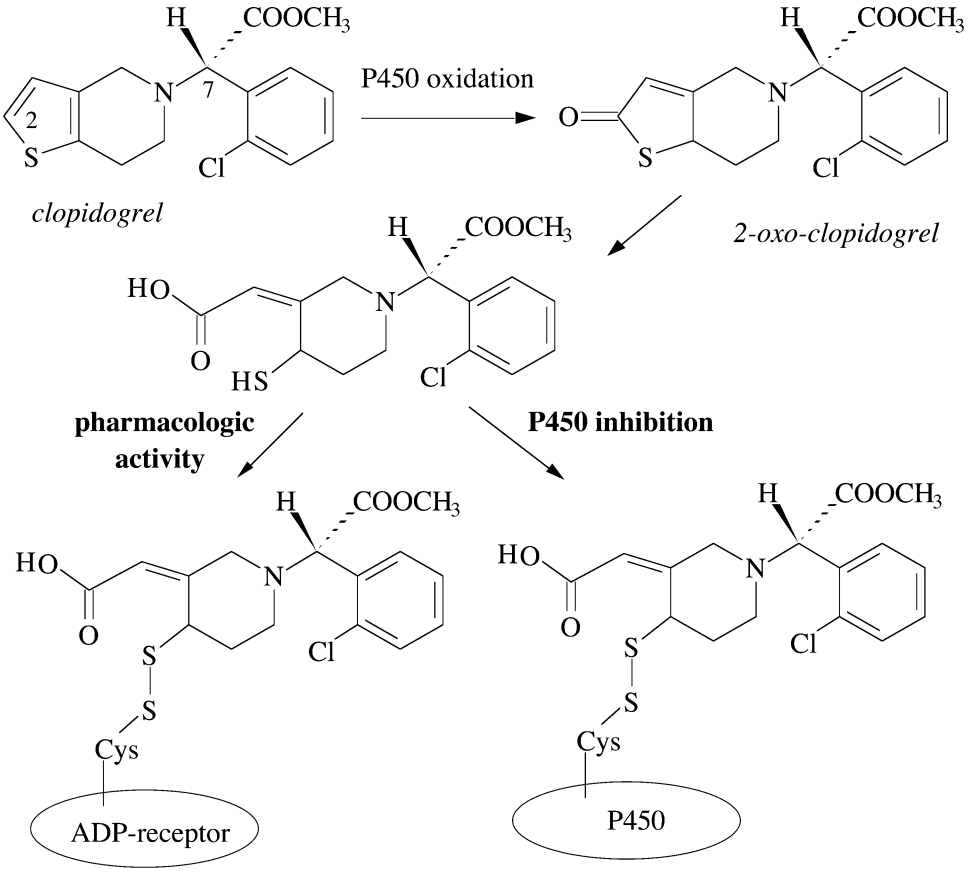


**Figure 39.** Mechanism of inhibition of cytochrome P450 by clopidogrel, an antithrombotic drug.

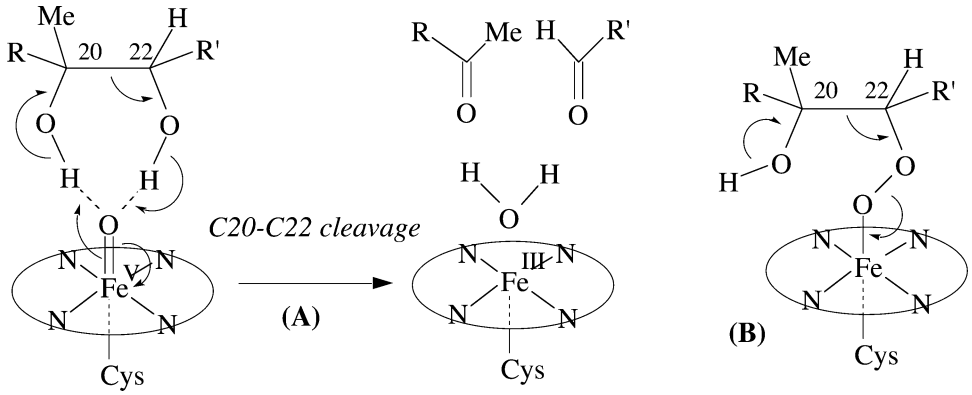


**Figure 40.** Two mechanistic proposals for the C−C bond cleavage of the side chain of cholesterol by cytochrome P450: (A) via a concerted mechanism and (B) with an intermediate iron-peroxo.

Up to now, neither of these two mechanistic proposals has been documented by suitable experiments.

## 9. Remarks in Conclusion

More than 40 years after the discovery of cytochrome P450 enzymes, the exact nature of the active species (the putative high-valent iron-oxo intermediate) is still a matter of intensive debates. These scientific debates are in fact highly fruitful: they forced trialogues among enzymologists, structural biologists, and chemists. Furthermore, they inspired the use of chemical models to generate data that could be compared with data obtained with the enzymes. Site-directed mutagenesis studies in conjunction with structural studies allowed different hypotheses to be checked. Theoretical calculations became available and enabled various hypotheses to be tested and new solutions to be offered. All these studies have enriched the knowledge on molecular enzymology and the coordination chemistry of metal-peroxo and high-valent metal-oxo species. This is physical chemical biology at its best!

## 10. Abbreviations

| | |
|---|---|
| ADME | adsorption−disposition−metabolism−excretion |
| ADP | adenosine diphosphate |
| Cpd I or II | compound I or II of a heme-peroxidase, an iron(IV)-oxo radical-cation species or an iron(IV)-oxo species, respectively (originally used only for peroxidases, but the new trend is also to use compound I to name the high-valent iron-oxo oxygenating species of cytochrome P-450) |
| DFT | density functional theory |
| FAD | flavin adenine dinucleotide |
| $Fe^{III}$−OOH | precursor of Cpd I |
| FMN | flavin mononucleotide |
| GSH | γ-L-glutamyl-L-cysteinyl-glycine (glutathione) |
| KIE | kinetic isotope effect |
| sMMO | soluble methane monooxygenase |
| NAD(P)H | reduced form of nicotinamide adenine dinucleotide (phosphate) |
| NOS | nitric oxide synthase |
| Por | porphyrin |
| PPIX | protoporphyrin-IX |
| dioxy-P450 | dioxygen complex of cytochrome P450−$Fe^{II}$ |
| QM/MM | hybrid quantum mechanical/molecular mechanical calculations |
| TMP | the dianion of *meso*-tetramesitylporphyrin ligand |
| TMPyP | the dianion of *meso*-tetrakis(4-methylpyridiniumyl)porphyrin ligand |

## 11. Acknowledgments

All the authors are deeply indebted to their collaborators and co-workers whose names are listed in several references of this review article. B.M. is also grateful to the Alexander Von Humboldt Foundation for the Von Humboldt−Gay Lussac Award that made possible most of his part of the manuscript preparation during a stay in the Chemistry Department of Dortmund University with Professor Bernhard Lippert in July 2003 (his hospitality is warmly acknowledged). Many references handled by B.M. were collected with the help of Philippe Erraud (LCC-CNRS). The work at the HU was supported in part by an ISF (Israeli Science Foundation) grant and a GIF (German−Israeli Foundation) grant to S.S.

## 12. References

(1) *Cytochrome P450*: *Structure, Mechanism and Biochemistry*; Ortiz de Montellano, P. R., Ed.; Plenum: New York, 1995.
(2) Hayaishi, O. *Molecular Mechanism of Oxygen Activation*; Academic Press: New York, 1974.
(3) Gunsalus, I. C.; Pederson, T. C.; Sligar, S. G. *Annu. Rev. Biochem.* **1975**, *44*, 377.
(4) Omura, T.; Ishimura, Y.; Fujii-Kuriyama, Y. *Cytochrome P450*; Kodansha: Tokyo, 1993.
(5) Guengerich, F. P. *Chem. Res. Toxicol.* **2001**, *14*, 611.
(6) Ortiz de Montellano, P. R.; De Voss, J. J. *Nat. Prod. Rep.* **2002**, *19*, 477.
(7) Meunier, B.; Bernadou, J. *Struct. Bonding* **2000**, *97*, 1.
(8) Loew, G. H.; Harris, D. L. *Chem. Rev.* **2000**, *100*, 407.
(9) (a) Sono, M.; Roach, M. P.; Coulter, E. D.; Dawson, J. H. *Chem. Rev.* **1996**, *96*, 2841. (b) Mansuy, D.; Battioni, P. *Bioinorganic Catalysis*; Reedijk, J., Ed.; Marcel Dekker: New York, 1993; pp 395−424. (c) Woggon, W.-D. *Top. Curr. Chem.* **1996**, *184*, 39.
(10) Filatov, M.; Reckien, W.; Peyerimhoff, S. D.; Shaik, S. *J. Phys. Chem. A* **2000**, *104*, 12014.
(11) Estabrook, R. W. *Drug Metab. Rev.* **2003**, *31*, 1461.
(12) Omura, T. *Biochem. Biophys. Res. Commun.* **1999**, *266*.
(13) Sheweita, S. A. *Curr. Drug Metab.* **2000**, *1*, 107.
(14) Axelrod, J. *J. Biol. Chem.* **1955**, *214*, 753.
(15) Klingenberg, M. *Arch. Biochem. Biophys.* **1958**, *75*, 376.
(16) Omura, T.; Sato, R. *J. Biol. Chem.* **1962**, *237*, 1375.
(17) Estabrook, R. W.; Cooper, D. Y.; Rosenthal, O. *Biochem. Z.* **1963**, *338*, 741.
(18) Ichikawa, Y.; Yamano, T. *Biochim. Biophys. Acta* **1967**, *131*, 490.
(19) Guengerich, F. P.; Hosea, N. A.; Parikh, A.; Bell-Parikh, L. C.; Johnson, W. W.; Gillam, E. M. J.; Shimida, T. *Drug Metab. Dispos.* **1998**, *26*, 1175.

(20) Roberts, G. A.; Grogan, G.; Greter, A.; Flitsch, S. L.; Turner, N. J. *J. Bacteriol.* **2002**, *184*, 3898.
(21) Maurer, S. C.; Schulze, H.; Schmid, R. D.; Urlacher, V. *Adv. Synth. Catal.* **2003**, *345*, 802.
(22) Nelson, D. R.; Strobel, H. W. *Mol. Biol. Evol.* **1988**, *4*, 572.
(23) Lewis, D. F. V.; Watson, E.; Lake, B. G. *Mutat. Res.* **1998**, *410*, 245.
(24) Nelson, D. R. In *Cytochrome P450*: *Structure, Mechanism and Biochemistry*; Ortiz de Montellano, P. R., Ed.; Plenum: New York, 1995; Appendix A, pp 575−606.
(25) Nebert, D. W.; Adesnik, M.; Coon, M. J.; Estabrook, R. W.; Gonzalez, F. J.; Guengerich, F. P.; Gunsalus, I. C.; Johnson, E. F.; Kemper, B.; Levin, W.; Phillips, I. R.; Sato, R.; Waterman, M. R. *DNA* **1987**, *6*, 1.
(26) Nebert, D. W.; Nelson, D. R.; Coon, M. J.; Estabrook, R. W.; Feyereisen, R.; Fujii-Kuriyama, Y.; Gonzalez, F. J.; Guengerich, F. P.; Gunsalus, I. C.; Johnson, E. F.; Loper, J. C.; Sato, R.; Waterman, M. R.; Waxman, D. J. *DNA Cell Biol.* **1991**, *10*, 1.
(27) Nelson, D. R.; Kamataki, T.; Waxman, D. J.; Guengerich, F. P.; Estabrook, R. W.; Feyereisen, R.; Gonzalez, F. J.; Coon, M. J.; Gunsalus, I. C.; Gotoh, O.; Okuda, K.; Nebert, D. W. *DNA Cell Biol.* **1993**, *12*, 1.
(28) Nelson, D. R. *Arch. Biochem. Biophys.* **1999**, *369*, 1.
(29) Lewis, D. F. V. *Cytochromes P450*: *Structure, Function and Mechanism*; Taylor and Francis: London, 1996.
(30) Tosha, T.; Yoshioka, S.; Hori, H.; Takahashi, S.; Ishimori, K.; Morishima, I. *Biochemistry* **2002**, *41*, 13883.
(31) Unno, M.; Shimada, H.; Toba, Y.; Makino, R.; Ishimura, Y. *J. Biol. Chem.* **1996**, *271*, 17869.
(32) Shimada, H.; Nagano, S.; Ariga, Y.; Unno, M.; Egawa, T.; Hishiki, T.; Ishimura, Y.; Masuya, F.; Obata, T.; Hori, H. *J. Biol. Chem.* **1999**, *274*, 9363.
(33) Modi, S.; Sutcliffe, M. J.; Primrose, W. U.; Lian, L. Y.; Roberts, G. C. K. *Nat. Struct. Biol.* **1996**, *3*, 414.
(34) Kirton, S. B.; Baxter, C. A.; Sutcliffe, M. J. *Adv. Drug Delivery* **2002**, *54*, 385.
(35) Rao, S.; Aoyama, R.; Schrag, M.; Trager, W. F.; Rettie, A.; Jones, J. P. *J. Med. Chem.* **2000**, *43*, 2789.
(36) Poulos, T. L. *Methods Enzymol.* **1991**, *206*, 11.
(37) Hodgson, J. *Nat. Biotechnol.* **2001**, *19*, 722.
(38) Rozman, D.; Strömstedt, M.; Tsui, L.-C.; Scherer, S. W.; Waterman, M. R. *Genomics* **1996**, *38*, 371.
(39) Ferrari, L.; Peng, N.; Halpert, J. R.; Morgan, E. T. *Mol. Pharmacol.* **2001**, *60*, 209.
(40) Singleton, D. W.; Lei, X.-D.; Webb, S. J.; Prough, R. A.; Geoghegan, T. E. *Drug Metab. Dispos.* **1999**, *27*, 193.
(41) Poulos, T. L.; Finzel, B. C.; Gunsalus, I. C.; Wagner, G. C.; Kraut, J. *J. Biol. Chem.* **1985**, *260*, 16122.
(42) Poulos, T. L.; Finzel, B. C.; Howard, A. J. *J. Mol. Biol.* **1987**, *195*, 687.
(43) Schlichting, I.; Jung, C.; Schulze, H. *FEBS Lett.* **1997**, *415*, 253.
(44) Chen, X.; Christopher, A.; Jones, J. P.; Bell, S. G.; Guo, Q.; Xu, F.; Rao, Z.; Wong, L.-L. *J. Biol. Chem.* **2002**, *277*, 37519.
(45) Ravichandran, K. G.; Boddupalli, S. S.; Hasemann, C. A.; Peterson, J. A.; Deisenhofer, J. *Science* **1993**, *261*, 731.
(46) Hi, H.; Poulos, T. L. *Nat. Struct. Biol.* **1997**, *4*, 140.
(47) Hasemann, C. A.; Ravichandran, K. G.; Peterson, J. A.; Deisenhofer, J. *J. Mol. Biol.* **1994**, *236*, 1169.
(48) Cupp-Vickery, J. R.; Poulos, T. L. *Nat. Struct. Biol.* **1995**, *2*, 144.
(49) Cupp-Vickery, J. R.; Poulos, T. L. *Steroids* **1997**, *62*, 112.
(50) Cupp-Vickery, J. R.; Garcia, C.; Hofacre, A.; McGee-Estrada, K. *J. Mol. Biol.* **2001**, *311*, 101.
(51) Shimizu, H.; Park, S.-Y.; Gomi, Y.; Arakawa, H.; Nakamura, H.; Adachi, S.-I.; Obayashi, E.; Iizuka, T.; Shoun, H.; Shiro, Y. *J. Biol. Chem.* **2000**, *275*, 4816.
(52) Yano, J. K.; Koo, L. S.; Schuller, D. J.; Li, H.; Ortiz de Montellano, P. R.; Poulos, T. L. *J. Biol. Chem.* **2000**, *275*, 31086.
(53) Podust, L. M.; Poulos, T. L.; Watermann, M. R. *Proc. Natl. Acad. Sci. U.S.A.* **2001**, *98*, 3068.
(54) Williams, P. A.; Cosme, J.; Sridhar, V.; Johnson, E. F.; McRee, D. E. *Mol. Cell.* **2000**, *5*, 121.
(55) Wester, M. R.; Johnson, E. F.; Marques-Soares, C.; Dijols, S.; Dansette, P. M.; Mansuy, D.; Stout, C. D. *Biochemistry* **2003**, *42*, 9335.
(56) Zerbe, K.; Pylypenko, O.; Vitali, F.; Zhang, W.; Rouset, S.; Heck, M.; Vrijbloed, J. W.; Bischoff, D.; Bister, B.; Süssmuth, R. D.; Pelzer, S.; Wohlleben, W.; Robinson, J. A.; Schlichting, I. *J. Biol. Chem.* **2002**, *277*, 47476.
(57) Podust, L. M.; Kim, Y.; Arase, M.; Neely, B. A.; Beck, B. J.; Bach, H.; Sherman, D. H.; Lamb, D. C.; Kelly, S. L.; Waterman, M. R. *J. Biol. Chem.* **2003**, *278*, 12214.
(58) Lee, D.-S.; Yamada, A.; Sugimoto, H.; Matsunaga, I.; Ogura, H.; Ichihara, K.; Adachi, S.-I.; Park, S.-Y.; Shiro, Y. *J. Biol. Chem.* **2003**, *278*, 9761.
(59) Yano, J. K.; Blasco, F.; Li, H.; Schmid, R. D.; Henne, A.; Poulos, T. J. *J. Biol. Chem.* **2003**, *278*, 608.
(60) Williams, P. A.; Cosme, J.; Ward, A.; Angove, H. C.; Matak Vinkovic, D.; Jhoti, H. *Nature* **2003**, *424*, 464.
(61) Sevrioukova, I. R.; Li, H.; Zhang, H.; Peterson, J. A.; Poulos, T. L. *Proc. Natl. Acad. Sci. U.S.A.* **1999**, *96*, 1863.
(62) Wong, L.-L.; Westlake, A. C. G.; Nickerson, D. P. *Struct. Bonding* **1997**, *88*, 175.
(63) Raag, R.; Li, H.; Jones, B. C.; Poulos, T. L. *Biochemistry* **1993**, *32*, 4571.
(64) Stevenson, J.-A.; Westlake, A. C. G.; Whittock, C.; Wong, L.-L. *J. Am. Chem. Soc.* **1996**, *118*, 12846.
(65) De Voss, J. J.; Sibbesen, O.; Zhang, Z.; Ortiz de Montellano, P. R. *J. Am. Chem. Soc.* **1997**, *119*, 5489.
(66) Dmochowski, I. J.; Crane, B. R.; Wilker, J. J.; Winkler, J. R.; Gray, H. B. *Proc. Natl. Acad. Sci. U.S.A.* **1999**, *96*, 12987.
(67) Li, Q.-S.; Schwaneberg, U.; Fischer, P.; Schmid, R. D. *Chem.—Eur. J.* **2000**, *6*, 1531.
(68) Loew, G. H.; Kert, C. J.; Hjelmeland, L. M.; Kirchner, R. F. *J. Am. Chem. Soc.* **1977**, *99*, 3534.
(69) Cramer, C. J. *Essentials of Computational Chemistry*: *Theories and Models*; Wiley: Chichester, 2002.
(70) Shaik, S.; de Visser, S. P.; Ogliaro, F.; Schwarz, H.; Schröder, D. *Curr. Opin. Chem. Biol.* **2002**, *6*, 556.
(71) Shaik, S.; Cohen, S.; de Visser, S. P.; Sharma, P. K.; Kumar, D.; Kozuch, S.; Ogliaro, F.; Danovich, D. *Eur. J. Inorg. Chem.* **2004**, 207.
(72) Shaik, S.; de Visser, S. P. In *Cytochrome P450*: *Structure, Mechanisms and Biochemistry*, 3rd ed.; Ortiz de Montellano, P. R., Ed.; Plenum Press: New York, 2003; Chapter 2, pp X−Y.
(73) Ullrich, V. *Top. Curr. Chem.* **1979**, *83*, 67.
(74) Groves, J. T.; Han, Y. Z. In *Cytochrome P450*: *Structure, Mechanism and Biochemistry*; Ortiz de Montellano, P. R., Ed.; Plenum: New York, 1995; Chapter 1, pp 3−48.
(75) (a) Meunier, B. *Chem. Rev.* **1992**, *92*, 1411. (b) Bernadou, J.; Meunier, B. *Adv. Synth. Catal.* **2004**, *346*, 171.
(76) Mansuy, D. *Pure Appl. Chem.* **1994**, *66*, 737.
(77) Dolphin, D.; Traylor, T. G.; Xie, L. Y. *Acc. Chem. Res.* **1997**, *30*, 259.
(78) Bernadou, J.; Meunier, B. *Chem. Commun.* **1998**, 2167.
(79) Meunier, B. *Biomimetic Oxidations Mediated by Metal Complexes*; Imperial College Press: London, 2000.
(80) Meunier, B.; Robert, A.; Pratviel, G.; Bernadou, J. In *The Porphyrin Handbook*; Kadish, K. M., Smith, K., Guilard, R., Eds.; Academic Press: San Diego, 2000; Vol. 4, Chapter 31, pp 119−187.
(81) (a) Vaz, A. D. N.; McGinnity, D. F.; Coon, M. J. *Proc. Natl. Acad. Sci. U.S.A.* **1998**, *95*, 3555. (b) Chandrasena, R. E. P.; Vatsis, K. P.; Coon, M. J.; Hollenberg, P. F.; Newcomb, M. *J. Am. Chem. Soc.* **2004**, *126*, 115.
(82) Burger, R. M. *Struct. Bonding* **2000**, *97*, 289.
(83) Griffin, B. W.; Peterson, J. A. *Biochemistry* **1972**, *11*, 4740.
(84) Atkins, W. A.; Sligar, S. G. *Biochemistry* **1990**, *29*, 1271.
(85) Helms, V.; Wade, R. C. *Proteins* **1998**, *32*, 381.
(86) Lüdemann, S. K.; Lounnas, V.; Wade, R. C. *J. Mol. Biol.* **2000**, *303*, 797, 813.
(87) Winn, P. J.; Lüdemann, S. K.; Gauges, R.; Lounnas, V.; Wade, R. C. *Proc. Natl. Acad. Sci. U.S.A.* **2002**, *99*, 5361.
(88) Raag, R.; Poulos, T. L. *Biochemistry* **1989**, *28*, 7586.
(89) Hanson, L. K.; Eaton, W. A.; Sligar, S. G.; Gunsalus, I. C.; Gouterman, M.; Connell, C. R. *J. Am. Chem. Soc.* **1976**, *98*, 2672.
(90) Caron, C.; Mitschler, A.; Rivere, G.; Ricard, L.; Schappacher, M.; Weiss, R. *J. Am. Chem. Soc.* **1979**, *101*, 7401.
(91) Ueno, T.; Kuosumi, Y.; Yoshizawa-Kumagaye, K.; Nakajima, K.; Ueyama, N.; Okamura, T. A.; Nakamura, A. *J. Am. Chem. Soc.* **1998**, *120*, 12264.
(92) Auclair, K.; Moënne-Loccoz, P.; Ortiz de Montellano, P. R. *J. Am. Chem. Soc.* **2001**, *123*, 4877.
(93) (a) Harris, D. L.; Loew, G. H. *J. Am. Chem. Soc.* **1993**, *115*, 5799. (b) Harris, D. L.; Loew, G. H. *J. Am. Chem. Soc.* **1993**, *115*, 8775.
(94) Aissaoui, H.; Bachmann, R.; Schweiger, A.; Woggon, W.-D. *Angew. Chem., Int. Ed.* **1998**, *37*, 2998.
(95) Green, M. T. *J. Am. Chem. Soc.* **1998**, *120*, 10772.
(96) Filatov, M.; Harris, N.; Shaik, S. *J. Chem. Soc., Perkin Trans. 2* **1999**, 399.
(97) (a) Scherlis, D. A.; Cymeryng, C. B.; Estrin, D. A. *Inorg. Chem.* **2000**, *39*, 2352. (b) Scherlis, D. A.; Martí, M. A.; Ordejón, P.; Estrin, D. A. *Int. J. Quantum Chem.* **2002**, *90*, 1505.
(98) Ogliaro, F.; de Visser, S. P.; Shaik, S. *J. Inorg. Biochem.* **2002**, *91*, 554.
(99) Loida, P. J.; Sligar, S. G. *Biochemistry* **1993**, *32*, 11530.
(100) Egawa, T.; Ogura, T.; Makino, R.; Ishimura, Y.; Kitagawa, T. *J. Biol. Chem.* **1991**, *266*, 10246.
(101) MacDonald, I. D. G.; Sligar, S. G.; Christian, J. F.; Unno, M.; Champion, P. M. *J. Am. Chem. Soc.* **1999**, *121*, 376.
(102) Benson, D. E.; Suslick, K. S.; Sligar, S. G. *Biochemistry* **1997**, *36*, 5104.
(103) Vidakovic, M.; Sligar, S. G.; Li, H.; Poulos, T. L. *Biochemistry* **1998**, *37*, 9211.
(104) Harris, D. L.; Loew, G. H. *J. Am. Chem. Soc.* **1998**, *120*, 8941.
(105) Harris, D. L.; Loew, G. H.; Waskell, L. *J. Am. Chem. Soc.* **1998**, *120*, 4308.
(106) Harris, D. L.; Loew, G. H. *J. Am. Chem. Soc.* **1994**, *116*, 11671.

(107) Harris, D. L.; Loew, G. H. *J. Am. Chem. Soc.* **1996**, *118*, 6377.
(108) Gerber, N. C.; Sligar, S. G. *J. Am. Chem. Soc.* **1992**, *114*, 8742.
(109) Raag, R.; Martinis, S. A.; Sligar, S. G.; Poulos, T. L. *Biochemistry* **1991**, *30*, 11420.
(110) Yeom, H.; Sligar, S. G.; Li, H.; Poulos, T. L.; Fulco, A. J. *Biochemistry* **1995**, *34*, 14733.
(111) Toy, P. H.; Newcomb, M.; Coon, M. J.; Vaz, A. D. N. *J. Am. Chem. Soc.* **1998**, *120*, 9718.
(112) Newcomb, M.; Toy, P. H. *Acc. Chem. Res.* **2000**, *33*, 449.
(113) Davydov, R.; Makris, T. M.; Kofman, V.; Werst, D. E.; Sligar, S. G.; Hoffmann, B. M. *J. Am. Chem. Soc.* **2001**, *13*, 1403.
(114) Schlichting, I.; Berendzen, J.; Chu, K.; Stock, A. M.; Maves, S. A.; Benson, D. E.; Sweet, R. M.; Ringe, D.; Pestko, G. A.; Sligar, S. G. *Science* **2000**, *287*, 1615.
(115) Schlichting, I. Personal communication with B.M., Dortmund, July 2003.
(116) Ogliaro, F.; de Visser, S. P.; Cohen, S.; Sharma, P. K.; Shaik, S. *J. Am. Chem. Soc.* **2002**, *124*, 2806.
(117) Kamachi, T.; Yoshizawa, K. *J. Am. Chem. Soc.* **2003**, *125*, 4652.
(118) Gualar, V.; Harris, D. L.; Batista, V. S.; Miller, W. H. *J. Am. Chem. Soc.* **2002**, *124*, 1430.
(119) Harris, D. L. *J. Inorg. Biochem.* **2002**, *91*, 568.
(120) Shaik, S.; Filatov, M.; Schröder, D.; Schwarz, H. *Chem.—Eur. J.* **1998**, *4*, 193.
(121) *Peroxidases in Chemistry and Biology*; Everse, J., Everse, K. E., Grisham, M. B., Eds.; CRC Press: Boca Raton, FL, 1991; 2 volumes.
(122) Meunier, B. In *Comprehensive Coordination Chemistry II*; McClaverty, J., Meyer, T. J., Eds.; Elsevier: New York, 2003; Vol. 8, pp 261−280.
(123) Yamamoto, S.; Teraoka, J.; Kashiwagi, H. *J. Chem. Phys.* **1988**, *88*, 303.
(124) Harris, D. L.; Loew, G. H.; Waskell, L. *J. Inorg. Biochem.* **2001**, *83*, 309.
(125) Ogliaro, F.; Cohen, S.; Filatov, M.; Harris, N.; Shaik, S. *Angew. Chem., Int. Ed.* **2000**, *39*, 3851.
(126) Ogliaro, F.; de Visser, S. P.; Cohen, S.; Kaneti, J.; Shaik, S. *ChemBioChem* **2001**, *2*, 848.
(127) Antony, J.; Grodzicki, M.; Trautwein, A. X. *J. Phys. Chem. A* **1997**, *101*, 2692.
(128) Green, M. T. *J. Am. Chem. Soc.* **1999**, *121*, 7939.
(129) Ohta, T.; Matsuura, K.; Yoshizawa, K.; Morishima, I. *J. Inorg. Biochem.* **2000**, *82*, 141.
(130) Ogliaro, F.; Harris, N.; Cohen, S.; Filatov, M.; de Visser, S. P.; Shaik, S. *J. Am. Chem. Soc.* **2000**, *122*, 8977.
(131) Ogliaro, F.; Cohen, S.; de Visser, S. P.; Shaik, S. *J. Am. Chem. Soc.* **2000**, *122*, 12892.
(132) Schöneboom, J. C.; Lin, H.; Reuter, N.; Thiel, W.; Cohen, S.; Ogliaro, F.; Shaik, S. *J. Am. Chem. Soc.* **2002**, *124*, 8142.
(133) Rutter, R.; Hager, L. P.; Dhonau, H.; Hendrich, M.; Valentine, M.; Debrunner, P. *Biochemistry* **1984**, *23*, 6809.
(134) Sisemore, M. F.; Selke M.; Burstyn, J. N.; Valentine, J. S. *Inorg. Chem.* **1997**, *36*, 979.
(135) Selke, M.; Valentine, J. S. *J. Am. Chem. Soc.* **1998**, *120*, 2652.
(136) Wertz, D. L.; Valentine, J. S. *Struct. Bonding* **2000**, *97*, 37.
(137) Wertz, D. L.; Sisemore, M. F.; Selke, M.; Driscoll, J.; Valentine, J. S. *J. Am. Chem. Soc.* **1998**, *120*, 5331.
(138) Ozette, K.; Leduc, P.; Palacio, M.; Bartoli, J. F.; Barkigia, K. M.; Fajer, J.; Battioni, P.; Mansuy, D. *J. Am. Chem. Soc.* **1997**, *119*, 6442.
(139) Bartoli, J.-F.; Le Barch, K.; Palacio, M.; Battioni, P.; Mansuy, D. *Chem. Commun.* **2001**, 1718.
(140) Chen, K.; Costas, M.; Kim, J.; Tipton, A. K.; Que, L. *J. Am. Chem. Soc.* **2002**, *124*, 3026.
(141) Rohde, J.-U.; In, J.-H.; Lim, M. I.; Brennessel, W. W.; Bukowski, M. R.; Stubna, A.; Münck, E.; Nam, W.; Que, L. *Science* **2003**, *299*, 1037.
(142) Groves, J. T.; Haushalter, R. C.; Nakamura, M.; Nemo, T. E.; Evans, B. J. *J. Am. Chem. Soc.* **1981**, *103*, 2884.
(143) Mandon, D.; Weiss, R.; Jayaraj, K.; Gold, A.; Terner, J.; Bill, E.; Trautwein, A. X. *Inorg. Chem.* **1992**, *31*, 4404.
(144) Watanabe, Y.; Fujii, H. *Struct. Bonding* **2000**, *97*, 61.
(145) Urano, Y.; Higuchi, T.; Hirobe, M.; Nagano, T. *J. Am. Chem. Soc.* **1997**, *119*, 12008.
(146) Woggon, W. D.; Wagenknecht, H. A.; Claude, C. *J. Inorg. Biochem.* **2001**, *83*, 289.
(147) Robert, A.; Loock, B.; Momenteau, M.; Meunier, B. *Inorg. Chem.* **1991**, *30*, 706.
(148) Bortolini, O.; Ricci, M.; Meunier, B.; Friant, P.; Ascone, I.; Goulon, J. *Nouv. J. Chim.* **1986**, *10*, 39.
(149) Ayougou, K.; Bill, E.; Charnock, J. M.; Garner, C. D.; Mandon, D.; Trautwein, A. X.; Weiss, R.; Winkler, H. *Angew. Chem., Int. Ed. Engl.* **1995**, *34*, 343.
(150) Groves, J. T.; Lee, J.; Marla, S. S. *J. Am. Chem. Soc.* **1997**, *119*, 6269.
(151) Jin, N.; Groves, J. T. *J. Am. Chem. Soc.* **1999**, *121*, 2923.
(152) de Visser, S. P.; Ogliaro, F.; Gross, Z.; Shaik, S. *Chem.—Eur. J.* **2001**, *7*, 4954.
(153) Ghosh, A.; Taylor, P. R. *Curr. Opin. Chem. Biol.* **2003**, *7*, 113.
(154) Robert, A.; Meunier, B. *New J. Chem.* **1988**, *12*, 885.
(155) Nam, W.; Valentine, J. S. *J. Am. Chem. Soc.* **1993**, *115*, 1772.
(156) Bernadou, J.; Fabiano, A. S.; Robert, A.; Meunier, B. *J. Am. Chem. Soc.* **1994**, *116*, 9375.
(157) Ingold, K. U.; MacFaul, P. A. In *Biomimetic Oxidations Catalyzed by Transition Metals*; Meunier, B., Ed.; Imperial College Press: London, 2000; Chapter 2, pp 45−89.
(158) Balahura, R. J.; Sorokin, A.; Bernadou, J.; Meunier, B. *Inorg. Chem.* **1997**, *36*, 3488.
(159) Lee, K. A.; Nam, W. *J. Am. Chem. Soc.* **1997**, *119*, 1916.
(160) Yang, S. J.; Nam, W. *Inorg. Chem.* **1998**, *37*, 606.
(161) Nam, W.; Goh, Y. M.; Lee, Y. L.; Lim, M. H.; Kim, C. *Inorg. Chem.* **1999**, *38*, 3238.
(162) Wietzerbin, K.; Muller, J. G.; Jameton, R. A.; Pratviel, G.; Bernadou, J.; Meunier, B.; Burrows, C. J. *Inorg. Chem.* **1999**, *38*, 4123.
(163) Song, R.; Sorokin, A.; Bernadou, J.; Meunier, B. *J. Org. Chem.* **1997**, *62*, 673.
(164) Sorokin, A.; Meunier, B. *Eur. J. Inorg. Chem.* **1998**, 1269.
(165) Pitié, M.; Bernadou, J.; Meunier, B. *J. Am. Chem. Soc.* **1995**, *117*, 2935.
(166) Atkinson, J. F.; Ingold, K. U. *Biochemistry* **1993**, *32*, 9209.
(167) Toy, P. H.; Newcomb, N.; Hollenberg, P. F. *J. Am. Chem. Soc.* **1998**, *120*, 7719.
(168) (a) Groves, J. T.; McClusky, G. A.; White, R. E.; Coon, M. J. *Biochem. Biophys. Res. Commun.* **1978**, *81*, 154. (b) Traylor, T. G.; Hill, K. W.; Fan, W.-P.; Tsuchiya, S.; Dunlap, B. E. *J. Am. Chem. Soc.* **1992**, *114*, 1308.
(169) Iyer, K. R.; Jones, J. P.; Darbyshire, J. F.; Trager, W. F. *Biochemistry* **1997**, *36*, 7039.
(170) Manchester, J. I.; Dinnocenzo, J. P.; Higgins, L. A.; Jones, J. P. *J. Am. Chem. Soc.* **1997**, *119*, 5069.
(171) Higgins, L. A.; Bennett, G. A.; Shimoji, M.; Jones, J. P. *Biochemistry* **1998**, *37*, 7039.
(172) Newcomb, M.; Aebisher, D.; Shen, R.; Esala, P.; Chandrasena, R.; Hollenberg, P. F.; Coon, M. J. *J. Am. Chem. Soc.* **2003**, *125*, 6064.
(173) Kumar, D.; de Visser, S. P.; Shaik, S. *J. Am. Chem. Soc.* **2003**, *125*, 13025.
(174) Fujita, M.; Costas, M.; Que, L. *J. Am. Chem. Soc.* **2003**, *125*, 9912.
(175) Lee, H.; Ortiz de Montellano, P. R.; McDermott, A. E. *Biochemistry* **1999**, *38*, 10808.
(176) Audergon, C.; Iyer, K. R.; Jones, J. P.; Darbyshire, J. F.; Trager, W. F. *J. Am. Chem. Soc.* **1999**, *121*, 41.
(177) Filatov, M.; Harris, N.; Shaik, S. *Angew. Chem., Int. Ed.* **1999**, *38*, 3510.
(178) Harris, N.; Cohen, S.; Filatov, M.; Ogliaro, F.; Shaik, S. *Angew. Chem., Int. Ed.* **2000**, *39*, 2003.
(179) Ogliaro, F.; Filatov, M.; Shaik, S. *Eur. J. Inorg. Chem.* **2000**, 2455.
(180) (a) De Visser, S. P.; Ogliaro, F.; Sharma, P. K.; Shaik, S. *Angew. Chem., Int. Ed.* **2002**, *41*, 1947. (b) de Visser, S. P.; Ogliaro, F.; Sharma, P. K.; Shaik, S. *J. Am. Chem. Soc.* **2002**, *124*, 11809.
(181) Yoshizawa, K. *Coord. Chem. Rev.* **2002**, *226*, 251.
(182) Yoshizawa, K.; Ohta, T.; Eda, M.; Yamabe, T. *Bull. Chem. Soc. Jpn.* **2000**, *73*, 401.
(183) (a) Yoshizawa, K.; Shiota, Y.; Kagawa, Y. *Bull. Chem. Soc. Jpn.* **2000**, *73*, 2669. (b) Yoshizawa, K.; Kagawa, Y.; Shiota, Y. *J. Phys. Chem. B* **2000**, *104*, 12365. (c) Yoshizawa, K.; Kamachi, T.; Shiota, Y. *J. Am. Chem. Soc.* **2001**, *123*, 9806.
(184) Newcomb, M.; Shen, R.; Choi, S.-Y.; Toy, P. H.; Hollenberg, P. F.; Vaz, A. D. N.; Coon, M. J. *J. Am. Chem. Soc.* **2000**, *122*, 2677.
(185) Robert, A.; Cazelles, J.; Meunier, B. *Angew. Chem., Int. Ed.* **2001**, *40*, 1954.
(186) Robert, A.; Cazelles, J.; Dechy-Cabaret, O.; Meunier, B. *Acc. Chem. Res.* **2002**, *35*, 167.
(187) Robert, A.; Coppel, Y.; Meunier, B. *Inorg. Chim. Acta* **2002**, *339*, 488.
(188) Auclair, K.; Hu, Z.; Little, D. M.; Ortiz de Montellano, P. R.; Groves, J. T. *J. Am. Chem. Soc.* **2002**, *124*, 6020.
(189) Newcomb, M.; Shen, R.; Lu, Y.; Coon, M. J.; Hollenberg, P. F.; Kopp, D. A.; Lippard, S. J. *J. Am. Chem. Soc.* **2002**, *124*, 6879.
(190) Bell-Parikh, L.; Guengerich, F. P. *J. Biol. Chem.* **1999**, *274*, 23833.
(191) Hecht, S. S.; Hochalter, J. B.; Villalta, P. W.; Murphy, S. E. *Proc. Natl. Acad. Sci. U.S.A.* **2000**, *97*, 12493.
(192) Ortiz de Montellano, P. R.; Stearns, R. A.; Langry, K. C. *Mol. Pharmacol.* **1984**, *25*, 310.
(193) Miller, R. E.; Guengerich, F. P. *Biochemistry* **170**, *21*, 1090.
(194) Jin, S. J.; Makris, T. M.; Bryson, T. A.; Sligar, S. G.; Dawson, J. H. *J. Am. Chem. Soc.* **2003**, *125*, 3406.
(195) Renz, M.; Meunier, B. *Eur. J. Org. Chem.* **1999**, 737.
(196) Kamachi, T.; Shiota, Y.; Ohta, T.; Yoshizawa, K. *Bull. Chem. Soc. Jpn.* **2003**, *76*, 721.
(197) (a) De Visser, S. P.; Ogliaro, F.; Harris, N.; Shaik, S. *J. Am. Chem. Soc.* **2001**, *123*, 3037. (b) de Visser, S. P.; Ogliaro, F.; Shaik, S. *Chem. Commun.* **2001**, 2322.

(198) de Visser, S. P.; Ogliaro, F.; Shaik, S. *Angew. Chem., Int. Ed.* **2001**, *40*, 2871.
(199) de Visser, S. P.; Kumar, D.; Shaik, S. *J. Inorg. Biochem.*, in press.
(200) Mayer, J. M. In *Biomimetic Oxidations Catalyzed by Transition Metal Complexes*; Meunier, B., Ed.; Imperial College Press: London, 2000; Chapter 1, pp 1−43.
(201) Sato, H.; Guengerich, F. P. *J. Am. Chem. Soc.* **2000**, *122*, 8099.
(202) Guroff, G.; Daly, J. W.; Jerina, D. M.; Renson, J.; Witkop, B.; Udenfriend, S. *Science* **1967**, *157*, 1524.
(203) Korzekwa, K. R.; Swinney, D. C.; Trager, W. F. *Biochemistry* **1989**, *28*, 9019.
(204) Vannelli, T.; Hooper, A. B. *Biochemistry* **1995**, *34*, 11743.
(205) Darbyshire, J. F.; Iyer, K. R.; Grogan, J.; Korzekwa, K. R.; Trager, W. F. *Drug Metab. Dispos.* **1996**, *24*, 1038.
(206) de Visser, S. P.; Shaik, S. *J. Am. Chem. Soc.* **2003**, *125*, 7413.
(207) (a) Bathelt, C. M.; Ridder, L.; Mulholland, A. J.; Harvey, J. N. *J. Am. Chem. Soc.* **2003**, *125*, 15004. (b) Harvey, J. N. Personal correspondence with Shaik, S.
(208) Mulder, P. P. J.; Devanesan, P.; Van Alem, K.; Lodder, G.; Rogan, E. G.; Cavalieri, E. L. *Free Radical Biol. Med.* **2003**, *34*, 734.
(209) Meunier, G.; Meunier, B. *J. Biol. Chem.* **1985**, *260*, 10576.
(210) Hissink, A. M.; Oudshoorn, M. J.; van Ommen, B.; Haenen, G. R. M. M.; van Bladeren, P. J. *Chem. Res. Toxicol.* **1996**, *9*, 1249.
(211) Guengerich, F. P.; MacDonald, T. L. *Acc. Chem. Res.* **1984**, *17*, 9.
(212) Guengerich, F. P. *J. Biol. Chem.* **1989**, *264*, 17198.
(213) Seto, Y.; Guengerich, F. P. *J. Biol. Chem.* **1993**, *268*, 9986.
(214) Guengerich, F. P.; Vaz, A. D. N.; Raner, G. N.; Pernecky, S. J.; Coon, M. J. *Mol. Pharmacol.* **1997**, *51*, 147.
(215) Ortiz de Montellano, P. R.; Correia, M. A. In *Cytochrome P450*: *Structure, Mechanism and Biochemistry*; Ortiz de Montellano, P. R., Ed.; Plenum: New York, 1995; Chapter 9, p 305.
(216) Goto, Y.; Matsui, T.; Ozaki, S.-I.; Watanabe, Y.; Fukuzumi, S. *J. Am. Chem. Soc.* **1999**, *121*, 9497.
(217) Moroni, P.; Burofosse, T.; Longin-Sauvageon, C.; Delatour, P.; Benoit, E. *Drug Metab. Dispos.* **1995**, *23*, 160.
(218) Volz, T. J.; Rock, D. A.; Jones, J. P. *J. Am. Chem. Soc.* **2002**, *124*, 9724.
(219) Sharma, P. K.; de Visser, S. P.; Shaik, S. *J. Am. Chem. Soc.* **2003**, *125*, 8698.
(220) Kedderis, G. L.; Dwyer, L. A.; Rickert, D. E.; Hollenberg, P. F. *Mol. Pharmacol.* **1983**, *23*, 758.
(221) (a) Karki, S. B.; Dinnocenzo, J. P.; Jones, J. P.; Korzekwa, K. R. *J. Am. Chem. Soc.* **1995**, *117*, 3657. (b) Guengerich, F. P.; Yun, C.-H.; MacDonald, T. L. *J. Biol. Chem.* **1996**, *271*, 27321.
(222) Nelson, S. D.; Trager, W. F. *Drug Metab. Dispos.* **2003**, *31*, 1481.
(223) Guengerich, F. P.; Peterson, L. A.; Böcker, R. H. *J. Biol. Chem.* **1988**, *263*, 8176.
(224) Shaffer, C. L.; Harriman, S.; Koen, Y. M.; Hanzlik, R. P. *J. Am. Chem. Soc.* **2002**, *124*, 8268.
(225) Bhakta, M. N.; Wimalasena, K. *J. Am. Chem. Soc.* **2002**, *124*, 1844.
(226) Wu, W.; Shaik, S. Preliminary calculations on $N(CH_3)_3$ + compound I.
(227) Yun, C.-H.; Miller, G. P.; Guengerich, F. P. *Biochemistry* **2000**, *39*, 11319.
(228) Moncada, S.; Palmer, R. M. J.; Higgs, E. A. *Pharmacol. Rev.* **1991**, *43*, 109.
(229) Kerwin, J. F., Jr.; Lancaster, J. R., Jr.; Feldman, P. L. *J. Med. Chem.* **1995**, *38*, 4343.
(230) Nathan, C. *J. Clin. Invest.* **1997**, *100*, 2417.
(231) Mansuy, D.; Renaud, J. P. In *Cytochrome P450*: *Structure, Mechanism and Biochemistry*; Ortiz de Montellano, P. R., Ed.; Plenum: New York, 1995; Chapter 15, pp 537−574.
(232) Crane, B. R.; Arval, A. S.; Ghosh, D. K.; Wu, C.; Getzoff, E. D.; Stuehr, D. J.; Tainer, J. A. *Science* **1998**, *279*, 2121.
(233) Fishmann, T. O.; Hruza, A.; Niu, X. D.; Fossetta, J. D.; Lunn, C. A.; Dolphin, E.; Prongay, A. J.; Reichert, P.; Lundell, D. J.; Narula, S. K.; Weber, P. C. *Nat. Struct. Biol.* **1999**, *6*, 233.
(234) Li, H.; Raman, C. S.; Glaser, C. B.; Blasko, E.; Young, T. A.; Parkinson, J. F.; Whitlow, M.; Poulos, T. L. *J. Biol. Chem.* **1999**, *274*, 21276.
(235) Pant, K.; Bilwes, A. M.; Adak, S.; Stuehr, D. J.; Crane, B. R. *Biochemistry* **2002**, *41*, 11071.
(236) Bird, L. E.; Ren, J.; Zhang, J.; Fowwell, N.; Hawkins, A. R.; Charles, I. G.; Stammers, D. K. *Structure* **2002**, *10*, 1687.
(237) Renodon-Corniere, A.; Dijols, S.; Perollier, C.; Lefevre-Groboillot, D.; Boucher, J.-L.; Attias, R.; Sari, M.-A.; Stuehr, D.; Mansuy, D. *J. Med. Chem.* **2002**, *45*, 944.
(238) Lefevre-Groboillot, D.; Frapart, Y.; Desbois, A.; Zimmermann, J.-L.; Boucher, J.-L.; Gorren, A. C. F.; Mayer, B.; Stuehr, D. J.; Mansuy, D. *Biochemistry* **2003**, *42*, 3858.
(239) Li, H.; Shimizu, H.; Flinspach, M.; Jamal, J.; Yang, W.; Xian, M.; Cai, T.; Wen, E. Z.; Jia, Q.; Wang, P. G.; Poulos, T. L. *Biochemistry* **2002**, *41*, 13868.
(240) Jia, Q.; Cai, T.; Huang, M.; Li, H.; Xian, M.; Poulos, T. L.; Wang, P. G. *J. Med. Chem.* **2003**, *46*, 2271.
(241) Vaz, A. D. N.; Roberts, E. S.; Coon, M. J. *J. Am. Chem. Soc.* **1991**, *113*, 5886.
(242) Vaz, A. D. N.; Pernecky, S. J.; Raner, G. M.; Coon, M. J. *Proc. Natl. Acad. Sci. U.S.A.* **1996**, *93*, 4644.
(243) Roberts, E. S.; Vaz, A. D. N.; Coon, M. J. *Proc. Natl. Acad. Sci. U.S.A.* **1991**, *88*, 8963.
(244) Kuo, C.-L.; Raner, G. M.; Vaz, A. D. N.; Coon, M. J. *Biochemistry* **1999**, *38*, 10511.
(245) Raner, G. M.; Hatchell, A. J.; Morton, P. E.; Ballou, D. P.; Coon, M. J. *J. Inorg. Biochem.* **2000**, *81*, 153.
(246) Rettie, A. E.; Boberg, M.; Rettenmeier, A. W.; Baillie, T. A. *J. Biol. Chem.* **1989**, *263*, 13733.
(247) Skiles, G. L.; Yost, G. S. *Chem. Res. Toxicol.* **1996**, *9*, 291.
(248) Obach, R. S. *Drug Metab. Dispos.* **2001**, *29*, 1599.
(249) Reilly, C. A.; Ehlhardt, W. J.; Jackson, D. A.; Kulanthaivel, P.; Mutlib, A. E.; Espina, R. J.; Moody, D. E.; Crouch, D. J.; Yost, G. S. *Chem. Res. Toxicol.* **2003**, *16*, 336.
(250) Corbin, C. J.; Graham-Lorence, S.; McPhaul, M.; Mason, J. I.; Mendelson, C. R.; Simpson, E. R. *Proc. Natl. Acad. Sci. U.S.A.* **1988**, *85*, 8948.
(251) Caspi, E.; Arunachalam, T.; Nelson, P. A. *J. Am. Chem. Soc.* **1986**, *108*, 1847.
(252) Ortiz de Montellano, P. R. In *Cytochrome P450*: *Structure, Mechanism and Biochemistry*; Ortiz de Montellano, P. R., Ed.; Plenum: New York, 1995; Chapter 8, pp 245−303.
(253) Graham-Lorenze, S.; Amarneh, B.; White, R. E.; Peterson, J. A.; Simpson, E. R. *Protein Sci.* **1995**, *4*, 1065.
(254) Akhtar, M.; Lee-Robichaud, P.; Akhtar, M. E.; Wright, J. N. *J. Steroid Biochem. Mol. Biol.* **1997**, *61*, 127.
(255) Akhtar, M.; Corina, D.; Miller, S.; Shyadehi, A. Z.; Wright, J. N. *Biochemistry* **1994**, *33*, 4410.
(256) Ortiz de Montellano, P. R. *Acc. Chem. Res.* **1998**, *31*, 543.
(257) Lad, L.; Wang, J.; Friedman, J.; Bhaskar, B.; Ortiz de Montellano, P. R.; Poulos, T. J. *J. Mol. Biol.* **2003**, *330*, 527.
(258) Sharma, P. K.; Kevorkiants, R.; de Visser, S. P.; Kumar, D.; Shaik, S. *Angew. Chem., Int. Ed.* **2004**, *43*, 1129.
(259) MacDougall, J. M.; Fandrick, K.; Zhang, X.; Serafin, S. V.; Cashman, J. R. *Chem. Res. Toxicol.* **2003**, *16*, 988.
(260) Susnow, R. G.; Dixon, S. L. *J. Chem. Inf. Comput. Sci.* **2003**, *43*, 1308.
(261) Lin, J. H.; Lu, A. Y. H. *Annu. Rep. Med. Chem.* **1997**, *32*, 295.
(262) Ha-Doung, N.-T.; Dijols, S.; Marques-Soares, C.; Minoletti, C.; Dansette, P. M.; Mansuy, D. *J. Med. Chem.* **2001**, *44*, 3622.
(263) Jean, P.; Lopez-Garcia, P.; Dansette, P.; Mansuy, D.; Godlstein, J. L. *Eur. J. Biochem.* **1996**, *241*, 797.
(264) Koenigs, L. L.; Peter, R. M.; Hunter, A. P.; Haining, R. L.; Rettie, A. E.; Friedberg, T.; Pritchard, M. P.; Shou, M.; Rushmore, T. H.; Trager, W. F. *Biochemistry* **1999**, *38*, 2312.
(265) Koenigs Lightning, L.; Jones, J. P.; Friedberg, T.; Pritchard, M. P.; Shou, M.; Rushmore, T. H.; Trager, W. F. *Biochemistry* **2000**, *39*, 4276.
(266) Pereillo, J.-M.; Maftouh, M.; Andrieu, A.; Uzabiaga, M.-F.; Fedeli, O.; Savi, P.; Pascal, M.; Herbert, J.-M.; Maffrand, J. P.; Picard, C. *Drug Metab. Dispos.* **2002**, *30*, 1288.
(267) Richter, T.; Mürdter, T. E.; Heinkele, G.; Pleiss, J.; Tatzel, S.; Schwab, M.; Eichelbaum, M.; Zanger, U. M. *J. Pharmacol. Exp. Ther.* **2003**, *308*, 189.
(268) Lambeth, J. D.; Kitchen, S. E.; Farooqui, A. A.; Tuckey, R.; Kamin, H. *J. Biol. Chem.* **1982**, *257*, 1876.
(269) Lieberman, S.; Lin, Y. Y. *J. Steroid Biochem. Mol. Biol.* **2001**, *78*, 1.
(270) Wietzerbin, K.; Bernadou, J.; Meunier, B. *Eur. J. Inorg. Chem.* **1999**, 1467.
(271) Wietzerbin, K.; Bernadou, J.; Meunier, B. *Eur. J. Inorg. Chem.* **2000**, 1391.

CR020443G